

**ANALYSIS OF SURFACE SOIL MOISTURE
PATTERNS IN AN AGRICULTURAL LANDSCAPE
UTILIZING MEASUREMENTS AND
ECOHYDROLOGICAL MODELING**

Inaugural-Dissertation

zur

Erlangung des Doktorgrades

der Mathematisch-Naturwissenschaftlichen Fakultät

der Universität zu Köln

vorgelegt von

Wolfgang Korres

aus Bonn

2013

Berichterstatter:

Prof. Dr. Karl Schneider

Prof. Dr. Georg Bareth

Tag der mündlichen Prüfung:

14.01.2013

Abstract

Soil moisture and its distribution in space and time plays a decisive role in terrestrial water and energy cycles. It controls the partitioning of precipitation into infiltration and runoff as well as the partitioning of solar radiation into latent and sensible heat flux. Therefore it has a strong impact on numerous processes, e.g., controlling floods, crop yield, erosion, and climate processes. Soil moisture, and surface soil moisture in particular, is highly variable in space and time and its spatial and temporal patterns in an agricultural landscape are affected by multiple natural (precipitation, soil, etc.) and agricultural (soil management, fertilization etc.) parameters. Against this background, the current study investigates the spatial and temporal patterns of surface soil moisture in an agricultural landscape, to determine the dominant parameters and the underlying processes controlling these patterns. The study was conducted on different spatial scales, from the field scale to the whole catchment scale of the river Rur (2364 km²) in Western Germany, because observed patterns are intrinsically connected to the scale on which they are observed. For the investigation three different approaches were used: Analysis based on A) Field measurements, B) Radar remote sensing, and C) Ecohydrological modeling. Extensive field measurements were carried out in a small arable land and grassland test site, measuring surface soil moisture, plant parameters, meteorological parameters, and soil parameters. These measurements were used to analyze the small scale (field scale) patterns of surface soil moisture and for the validation of the two other methods. Since large scale investigations based on field measurements are generally not feasible, surface soil moisture maps from radar remote sensing and ecohydrological modeling were used to analyze large scale patterns of surface soil moisture and their scaling properties.

Precipitation, vegetation patterns, topography and soil properties were found to be the dominant parameters for soil moisture patterns in an agriculturally used landscape. Precipitation can be assumed to be homogeneous on the small scale, but can be very heterogeneous on the large scale at the same time. Evapotranspiration causes high small scale variability, especially during the growing season. If analyzed on coarser resolutions, this small scale pattern is smoothed out. Topography is a source of small scale patterns only on wet surface soil moisture states, because of the lateral redistribution of water during or shortly after precipitation events. Soils have a major influence on the variability of surface soil

moisture on all scales, due to the large heterogeneity of soil properties within a given soil type (small scale) and between different soil types (large scale). Altogether, the variability of surface soil moisture increases with an increasing size of the investigation area and with an increasing resolution within the investigation area. During the course of the year surface soil moisture variability and its scaling properties are being influenced by different parameters with temporally varying intensities. During the growing season, at the time of high small scale variability of evapotranspiration, the variability of surface soil moisture is high and decreases much stronger with decreasing spatial resolution of the investigation, than during times outside the growing season. In the beginning and towards the end of the year (outside the growing season, when the soil is wet) the patterns and their scaling properties are mainly determined by soil properties. Precipitation events generally superimpose their large scale patterns for a short period of time and diminish the small scale variability induced by evapotranspiration.

This thesis improves the knowledge about surface soil moisture patterns in agriculturally used areas and their underlying processes. The results of the scaling analysis indicate the potential to use vegetation and precipitation parameters for downscaling purposes. Understanding the subscale soil moisture heterogeneity is, for example, particularly relevant to better utilize coarse scale soil moisture data derived from SMOS (Soil Moisture and Ocean Salinity) or the upcoming SMAP (Soil Moisture Active Passive) satellite measurements.

Kurzzusammenfassung

Bodenfeuchte und ihre räumliche und zeitliche Verteilung spielen eine entscheidende Rolle im terrestrischen Wasser- und Energiekreislauf. Sie kontrolliert die Aufteilung von Niederschlägen in Versickerung und Oberflächenabfluss und die Aufteilung von Sonnenenergie in latenten und fühlbaren Wärmestrom. Dies begründet den unmittelbaren Einfluss dieser Größe auf vielfältigste Prozesse, wie zum Beispiel auf Überflutungs- oder Erosionsereignisse, auf Erntemengen oder klimatisch wichtige Größen wie zum Beispiel die Lufttemperatur. Insbesondere die oberflächennahe Bodenfeuchte ist räumlich und zeitlich sehr variabel und ihre Muster werden auf landwirtschaftlich genutzten Flächen von einer Vielzahl natürlicher (z.B. Niederschlag, Bodeneigenschaften) und Bewirtschaftungsfaktoren (z.B. Bodenbearbeitung, Saattermine, Erntetermine) bestimmt. Vor diesem Hintergrund untersucht diese Studie die räumlichen und zeitlichen Muster der oberflächennahen Bodenfeuchte auf landwirtschaftlich genutzten Flächen und analysiert die wichtigsten Einflussfaktoren und zugrundeliegenden Prozesse, die diese Muster verursachen. Da ein beobachtetes Muster immer direkt mit der Skala, auf der diese Beobachtung gemacht wurde, verknüpft ist, wurde diese Studie auf verschiedenen räumlichen Skalen durchgeführt, die von der Feldskala bis hin zur Skala des Gesamteinzugsgebiets der Rur mit einer Größe von 2364 km² reicht. Für diese Arbeit wurden drei unterschiedliche methodische Herangehensweisen verwendet: Analysen basierend auf A) Feldmessungen, B) Radar-Fernerkundung und C) ökohydrologischer Modellierung. In einem ackerbaulich genutzten Testgebiet und in einem Grünlandtestgebiet wurden umfangreiche Feldmessungen der Bodenfeuchte, von Pflanzenparametern, von meteorologischen Parametern und Bodenparametern durchgeführt. Diese wurden zur Analyse der oberflächennahen Bodenfeuchtemuster auf der kleinen Skala (Feldgröße) und zur Validierung der beiden weiteren Methoden verwendet. Da großflächige Untersuchungen auf der Basis von Feldmessungen nicht durchführbar sind, wurden für die Untersuchung der Bodenfeuchtemuster auf großen Skala und deren Skalierungseigenschaften Bodenfeuchtekarten genutzt, die aus der Radar-Fernerkundung abgeleitet wurden oder aus der ökohydrologischen Modellierung stammen.

Als Haupteinflussfaktoren für oberflächennahe Bodenfeuchtemuster in landwirtschaftlich genutzten Gebieten wurden Niederschlag, Landnutzung, Topographie und Boden ermittelt. Niederschlag kann zwar auf der kleinen Skala als homogen angenommen werden, aber gleichzeitig große Heterogenität auf der großen Skala zeigen. Evapotranspiration im Zusammenhang mit kleinräumigen Landnutzungsmustern verursacht kleinräumige Variabilität, vor allem in der Hauptwachstumsperiode der Pflanzen. Mit einer Verkleinerung der Auflösung der Untersuchung werden diese kleinräumigen Muster durch Mittelung geglättet. Topographie verursacht ebenfalls kleinräumige Muster der Bodenfeuchte unter feuchten Bedingungen, da Wasser aus Niederschlagsereignissen lateral in tieferliegende Gebiete abgeleitet wird und dort zu einem Anstieg der Versickerung führen kann. Böden haben einen sehr großen Einfluss auf die Variabilität der Bodenfeuchte auf allen Skalen, da die Heterogenität der hydraulischen Bodeneigenschaften innerhalb eines Bodentyps auf der kleinen Skala ebenso groß sein kann wie zwischen unterschiedlichen Bodentypen auf der großen Skala. Insgesamt nimmt die Variabilität der oberflächennahen Bodenfeuchte mit der Vergrößerung der Auflösung der Untersuchung und der Größe des Untersuchungsgebietes zu. Im Laufe eines Jahres verändern sich der Einfluss verschiedener Faktoren und deren Intensität auf die Muster und deren Skalierungsverhalten. Während der Hauptwachstumsperiode ist die durch die Evapotranspiration verursachte kleinräumige Variabilität sehr hoch, sinkt dann allerdings auch wesentlich schneller mit der Verringerung der Auflösung der Untersuchung als außerhalb der Hauptwachstumsperiode. In dieser Zeit, am Anfang und gegen Ende des Jahres, wenn der Boden feucht ist, bestimmen hauptsächlich Bodeneigenschaften das Muster und die Skalierung. Niederschlagsereignisse mit ihrem großskaligen Muster überlagern und dämpfen die durch die Evapotranspiration verursachte kleinskalige Heterogenität für einen kurzen Zeitraum.

Insgesamt verbesserte diese Arbeit das Verständnis von oberflächennahen Bodenfeuchtemustern auf landwirtschaftlich genutzten Flächen und deren zugrundeliegenden Prozessen. Die Ergebnisse der Skalierungsanalyse zeigen das Potenzial von Vegetations- und Niederschlagsparametern zur Anwendung eines Downscaling-Verfahrens. Das Verständnis der subskaligen Heterogenität von oberflächennaher Bodenfeuchte ist von besonderem Interesse, um zum Beispiel großskalige aber gering aufgelöste Bodenfeuchtedaten aus SMOS (Soil Moisture and Ocean Salinity) oder den kommenden SMAP (Soil Moisture Active Passive) Satellitenmessungen besser nutzen zu können.

Acknowledgements

This thesis was prepared during the first phase of the Transregional Collaborative Research Center 32 (SFB/TR32) “Patterns in Soil-Vegetation-Atmosphere Systems: Monitoring, Modeling, and Data Assimilation”, funded by the German Research Foundation (DFG). I gratefully acknowledge their financial support.

I wish to express my gratitude to my supervisor Prof. Dr. Karl Schneider for giving me the opportunity to work in his research group and in the SFB/TR32 project, for providing me with all essential background conditions that made this thesis possible and also for his guidance and invaluable suggestions for improving this work.

I also sincerely thank Prof. Dr. Georg Bareth for consenting to act as second examiner and Prof. Dr. Susanne Crewell for chairing the examination committee.

I am indebted to Prof. Dr. Peter Fiener, Dr. Tim Reichenau and Dr. Christian Koyama for many inspiring and fruitful discussions and collaborations.

I thank my colleagues within the research group for a stimulating and friendly working atmosphere: Dr. Verena Dlugoß, Dr. Christian Klar, Dr. Victoria Lenz-Wiedemann, Paul Wagner and Marius Schmidt.

Furthermore, I thank Sven Bremenfeld, Alexander Schlote, Florian Wilken and the many student helpers for their assistance during the field campaigns and the laboratory analyses. Many thanks also go to the farmers in Rollesbroich and Selhausen for their permission to carry out our measurements on their fields.

I am grateful to all colleagues within the SFB/TR32 project for their friendly conversations and collaborations.

Last but not least, my heartfelt thanks to my family, my brother Martin, and especially my parents, Brigitte and Lothar, for their support throughout my entire life.

Contents

Abstract	III
Kurzzusammenfassung.....	V
Acknowledgements	VII
Contents.....	VIII
1. Introduction	1
1.1. The importance of soil moisture in the soil-plant-atmosphere system.....	1
1.2. Scope and outline of this thesis	2
2. Soil moisture.....	5
2.1. Definition of soil moisture	5
2.2. Soil moisture measurements.....	5
2.2.1. Frequency Domain Reflectometry	8
2.2.2. Advanced Synthetic Aperture Radar.....	9
2.3. Soil moisture modeling	9
2.4. Patterns of surface soil moisture	11
3. Analysis of surface soil moisture patterns based on field measurements.....	14
4. Analysis of surface soil moisture patterns based on radar remote sensing	28
5. Analysis of surface soil moisture patterns based on ecohydrological modeling.....	39
6. Summary of results and conclusions	80
6.1. Small scale surface soil moisture patterns.....	81
6.2. Large scale surface soil moisture patterns.....	82
6.2.1. Validation of methods	82
6.2.2. Large scale patterns	83
6.3. Scaling properties of surface soil moisture patterns.....	85
6.4. General conclusions	86
6.5. Outlook.....	87
References	89

1. Introduction

1.1. The importance of soil moisture in the soil-plant-atmosphere system

The water cycle is a key part of the global climate system. Water plays an important role in the Earth's energy budget, due to its high latent heat of fusion and vaporization. Only 0.0012 % of the global water and 0.035 % of the global fresh water (excluding Antarctica) is stored in soils (Oki and Kanae, 2006). Despite its seemingly negligible quantity when compared to global water resources, soil moisture is a key variable in hydrology, meteorology, and agriculture.

Soil moisture plays a central role in terrestrial water and energy cycles. Its distribution controls the partitioning of precipitation into infiltration and runoff (Western et al., 1999), hence it has a strong impact on the response of stream discharge to rainfall events, plays a significant role in producing floods (Kitanidis and Bras, 1980) and affects erosion processes from overland flow and the generation of gullies (Moore et al., 1988). Soil moisture controls the partitioning of incoming radiation into latent and sensible heat, due to its effects on evaporation and transpiration (Entekhabi and Rodriguez-Iturbe, 1994) and thus determines energy and mass fluxes in the soil-vegetation-atmosphere system.

Moreover, soil moisture enables and modulates plant growth and hence has a major influence on crop yield and food production. Root zone soil moisture determines how much water is available to plants for photosynthesis, which is regulated by their stomatal conductance to water transfer. Through their roots, plants extract water from deeper soil layers and reduce percolation of precipitation to the groundwater. The fact, that evapotranspiration returns about 60 % of the land precipitation back to the atmosphere (Oki and Kanae, 2006) and most of the evapotranspiration takes place through the stomata of plants emphasizes the major importance of the feedback loop between soil moisture and plants in the terrestrial water and energy cycles. Because of the influence on the partitioning of incoming radiation into latent and sensible heat, soil moisture impacts on a variety of climate processes, in particular air temperature, boundary layer stability and in some instances precipitation (Seneviratne et al., 2010).

In addition, soil moisture plays a major role in the global carbon cycle (Falloon et al., 2011), since microbiological activity and the decomposition of soil organic matter are controlled by temperature and moisture conditions. It is also of great socio-economic interest. Global population growth, rapid economic development and climate change intensify the demand of fresh water, e.g., for drinking, irrigation, and cooling (Arnell, 1999).

Consequently, information about the spatial and temporal patterns of soil moisture is a very important parameter in weather forecast and global climate models, due to the improved representation of interactive land surface processes, in predicting extreme events like droughts or floods, erosion modeling, water resource management, and agricultural applications, e.g., determination of sowing dates, rational irrigation practices, cultural practices or selective application of pesticides. However, soil moisture and surface soil moisture in particular, is highly variable in space and time, impacted by the heterogeneity of soil properties, topography, land cover, and meteorological conditions.

1.2. Scope and outline of this thesis

This thesis was embedded within the framework of the Transregional Collaborative Research Center 32 (SFB/TR32) with the title “Patterns in Soil-Vegetation-Atmosphere Systems: Monitoring, Modelling, and Data Assimilation” funded by the German Research Foundation (DFG). This multidisciplinary project involves research groups in the field of geophysics, soil and plant science, hydrology and meteorology located at the Universities of Aachen, Bonn, and Cologne and the Research Centre Jülich. The project aims at extending the knowledge about the origins of and the interrelations between spatial and temporal patterns within the soil-vegetation-atmosphere system and their relation to energy and matter. The research area is the Rur catchment in Western Germany. The research of our subproject within the SFB/TR32 focuses on the subject of surface soil moisture, an essential quantity in the context of the overall research of the SFB/TR32 project. This dissertation thesis aims at answering the following main research questions:

- What are the dominant parameters and underlying processes for spatial and temporal patterns of surface soil moisture in an agriculturally used landscape?
- How does the spatial variability of surface soil moisture change from the field scale to the catchment scale?

- How do surface soil moisture patterns and their scaling behavior change during the course of the year? What parameters determine the patterns and their scaling behavior at different times?

To address these main questions three different approaches were used: Analysis based on A) Field measurements, B) Radar remote sensing, and C) Ecohydrological modeling. Extensive spatially distributed field measurements of surface soil moisture in a grassland and an arable land test site were conducted. To analyze the patterns and dominant parameters at the small catchment scale an Empirical Orthogonal Function (EOF) and a correlation analysis were used (see chapter 3). The measurements were also used to validate an empirical soil moisture retrieval algorithm for Advanced Synthetic Aperture Radar (ASAR) remote sensing data. Retrieved soil moisture data and the field measurements served as a basis for the analysis of statistical properties of surface soil moisture from the field scale to the whole catchment scale in terms of the relationship between soil moisture variability and mean soil moisture (see chapter 4). To identify and assess the influence of the main parameters and processes leading to the scale dependent variability of surface soil moisture, a process based, dynamic ecohydrological model was deployed and validated. The use of this model accounted for the complex interactions and feedbacks between soil, plant, and atmosphere. An autocorrelation and scaling analysis of the surface soil moisture data from different model runs was used to investigate the varying impact of soil, precipitation and vegetation on the autocorrelation structure and scaling properties of surface soil moisture patterns during the course of the year (see chapter 5).

This thesis is organized in the following manner:

This introduction (*Chapter 1*) is followed by a general chapter (*Chapter 2*), with definitions of the variable of interest (2.1), an introduction of soil moisture measurement methods (2.2), a short introduction of soil moisture modeling in the context of ecohydrology (2.3) and an integrated overview of the research on patterns of soil moisture (2.4). *Chapters 3 to 5* contain three research papers corresponding to the research approaches:

Chapter 3: Analysis of surface soil moisture patterns based on field measurements with the paper title: “Analysis of surface soil moisture patterns in agricultural landscapes using Empirical Orthogonal Functions”.

Chapter 4: Analysis of surface soil moisture patterns based on radar remote sensing with the paper title: “Variability of Surface Soil Moisture Observed from Multitemporal C-Band Synthetic Aperture Radar and Field Data”.

Chapter 5: Analysis of surface soil moisture patterns based on ecohydrological modeling with the paper title: “Patterns and scaling properties of surface soil moisture in an agricultural landscape: An ecohydrological modeling study”.

Chapter 6 summarizes the results and conclusions of this thesis regarding the small scale patterns (6.1), the large scale patterns (6.2), and the scaling properties (6.3) of surface soil moisture. Furthermore, in the general conclusions (6.4) the main research questions will be addressed and a short outlook is given (6.5).

2. Soil moisture

2.1. Definition of soil moisture

Soil is a three phase system, consisting of soil particles, soil water, and soil air. The water contained in the unsaturated soil is defined as soil moisture (Hillel, 1998). The amount of water in the soil can be expressed in relative terms (volumetric soil moisture [$\text{m}^3 \text{m}^{-3}$], gravimetric soil moisture [kg kg^{-1}] or saturation ratio) and in absolute terms (water depth [mm] or mass [kg]). The value of soil moisture is considered with regard to a given soil volume. This is highly relevant, when comparing different soil moisture measurements or estimations, because the considered volumes range from the top few centimeters of the soil (e.g., from radar remote sensing) or a small volume (e.g., from Frequency Domain Reflectometry measurements) to discrete soil layers (e.g., from modeling) or an extremely large volume (e.g., from Gravity Recovery and Climate Experiment, GRACE). For the definition of root zone soil moisture and total soil moisture the relevant soil volume will vary as a function of space and time, depending on the rooting depth of plants and the water table depth, respectively. Two other important quantities in hydrology and agricultural applications are field capacity and permanent wilting point. Above field capacity, water cannot be held against gravity and drains towards the groundwater table, and below wilting point the water is strongly bound to the soil matrix and not accessible to plants. The binding of the soil moisture to the soil matrix is characterized by the soil moisture potential. Field capacity and permanent wilting point are typically defined as corresponding to suction heads of pF 1.8-2.5, with pF being the logarithm of the cm of water column suction, and pF 4.2, respectively. These are approximated values, and the wilting point is depending on the vegetation type.

2.2. Soil moisture measurements

There are multiple techniques that are used to measure soil moisture. However, a method to continuously measure the spatial patterns of soil moisture at larger scales is currently not available. The available measurement methods can be differentiated in direct (measurement of hydrological variable, e.g., rainfall depth) or indirect methods. Most soil moisture measurement techniques employ indirect measurements methods, utilizing the measurements

of features which are closely linked to soil moisture (e.g. frequency modulation of an emitted signal for FDR measurements or electromagnetic emissions for remote sensing). These measurements are then converted by a rating function to a soil moisture value (Grayson and Blöschl, 2000). These conversions can introduce additional measurement errors. In the following section different methods of soil moisture measurement are introduced, however this short outline is not intended to be exhaustive.

The thermogravimetric method is a one of the few direct methods and determines the weight loss of a known volume of soil after oven drying at 105°C (Reynolds, 1970a). But it is a very time-consuming and destructive method, used for calibration and evaluation purposes. Time and Frequency Domain Reflectometry (TDR, FDR) are used most often to investigate soil moisture at the point scale (Navarro et al., 2006; Roth et al., 1992). These techniques are based on the change of an emitted electromagnetic wave along some wave guides inserted in the soil depending on the dielectric constant of the wet soil (see 2.2.1). The sensors are either used on fixed locations to monitor temporal dynamics or as portable probes to study spatially distributed soil moisture patterns. To enlarge the number of measurement locations while simultaneously retain the high temporal resolution of the measurements, wireless sensor networks have been developed (Bogena et al., 2007), but they cannot be applied to surface soil moisture investigations in an arable land test site, due to the cultivation practices and the high effort of installation and deinstallation.

Geophysical methods like ground penetrating radar (GPR, Huisman et al., 2001), electromagnetic induction (EMI, Sheets and Hendrickx, 1995) or electric resistivity tomography (ERT, Kemna et al., 2002) make it possible to measure soil moisture in a less invasive or even noninvasive way on larger areas, but they rely on highly detailed information of subsurface properties and a site specific calibration. The GPR method uses the same principle as TDR, only it uses a non-guided electromagnetic wave, measured between a transmitter and a receiver. EMI measures the apparent electric conductivity of the soil, depending on the water content of the soil, with a magnetic field. ERT measures the bulk soil electric conductivity, related to the water content, between two or more electrodes inserted into the soil. Other ground based methods are utilizing the sensitivity of cosmic ray neutrons to water content changes to estimate surface soil moisture non-invasive for a spatial scale of 300 m radius around the measurement device (Zreda et al., 2008) or using fibre optic cables (Sayde et al., 2010; Steele-Dunne et al., 2010) to estimate soil moisture along cables of over 10 km length, using the dependence of soil thermal properties on soil moisture, but with a strongly invasive and very complex installation process.

Remote sensing can be used to observe larger scale soil moisture patterns with different spatial and temporal resolutions. All remote sensing based approaches are indirect methods, measuring the color (at optical to mid-infrared wavelengths), parameters of the surface energy balance (e.g., temperature, at thermal infrared wavelengths) or dielectric properties (at microwave wavelengths) of the soil. For the retrieval of soil moisture the following microwave frequency bands are most important: L-band (wavelength 15 - 30 cm), C-band (3.8 - 7.5 cm) and X-band (2.5 - 3.8 cm). There are three types of remote sensing platforms, towers, aircrafts (airborne) and satellites (spaceborne), but for operational purposes spaceborne platforms are the prime choice, because of their global coverage and the regular nature of their overpasses (Wagner et al., 2007). Active radar systems measure the backscattering coefficient (reflectivity of the surface) of the emitted beam, whereas passive systems (Radiometers) measure the brightness temperature of the surface (product of emissivity and temperature). Active measurements are more sensitive to roughness and vegetation structure than passive measurements, but they provide a much better spatial resolution. Examples for Microwave radiometers (passive systems) are: Advanced Microwave Scanning Radiometer (AMSR-E) or Soil Moisture and Ocean Salinity (SMOS). Examples for Synthetic Aperture Radar (SAR, active systems) platforms are: RADARSAT-1, RADARSAT-2, ERS-1, ERS-2 and ENVISAT (all C-band) or JERS-1 and ALOS (L-band). SAR systems allow monitoring patterns at higher spatial and lower temporal resolutions, while passive systems allow assessing patterns at lower spatial and higher temporal resolutions (Wagner et al., 2007).

In our study, we used FDR probes both for the spatial surface soil moisture measurements and the measurements of soil moisture time series on single locations. Moreover, we used data from the Advanced Synthetic Aperture Radar (ASAR) onboard the ENVIRONMENTAL SATellite (ENVISAT) launched by the European Space Agency (ESA). Therefore these techniques are described in the following sections 2.2.1 and 2.2.2. in more detail.

The organization of measurements can be characterized by three scales (spacing, extent, and support) and has been termed “scale triplet” by Blöschl and Sivapalan (1995). The term scale refers to a characteristic length or time scale. Spacing refers to the distance (or time) between the measurements, extent to the overall coverage of the measurements (in time or space), and support to the averaging volume or area (or time) of a single measurement. For example, the FDR measurements in our grassland test site had 50 meter spacing (between the measurements), 1000 meter extent (length of the test site), and 0.1 meter support (area influencing or representing a single measurement). The measurements should be taken at a

scale that is able to resolve all variability of the processes that influences the soil moisture patterns. If the spacing is too large, small scale variability will not be captured. If the extend is too small, large scale variability will not be captured and if the support is too large, variability will be smoothed out (Grayson and Blöschl, 2000). Thus, ideally the process scale equals the measurement scale (equals the model scale).

2.2.1. Frequency Domain Reflectometry

Frequency Domain Reflectometry (FDR) measurements (Navarro et al., 2006) are used in this study as a standard for in situ soil moisture measurements. The FDR probes (Delta-T Devices Ltd., Cambridge, UK) consist of a waterproof casing for the electronics and four 6 cm long parallel stainless steel rods (to be inserted into the soil) and a data logger. This system provides a quick and efficient method for measuring soil moisture patterns (with a handheld logging device) or soil moisture time series (with a stationary data logger). The soil moisture value is averaged over a sampling volume with about 6 cm in length (along the rods) and a diameter of approximately 10 cm.

FDR is an indirect method and it is based on the change of the amplitude of an emitted 100 MHz sinusoidal wave signal as a function of the soil dielectric constant, also known as permittivity or specific inductive capacity (Gaskin and Miller, 1996). The dielectric constant is a measure of how polarizable a material is, when subjected to an electric field and is measured usually in relation to the dielectric constant of free space (then called relative dielectric constant). The relative dielectric constant of soil consists of the relative dielectric properties of liquid water (approximately 80) and dry soil (2-5, depending on bulk density), and the volume fraction of each component involved. Thus, when the soil moisture content in the soil increases, the relative dielectric constant increases. However, the dielectric constant of moist soil is more complex than a simply weighted average of its components and the mixing model has many influencing factors (Jackson and Schmugge, 1989). A comprehensive overview over the topic complex dielectric constant is given by Von Hippel and Labounsky (1995). The most commonly used relationship to convert the dielectric constant to volumetric soil moisture is an empirical third order polynomial expression established by Topp et al. (1980). This conversion is almost independent from soil density, soil texture, soil salinity and soil temperatures (for temperatures between 10°C and 36°C) and has been used as a quasi-standard method in various investigations.

2.2.2. Advanced Synthetic Aperture Radar

The Advanced Synthetic Aperture Radar (ASAR) was launched as one of ten instruments onboard the ENVISAT-1 satellite by the European Space Agency (ESA) with a sun-synchronous polar orbit in 2002. It is an active radar instrument, operating in C-band with a center frequency of 5.331 GHz (the corresponding wavelength is 5.62 cm) and can perform multiple acquisition modes. The penetration depth of the radar determines the sample volume and varies between half of the wavelength to the order of some tenths of the wavelength (in wet soil conditions). In our study wide swath images with a resolution of approximately 150 m and a swath width (width the sensor can observe) of 400 km were used, because this mode is suitable for the derivation of large scale surface soil moisture patterns. The single scenes were acquired on the same orbit, hence the time lag between the different images equals the orbital repeat cycle of the satellite of 35 days.

The derivation of surface soil moisture values from radar remote sensing is based on the sensitivity of the SAR backscatter intensity to the dielectric constant of the moist soil (see FDR measurements). But the backscatter signal at the C-band is also significantly influenced by vegetation and surface roughness, thus for the estimation of spatial soil moisture patterns, correction procedures for these two factors are required. Physically based backscatter models for the inversion of soil moisture from the radar data are only available for bare soil conditions and require either detailed independent soil data or additional radar data to isolate the effects of surface roughness and surface soil dielectric constant. This detailed additional data is often unavailable, particularly for larger areas. Empirical and semiempirical algorithms have shown their potential to derive soil moisture from single-frequency SAR data, but their applicability might be limited to the region where they are developed (Oh et al., 1992; Rombach and Mauser, 1997). If transferred to a different area, they must be validated again. An overview of the existing inversion approaches is given by Verhoest et al. (2008).

2.3. Soil moisture modeling

Soil moisture modeling in the context of ecohydrology can be characterized by two main types of concepts: i) empirical modeling concepts, with only a statistical or conceptual (high degree of abstraction) description of the processes and their underlying controlling factors and ii) process based dynamic modeling concepts, with a process based description of the physical processes and the capability of simulating nonlinear interactions. Process based dynamic models are suitable for climate change studies, the analysis of complex cause and effect

principles and have a high transferability to other areas. The transferability of models or modeling concepts from the point or small scale, where they are being developed and validated, to the larger or even global scales is another big challenge and a large source of uncertainty. Three examples of concepts for bridging this scale gap are effective parameters (Hansen et al., 2007), Geo-complexes (Ludwig et al., 2003), and hydrological response units (HRUs, Flügel, 1995). Due to the large variety of models and model concepts with various complexities of process descriptions at different scales, a short description of the concepts in the model we used in our investigation is given in the following section instead of a general overview over different models and concepts (for this, see Pitman, 2003; Sellers et al., 1997).

The ecohydrological model used in this study is the DANUBIA simulation system. It is a component and raster based modeling tool designed for coupling models of different complexity and temporal resolution and consist of 17 components in its complete structure, representing natural as well as socio-economic processes (Barth et al., 2004; Barthel et al., 2012). It was developed in the GLOWA-Danube Project to investigate the impacts of Global Change on the Upper Danube catchment in Southern Germany. For the current study in the northern part of the Rur catchment, only the ecohydrological components regarding plant growth, soil nitrogen transformation, hydrology, and energy balance were used. These components model fluxes of water, energy, nitrogen and carbon in the soil-vegetation-atmosphere system using physically based process descriptions.

The vertical water fluxes in the soil are modeled using a modified Eagleson approach (Eagleson, 1978). The modification particularly pertains to describing water fluxes in soil by a user defined number of soil layers. Percolation of the upper soil layer is interpreted as effective precipitation for the downward layer (Mauser and Bach, 2009). Volumetric soil moisture and matrix potential is calculated according to the one-dimensional, concentration dependent diffusivity equation (Philip, 1960). Eagleson (1978) presented an analytical solution of the Philips equation for simplified boundary conditions to model the key processes of soil water movement, namely infiltration, exfiltration, percolation and capillary rise. Most of the hydrological models use a numerical solution of the Richards' equation to describe soil water flow (e.g. HYDRUS, Šimůnek et al., 2008), but for our distributed soil moisture modeling at larger scales only an analytical algorithm like the Eagleson approach is practical. This analytical and physically based approach is computationally efficient and it avoids iterative solutions. It has proven its applicability (Mauser and Bach, 2009; Schneider, 2003) and all necessary input data can be derived from soil texture, which is extensively available from soil maps. Moreover, the use of the Richards' equation may be not valid, when used with

larger grid sizes comparable to our study (Vogel and Ippisch, 2008) and can in some cases lead to loss of the physical basis.

The crop growth model (Lenz-Wiedemann et al., 2010) simulates water, carbon, and nitrogen fluxes within the crops as well as the energy balance at leaf level. It models photosynthesis, respiration, soil layer-specific water and nitrogen uptake, dynamic allocation of carbon and nitrogen to four plant organs (root, stem, leaf, harvest organ), as well as phenological development and senescence. Resulting from the interplay of these processes, transpiration is a function of available energy, stomatal conductance (controlled by soil moisture and CO₂), and leaf area (emerging from carbon and nitrogen dynamics). The water and nitrogen uptake is differentiated between the different soil layers based on the distribution of the plant roots. The main concepts and algorithms are adopted and extended from the models GECROS (Yin and van Laar, 2005) and CERES (Jones and Kiniry, 1986). The soil nitrogen transformation model (Klar et al., 2008) is based on algorithms from the CERES maize model (Jones and Kiniry, 1986) and models nitrogen transformation processes: Mineralization from two organic carbon pools (easily decomposable fresh organic matter and stable humus pool), immobilization, nitrification, denitrification, urea hydrolysis, and nitrate leaching. The iterative solution of the energy and mass balance is calculated based on the results exchanged between the soil component (including a soil temperature model from Muerth and Mauser, 2012) and the plant growth component. Meteorological input was derived from meteorological station data, using the method described by Mauser and Bach (2009).

The full coupling of the different components as well as the dynamic plant growth component (in contrast to a prescribed vegetation) consider the manifold interactions and feedbacks between soil, plant, and atmosphere with regard to water and energy fluxes and their resulting effect on soil moisture and evapotranspiration. Thus, DANUBIA is a suitable model to investigate soil moisture patterns at larger scales in strongly managed agricultural areas.

2.4. Patterns of surface soil moisture

Many factors control the spatial patterns and temporal dynamics of surface soil moisture. Among these a distinction can be made between static and dynamic factors (Reynolds, 1970b). Static factors are particularly topography (e.g., slope and aspect affect runoff, infiltration, and evapotranspiration) and soil properties (e.g., texture, porosity and organic

matter content affecting water holding capacity). Dynamic factors are meteorological conditions (e.g., precipitation, solar radiation, air temperature, wind speed, humidity), vegetation dynamics (e.g., influencing transpiration, evaporation from intercepted precipitation) and human management (e.g., irrigation). The influence of the different factors can vary significantly over time in the same landscape. Grayson et al. (1997) distinguish between two states: A) a wet state, denoted as non-locally controlled, which is dominated by lateral water movement through both surface and subsurface paths, with catchment terrain leading to organization of wet areas along drainage lines, and B) a dry state, denoted as locally controlled, dominated by vertical fluxes (e.g., evapotranspiration), with soil properties and only local terrain (areas of high convergence) influencing spatial patterns. But also precipitation as the main driver of surface soil moisture can occur at different scales in space and time. Convective precipitation can be characterized by small spatial extent, high intensities and short durations, with typical spatial scales of 1–10 km and typical temporal scales ranging from 1 minute to 1 hour. Whereas frontal weather systems tend to produce wide areas of relatively uniform rainfall with typical spatial scales of 100–1000 km and typical temporal scales of 1 day (Grayson and Blöschl, 2000).

Autocorrelation length is often used to analyze the spatial structure of soil moisture fields and their driving parameters. For a small grassland catchment, Western and Grayson (1998) found shorter autocorrelation lengths on wet days, related to the smaller spatial scale of lateral redistribution, in contrast to longer autocorrelation lengths on dry dates, connected to the larger scale of evapotranspiration as the dominant driver. At the field scale (mainly on wheat fields) in a semi-arid climate, Green and Erskine (2004) found a spatial structure of surface soil moisture, but no clear connection of the autocorrelation length to dry or wet soil moisture conditions. Western et al. (2004) compared soil moisture autocorrelation lengths of soil moisture and terrain attributes, indicating the important role of topography at one test site and the variation of soil properties at other test sites. But these studies focused on small catchments, mostly with homogeneous vegetation, therefore the influence of the interacting factors topography, vegetation, soil, and precipitation on surface soil moisture patterns were not investigated. Other studies used Empirical Orthogonal Functions to analyze the variability of surface soil moisture and their driving factors over a large variety of scales, from the field scale for agricultural sites (Yoo and Kim, 2004) to small catchment scales (Perry and Niemann, 2007), and to regional scales (Jawson and Niemann, 2007). At the field and small catchment scale topography related factors were found to be most important for the spatial patterns, whereas soil texture was identified to be the most important factor on the regional

scale. This indicates that topographic characteristics influence soil moisture largely through lateral flows, which are not easily observed at larger scales.

Many studies have analyzed the statistical properties of the spatial structure of soil moisture in terms of the relationship between soil moisture variability and mean soil moisture using point measurements (e.g., Famiglietti et al., 1998; Western et al., 1998), remotely sensed images (e.g., Kim and Barros, 2002; Rodriguez-Iturbe et al., 1995) and model generated maps (e.g., Manfreda et al., 2007; Peters-Lidard et al., 2001). Contrasting findings of the relationship have been reported. Some studies found an increase of spatial variability with decreasing mean soil moisture (e.g., Choi and Jacobs, 2011; Famiglietti et al., 1999), others found opposite trends (e.g., Famiglietti et al., 1998; Western and Grayson, 1998) or were unable to detect a trend (e.g., Charpentier and Groffman, 1992; Hawley et al., 1983). Teuling and Troch (2005) explained these contrasting findings by analyzing that both, soil properties and vegetation dynamics, can act to either create or destroy spatial variability. The main discriminating factor between both behaviors is a critical moisture content in the soil, defined by the transition between stressed and unstressed conditions for transpiration. Moreover, Rodriguez-Iturbe et al. (1995) and Manfreda et al. (2007) showed that spatial soil moisture variability is not only depending on mean soil moisture, but also varies with the spatial scale of the analysis following a power-law relationship.

3. Analysis of surface soil moisture patterns based on field measurements

Journal article (published):

Korres, W., Koyama, C.N., Fiener, P., Schneider, K., 2010. Analysis of surface soil moisture patterns in agricultural landscapes using Empirical Orthogonal Functions. *Hydrology and Earth System Science*, 14(5): 751-764.

Permission to reprint:

The article and any associated published material is distributed under the Creative Commons Attribution 3.0. Copyright on this article is retained by the authors. Original page numbers are used.

Analysis of surface soil moisture patterns in agricultural landscapes using Empirical Orthogonal Functions

W. Korres, C. N. Koyama, P. Fiener, and K. Schneider

Department of Geography, University of Cologne, Cologne, Germany

Received: 30 July 2009 – Published in Hydrol. Earth Syst. Sci. Discuss.: 24 August 2009

Revised: 3 April 2010 – Accepted: 14 April 2010 – Published: 12 May 2010

Abstract. Soil moisture is one of the fundamental variables in hydrology, meteorology and agriculture. Nevertheless, its spatio-temporal patterns in agriculturally used landscapes that are affected by multiple natural (rainfall, soil, topography etc.) and agronomic (fertilisation, soil management etc.) factors are often not well known. The aim of this study is to determine the dominant factors governing the spatio-temporal patterns of surface soil moisture in a grassland and an arable test site that are located within the Rur catchment in Western Germany. Surface soil moisture (0–6 cm) was measured in an approx. 50×50 m grid during 14 and 17 measurement campaigns (May 2007 to November 2008) in both test sites. To analyse the spatio-temporal patterns of surface soil moisture, an Empirical Orthogonal Function (EOF) analysis was applied and the results were correlated with parameters derived from topography, soil, vegetation and land management to link the patterns to related factors and processes. For the grassland test site, the analysis resulted in one significant spatial structure (first EOF), which explained 57.5% of the spatial variability connected to soil properties and topography. The statistical weight of the first spatial EOF is stronger on wet days. The highest temporal variability can be found in locations with a high percentage of soil organic carbon (SOC). For the arable test site, the analysis resulted in two significant spatial structures, the first EOF, which explained 38.4% of the spatial variability, and showed a highly significant correlation to soil properties, namely soil texture and soil stone content. The second EOF, which explained 28.3% of the spatial variability, is linked to differences in land management. The soil moisture in the arable test site varied more strongly during dry and wet periods at locations

with low porosity. The method applied is capable of identifying the dominant parameters controlling spatio-temporal patterns of surface soil moisture without being affected by single random processes, even in intensively managed agricultural areas.

1 Introduction

Soil moisture is one of the fundamental variables in hydrology, meteorology and agriculture as it plays a major role in partitioning energy, water and matter fluxes at the boundary between the atmosphere and the pedosphere. Its spatio-temporal distribution influences the partitioning of precipitation into infiltration and runoff (Western et al., 1999a) and it partitions the incoming radiation into latent and sensible heat due to the control of evaporation and transpiration. It has a strong impact on the response of stream discharge to rainfall events, it plays a significant role in producing floods (Kitanidis and Bras, 1980) and affects erosion from overland flow and the generation of gullies (Moore et al., 1988). More discharge and erosion have been observed in areas with high soil moisture that are well connected to channels (Ntekos et al., 2006). The spatio-temporal variation of soil moisture is also reflected in spatial patterns of plant growth and crop yield (Jaynes et al., 2003). For example, crop yield is highly sensitive to early season soil moisture conditions, especially during seed germination (Green and Erskine, 2004).

Due to difficulties in measuring spatio-temporal patterns of soil moisture at larger scales and owing to the importance of these patterns for many environmental processes, great efforts were undertaken to derive spatially distributed soil moisture maps from remote sensing and modelling (Oppelt et al., 1998; Owe and Van de Griend, 1998; Schneider,



Correspondence to: W. Korres
(wolfgang.korres@uni-koeln.de)

2003). Since surface soil moisture data is potentially available for large areas using remote sensing products (Koyama et al., 2010), it is of great interest to analyse the driving parameters which explain these patterns. To build an adequate model, all relevant processes that affect spatial and temporal soil moisture variability must be identified and addressed. In case of strong spatial variations in soil properties or a dominance of vertical fluxes, such as evapotranspiration or infiltration, soil moisture patterns are controlled by local properties and processes (Grayson et al., 1997; Vachaud et al., 1985). If soil moisture is horizontally redistributed by lateral fluxes, non-local dependencies can play a decisive role (Herbst and Diekkrüger, 2003). Both, locally and non-locally controlled processes and their varying importance in time are essential for the determination of soil moisture patterns. Hawley (1983) determined that topography (relative elevation) is the most important driver of soil moisture in small agricultural watersheds. Even in watersheds with little slope, soil moisture values are consistently higher at the bottom of the slope. Vegetation tends to override this topographic influence. The effect of soil texture on surface soil moisture appears to be larger under wet conditions; minor variations in soil type seem to be insignificant. For all soil texture classes (except sands), soil moisture variability is typically high in a mid range between 18 and 23 Vol.-% (Vereecken et al., 2007). On a 1.4 ha hillslope, Burt and Butcher (1985) detected the development of saturated areas in downhill, low slope and convergent locations, indicating lateral redistribution of soil water via saturated flow above impermeable bedrock. The correlation between Wetness Index (WI; Beven and Kirkby, 1979) and soil moisture was generally better during wet conditions (Burt and Butcher, 1985). However, lateral water movement in unsaturated soils can also be observed and may reach the same order of magnitude as the vertical movement. This is caused by anisotropic permeability due to different soil layers (Zaslavsky and Sinai, 1981; Herbst et al., 2006). For the Tarrawarra grassland catchment in south eastern Australia (Western et al., 1999a), the highest correlation between soil moisture and topographic characteristics occurred for moderately wet conditions. This relationship deteriorates for dry and very wet (near saturation) conditions. The soil moisture autocorrelation calculated for different dates generally showed longer correlation length on dry dates, related to the larger spatial scale of evapotranspiration as the dominant driver. The shorter correlation length on wet days seems to be connected to the smaller spatial scale of lateral redistribution (Western et al., 1998). Green and Erskine (2004) found no clear correlation length of soil moisture at the field scale for a semi-arid climate. Western et al. (2004) compared soil moisture correlation lengths with the spatial correlation of terrain attributes indicating the important role of topography at one site and the variation of soil properties at other sites. Empirical Orthogonal Function (EOF) analysis can be used to identify the dominant processes and essential parameters controlling soil moisture

patterns. Since introduced to the analysis of geophysical fields by Lorenz (1956), EOF analysis has been widely applied for the analysis of the spatial and temporal variability of large multidimensional datasets and has been commonly used in meteorological studies. More recently it has also been used to analyse soil moisture patterns at a large variety of scales, from the field scale for agricultural sites (Yoo and Kim, 2004), to catchment scales (Perry and Niemann, 2007), and to regional scales (Jawson and Niemann, 2007; Kim and Barros, 2002). The result of this analysis is a small number of spatial structures (EOFs) that explain a high percentage of variation of the dataset and temporal varying coefficients (ECs), which modulate the influence of these spatial structures in time. Utilizing correlation analyses, these underlying (stable) patterns of soil moisture variations can be connected to parameters derived from topography, soil, vegetation, land management and meteorology. Our dataset contains “snapshots” in time and the intention of our analysis is not to analyse continuous soil moisture seasonality. The main objectives of this study are to identify the dominant parameters and underlying processes controlling the stable spatial and temporal patterns of surface soil moisture under different soil moisture states and to examine whether the application of this method in agriculturally used areas, which are affected by heterogeneous, land-use dependent management procedures, also provides reasonable results.

2 Test sites

Field measurements were carried out in a grassland test site in Rollesbroich and an arable test site in Selhausen, both located west of Cologne, Germany. The grassland site (50°37'25" N/6°18'16" E) covers an area of approximately 20 ha with nine fields of extensively used grassland (Fig. 1). This test site is typical for the low mountain ranges of the Eifel. Slopes range from 0 to 10°, while altitude ranges from 474 to 518 m a.s.l. Mean annual air temperature and average annual precipitation measured at a meteorological station 9 km west (altitude 505 m) of the test site are 7.7°C and 1033 mm, respectively. No pronounced seasonality in precipitation can be found. The dominant soils are (gleyic) Cambisol, Stagnosol and Cambisol-Stagnosol. The grassland vegetation is dominated by a ryegrass society, particularly perennial ryegrass (*Lolium perenne*) and smooth meadow grass (*Poa pratensis*).

The arable site (50°52'10" N/6°27'4" E) covers an area of approximately 34.3 ha and represents an intensively used agricultural area, where crops are grown on gentle slopes (0–4°). The altitude ranges from 102 to 110 m a.s.l. A mean annual air temperature of 9.8°C and an average precipitation of 690 mm with slightly higher values occurring in June and July were measured at a meteorological station 4.5 km to the north-west (altitude 90 m). Main soils are (gleyic) Cambisol and (gleyic) Luvisol with a high amount of coarse alluvial

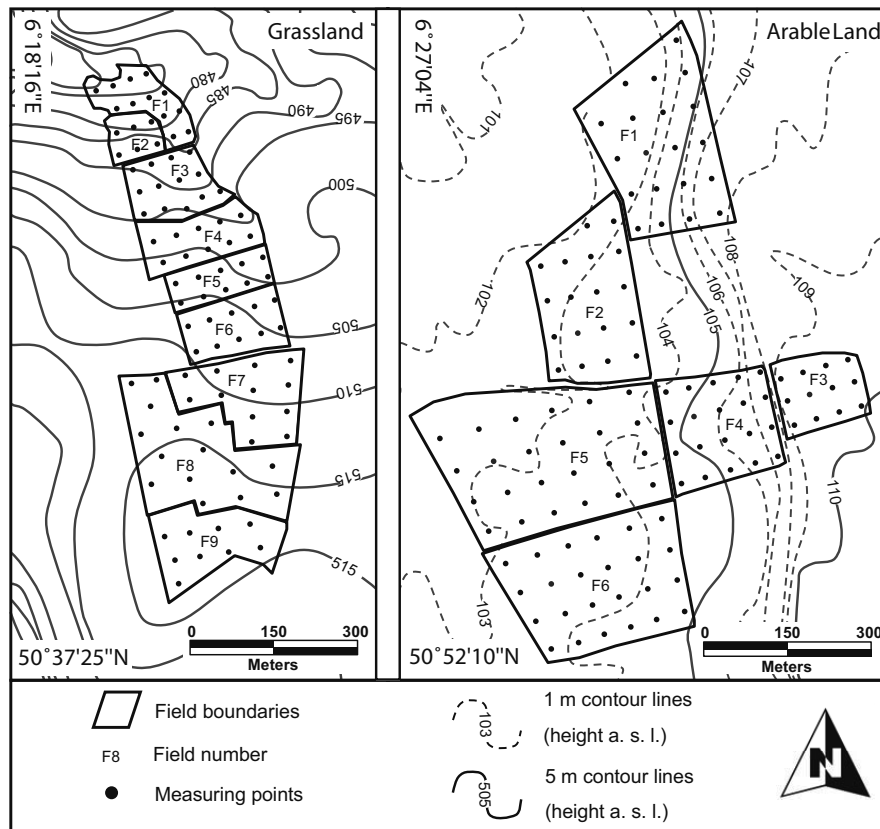


Fig. 1. Topography, field layout and measuring grid of the grassland (Rollesbroich) and the arable test site (Selhausen).

deposits on a former river terrace in the eastern part. The land cover types during the measurement period were sugar beet (*beta vulgaris*), wheat (*triticum aestivum*), rye (*secale cereale*), oilseed radish (*raphanus sativus oleiformes*) and fallow.

3 Field measurements

3.1 Grassland test site

Surface soil moisture measurements for the topsoil layer (0–6 cm) were performed on an approx. 50×50 m grid (Fig. 1). The measurement locations were slightly adjusted according to local conditions such as field boundaries. While the average distance to the next measurement location was 50 m, the minimum distance was 20 m and ranged up to 60 m. Measurements were taken during 14 campaigns from May 2007 to November 2008 at 41 to 96 locations. To provide representative values, each measurement location is represented by the average of six measurements carried out within a radius of 10 cm. Soil moisture was measured with handheld FDR probes (Delta-T Devices Ltd., Cambridge, UK). The probes were calibrated individually in the laboratory using a mixture of water and glass beads to provide well defined water

content and tested on soil samples from the test sites. Based on these lab procedures, the FDR probes yield an absolute accuracy of ± 3 Vol.-% and a relative accuracy of ± 1 Vol.-% (Delta-T Devices Ltd., Cambridge, UK). To investigate the influence of soil texture and soil organic carbon (SOC) on the surface soil moisture, soil samples in three depths (0–10 cm, 10–30 cm and 30–60 cm) were taken at every sampling location. Carbon content and soil texture were determined using mid-infrared-spectroscopy (Bornemann et al., 2008). The results from spectroscopy analysis were calibrated to carbon content using samples analysed with a CN Elemental Analysator (Elementar, Germany). In addition, topsoil (0–5 cm) porosity and soil organic matter (SOM) were measured at four locations in the northern part of the test site, where very high surface soil moisture values (up to 75 Vol.-%) were determined (especially field F2).

3.2 Arable test site

Similarly to the grassland test site, surface soil moisture (<6 cm) was measured in the arable test site on a grid of approx. 50×50 m (Fig. 1). Again the locations were adjusted according to local conditions and field boundaries. Measurements were taken during 17 campaigns between May 2007 and November 2008 at 44 to 118 locations. Soil information

was taken from a high resolution soil map (Bodenkarte 1:50 000, Geologischer Dienst, North-Rhine-Westphalia). A terrace slope with an elevation difference of about 2–3 m cuts through the test site. Soil translocation by tillage operations at the edge of the terrace result in a high percentage of stones at the surface in the vicinity of the terrace slope. The upper terrace plain has a high stone content, while the lower plain generally shows a lower stone content. The stone cover on the surface within a sample area of 0.4×0.4 m was visually estimated at each measuring location using a wooden frame. On every location, three replicate measurements were taken. Using previously measured data of the coarse fraction of soil material, a relationship between the stone cover and the coarse fraction of the top soil layer (0–30 cm) was established by correlation analysis for two parallel transects with 8 measurement points. This analysis resulted in a Pearson correlation coefficient of $r=0.89$. The stone cover analysis is subsequently used in the pattern analysis. The ground based data set was complemented by data on the tillage practice for each field.

4 Methods

4.1 Empirical Orthogonal Functions analysis

Empirical Orthogonal Functions (EOF) analysis is one of the best known data analysis techniques and a well established method of multivariate data analysis (Jolliffe, 2002). The EOF analysis, also known as principal component analysis, decomposes the observed variability of a dataset into a set of orthogonal spatial patterns (EOFs) and a set of time series called expansion coefficients (ECs). While single soil moisture patterns might be affected by random processes (e.g. rainfall shortly before measuring), significant EOFs represent stable patterns of a dataset and are by definition not random (definition of statistical significance in Sect. 4.2). The existing degree of randomness of a single soil moisture pattern is reflected by the associated EC, since the EC value represents the proportion of the significant EOF pattern in the soil moisture pattern of each date. In consequence, we did not use single soil moisture patterns (which might be random) but the EOF patterns for the subsequent correlation analysis.

Measurements, taken at location x_i ($i = 1, \dots, p$) and at time t_j ($j=1, \dots, n$), are arranged into a matrix \mathbf{D} (n by p : n sampling times and p sampling locations), in a so called S-mode. Each row of the matrix represents the measurements at one point in time at all locations and each column represents a time series of measurements for a given location. To analyse the spatial variability of the data, a matrix \mathbf{F} is computed from the matrix \mathbf{D} by subtracting the average of each row of the data matrix \mathbf{D} (average soil moisture for a given observation time over all measurements locations). Analogously, to analyse the temporal variability, the average of each column

is subtracted from matrix \mathbf{D} (average soil moisture for a given location for all measurements conducted at that location). In the next step, the covariance matrix \mathbf{R} (p by p) of the data matrix \mathbf{F} is calculated:

$$\mathbf{R} = \frac{1}{N-1} \mathbf{F}^t \mathbf{F} \quad (1)$$

where the superscript t indicates a transposed matrix and N is the number of observations.

\mathbf{R} is diagonalized to find the eigenvectors and eigenvalues:

$$\mathbf{R}\mathbf{C} = \mathbf{C}\mathbf{\Lambda} \quad (2)$$

where $\mathbf{\Lambda}$ (p by p) is a diagonal matrix containing the eigenvalues λ_i of \mathbf{R} , and \mathbf{C} (p by p) contains the eigenvectors c_i of \mathbf{R} in the column vectors, corresponding to the eigenvalues λ_i . For more details on the procedure see Jolliffe (2002); Hannachi (2007) or Preisendorfer (1988).

This procedure rotates the original coordinate axes in a multidimensional space to align the data along a new set of orthogonal axes in the direction of the largest variance. Thus, the first axis or eigenvector is oriented in the direction that explains the largest variance. The subsequent axes are constrained to be orthogonal to the axes computed before and consecutively explain the largest part due to the remaining covariance. The eigenvectors c_i in the columns of the matrix \mathbf{C} are the EOFs. The EOFs represent patterns or standing oscillations that are invariant in time. To analyse how the EOFs evolve in time, the expansion coefficients (ECs) associated with each EOF are calculated by projecting the matrix \mathbf{F} onto the matrix \mathbf{C} :

$$\mathbf{A} = \mathbf{F}\mathbf{C} \quad (3)$$

where the matrix \mathbf{A} contains the expansion coefficients a_i in the column vectors.

The EOF analysis produces p (p =sampling locations) EOF/EC pairs, but only $\min(n, p)$ eigenvalues (n =sampling times) are greater than zero and only a subset (usually a much smaller set) of these positive eigenvalues are meaningful. In general, the EOFs and ECs are rearranged in descending order due to their eigenvalues, so that the first EOF (EOF1) is associated with the largest eigenvalue. The fraction of variance explained (EV) by each EOF can be found by dividing the associated λ_i by the sum of all eigenvalues (the trace of $\mathbf{\Lambda}$):

$$EV_i = \frac{\lambda_i}{\sum_{i=1}^p \lambda_i} \quad (4)$$

Following Björnsson and Venegas (1997) and Hannachi et al. (2007), the EOFs and the ECs can be determined very efficiently by singular value decomposition (SVD) without computing the covariance matrix and solving the eigenvalue problem. This decomposition by SVD provides a compact representation, because it drops unnecessary zero singular values (equivalent to zero eigenvalues).

4.2 Selection of significant EOFs

After decomposition, the EOFs and ECs can be used to reconstruct the full variability of the dataset by selecting all EOF/EC pairs. However, to approximate and compress a dataset, only the first few EOF and EC pairs that explain the largest fraction of variance are usually selected. This results in a reduction of dimensionality. By truncating the system, a “cleaner” version of the dataset is constructed, because random noise contained in the higher order EOFs is eliminated (Björnsson and Venegas, 1997; Preisendorfer, 1988). In practice, this truncation is often achieved by selecting a threshold for the overall explained variance (e.g. 80%) and choosing the set of leading EOFs that cumulatively explain at least this amount of variance. A prerequisite for the physical interpretation of single EOFs is that the EOFs are significantly different from each other. The linear combination of two EOFs, which are not significantly different and therefore degraded, may be based upon the same underlying physical processes. Thus, any linear combination of patterns based on degraded EOFs is as significant as each one of them (Hannachi et al., 2007).

To estimate the correct number of significant patterns (EOFs) for the subsequent physical interpretation, two selection rules are applied. One rule utilizes a measure of uncertainty for the eigenvalues and is summarized by the rule of thumb (North et al., 1982) defining the typical error (Δ) of eigenvalues:

$$\Delta(\lambda_i) \approx \lambda_i \sqrt{\frac{2}{s}} \quad (5)$$

where s is the number of independent samples (or the number of degrees of freedom).

The 95% confidence interval (CI_{95}) for each eigenvalue is then given by:

$$CI_{95}(\lambda_i) \approx \lambda_i \left(1 \pm \sqrt{\frac{2}{s}}\right) \quad (6)$$

The EOFs are considered to be significantly non degenerate if the 95% confidence intervals of the neighbouring eigenvalues do not overlap.

An additional rule is to use Monte Carlo simulations to estimate the uncertainties of the eigenvalues (Rule N; Preisendorfer, 1988). The eigenvalues of the measured data set have to be significantly higher than the eigenvalues of a random dataset. To test this, one thousand realisations of normally distributed surrogate data sets with a zero mean and a standard deviation of one in the dimension of the matrix of the original dataset (n by p) are calculated and analysed by the EOF analysis. From the results of these one thousand realisations, the upper 95% confidence interval of the eigenvalues is calculated and taken as the limit for the significance of the eigenvalues of the measured dataset. Another calculation with randomized measured values instead of normally distributed surrogate data resulted in the same number

of significant EOFs and is not additionally presented here. In this calculation, the positions of the elements of the real measurement data matrix were randomized along one dimension. For the spatial Monte Carlo-analysis, the positions of the elements in every row (all measurements on every single date), for the temporal Monte Carlo-analysis, the positions of the elements in every column (all measurements at every single point) were randomized.

Both selection rules were used in our data analysis to determine the number of significant EOF/EC pairs. Both require knowledge of the number of independent samples (s). In Eq. (6), the number of independent samples was used directly to estimate the errors of the eigenvalues and in the Monte Carlo analysis, the dimensions of the surrogate data matrix were changed from (n by p : n sampling times and p sampling locations) to (n by s) for the spatial and to (s by p) for the temporal analysis, resulting in a higher limit for the first few EOFs to be considered significant. This number of independent samples (or degrees of freedom) is calculated in Sect. 5.2.

4.3 Secondary parameters and correlation analysis

The aim of the EOF analysis is to identify stable spatial and temporal patterns in a set of surface soil moisture measurements. To identify the dominant drivers governing the surface soil moisture patterns, the EOFs were correlated with secondary parameters derived from topographical, soil, vegetation, land management and meteorological data. The EOFs may only be correlated with parameters that are invariant in time. The temporal development of biomass may explain, to some degree, the soil moisture patterns at a given day due to growth, cutting or grazing for instance, but it does not provide a temporally invariant signal and is therefore not suitable to explain the EOF patterns. Accordingly, it is only useful to correlate the EC time series with parameters which are invariant in space. This condition can be assumed to be valid for the parameter precipitation, because of the small size of our test sites.

The parameters used in our correlation analysis are associated with parameters determining vertical/local (e.g. field capacity, soil texture, SOC etc.) and horizontal/non-local (e.g. elevation, flow accumulation, curvature etc.) water flow. Elevation, multiple flow accumulation (e.g. specific drainage area), natural log of the multiple flow accumulation, slope, slope⁻¹, horizontal curvature, vertical curvature and Wetness Index are computed from a 10 m DEM (Sci Lands, 2008) with ArcGis 9.2 (ESRI, USA). Soil type data in the grassland test site was derived from the 1:5000 soil map (Geologischer Dienst, North-Rhine-Westphalia) and was particularly used to delineate an gleyic area (Stagnosol; impermeable soil layer). Field capacity in the arable test site was derived from the 1:50 000 soil map (Geologischer Dienst, North-Rhine-Westphalia). The percent of surface stone cover in the arable test site and the percent clay, silt, sand and SOC

in the grassland test site were measured. Topographic parameters such as Wetness Index, Flow Accumulation, Slope and Curvature were not computed for the arable test site, since in this predominantly flat area, the flow path is affected by features such as field boundaries and tillage tracks within the field rather than the slope given in the DEM.

5 Results

5.1 Analysis of field measurements

Both test sites show a large range of different soil moisture conditions (Figs. 2, 3), ranging from very dry conditions (22.2 Vol.-% in the grassland test site, and 19.5 Vol.-% in the arable test site) to very wet conditions (54.3 Vol.-%, 32.5 Vol.-%, respectively). The soil moisture over all measurements generally indicates higher average values (46.5 Vol.-%) for the grassland site as compared to the arable test site (26.6 Vol.-%) and a lower spatial variability (coefficient of variance (CV): 9.6% for grassland, 14.2% for arable land). The average standard deviation of the soil moisture over all days of measurement in the grassland test site was 4.5 Vol.-% (Min.: 3.2 Vol.-%, Max.: 5.8 Vol.-%) and in the arable test site, it was 3.8 Vol.-% (Min.: 2.3 Vol.-%, Max.: 6.3 Vol.-%). Due to the higher soil moisture status in the grassland test site, the range of the average soil moisture in the grassland test site (32.1 Vol.-%) exceeded the respective range in the arable test site (13.1 Vol.-%). These differences are due to the higher precipitation, the higher soil porosity and the higher amount of soil organic carbon content (SOC) in the topsoil of the grassland test site. Extremely high surface soil moisture values were particularly measured in field F2 in the grassland test site, which is located in the lowest part of the test site. Due to the dense root network of the grass cover, the amount of soil organic matter (SOM) in the topsoil is higher than 8 Vol.-%. Hence low bulk densities (0.57 to 0.83 g cm⁻³) prevail, with smallest values measured in the lower northern part of the test site with dominating gleyic soils. Due to the high organic content in this area, the maximum porosity reached values of up to 70% in the topsoil. In the arable test site, the maximum measured soil moisture reached 40%. The length of the whiskers in Fig. 2 indicates a large spatial variability of the surface soil moisture in the grassland test site. The average range of the soil moisture values measured in the grassland test site is 25.3 Vol.-% (Min.: 14.3 Vol.-%, Max.: 36.1 Vol.-%) and 18.4 Vol.-% (Min.: 9.1 Vol.-%, Max.: 25.9 Vol.-%) in the arable test site. The measurements of the 14 measurement campaigns in the grassland test site and the 17 in the arable test site accumulate to a total number of 17124 FDR-measurements. To avoid the imputation of missing values and to keep the results interpretable, the EOF analysis was computed with a continuous data set without missing data. Thus only 8 of the 14 measurement

days from the grassland test site and 10 of the 17 measuring days from the arable test site were used for the subsequent analysis.

5.2 Degrees of freedom

For the evaluation of spatial interdependencies between the measurement locations, a spatial autocorrelation analysis was performed, calculating Moran's I statistic (Moran, 1950) for a number of distance classes. This statistic calculates values between 1 (indicating perfect correlation) and -1 (perfect dispersion) between the different distant classes, a value of 0 indicates a completely random pattern. A number of 25 distance classes, each containing 183 data pairs for each day of measurement, were calculated for the grassland. For the arable test site, 30 classes were computed. Over all measurement campaigns, we determined an average autocorrelation length of 117 m for the grassland test site and 123 m for the arable test site. Hence, 16% (grassland) and 9% (arable land) of all distance pairs are assumed to be autocorrelated. The number of significant EOFs is sensitive to the number of independent samples (degrees of freedom). Thus, to account for the influence of spatial autocorrelation on the evaluation of significant EOFs, the number of sampling locations was reduced by these percentages of autocorrelated distance pairs, resulting in 81 and 107 independent spatial sampling locations for the grassland test site and the arable test site, respectively. For the temporal analysis, dates of each measurement campaign were considered to be independent, if the time span between two measurement dates added up to at least 20 days. This resulted in 6 and 8 degrees of freedom for the calculation of significance in the time domain.

5.3 EOF-Analysis

The analysis of the spatial patterns in the grassland test site yields a set of 8 EOF/EC pairs. EOFs calculated for analysing spatial patterns are referred to as spatial EOFs. Analogously, EOFs calculated to investigate temporal patterns are referred to as temporal EOFs. The spatial EOF1 of the grassland test site explains 57.5% of the spatial variance of the dataset, while EOF2 explains only 10.2% (Fig. 4a). The 95% confidence limit of the Monte Carlo simulation exceeds the explained variance of EOF2 to EOF8. Also, the 95% confidence interval of EOF1 does not overlap with the neighbouring EOFs. As a result, the first EOF is significant. The pattern of the spatial EOF1 (Fig. 5a) shows high positive values. This indicates higher than average soil moisture values in the northern part (fields F1, F2 and F3), which is in the valley section of the test site. Highest positive values can be found in field F2. Minimum values with negative signs are located in the central part of the test site (field F6). The EOF values increase slightly towards the southern part. The associated expansion coefficient (spatial EC1, Fig. 5b) shows a maximum value on 29 April 2008 and a minimum value on

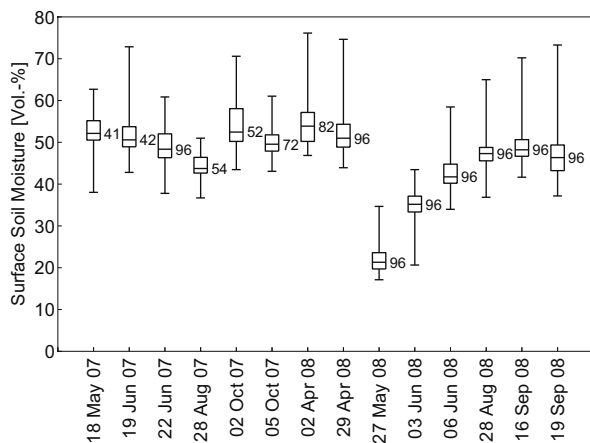


Fig. 2. Box-Whisker-Plot for the grassland site of all days of surface soil moisture measurements; the bottom and top of the box show the lower and upper quartiles, the band near the middle of the box is the median, the ends of the whiskers represent the measured minimum and maximum surface soil moisture; the number to the right of each box indicates the number of sampling locations for each date; data sets without gaps ($n=96$) were used for the EOF analysis.

3 June 2008. This maximum EC1 values coincides with the high average soil moisture values on these measuring dates, while the low EC values indicate dry conditions.

The analysis of the spatial patterns in the arable test site yields a set of 10 EOF/EC pairs. The spatial EOF1 explains 38.4% and EOF2 28.3% of the spatial variability of the dataset (Fig. 6a). Only these first two EOFs satisfy the significance requirements, because the 95% confidence intervals of their eigenvalues neither overlap with neighbouring confidence intervals nor are their eigenvalues within the 95% confidence interval of the eigenvalues of the Monte Carlo simulation. All eigenvalues and confidence limits can be converted into EV -values (see Figs. 4a, b, and 6a, b) according to Eq. (4). The spatial EOF1 (Fig. 7a) shows the lowest negative values in the eastern part of the test site and an irregular and patchy pattern with higher values in the rest of the test site. The EOF2 (Fig. 7b) shows a two peaked distribution with high positive values on some fields contrasted by low negative values on other fields with an abrupt change of the EOF values typically at the field boundaries. The values of the EC1 (Fig. 7c), which express the weight of the EOF1 on the different dates, are positive on all dates and reach a maximum value on 27 July 2007 and a minimum value on 24 April 2008. The values of the EC2 (Fig. 7d) show a minimum value with a negative sign on 19 September 2008 and a maximum and positive value on 27 July 2007. Thus, the influence of the EOF1 varies only gradually during the dates of measurements, while the EOF2 reverses its influence in an annual cycle.

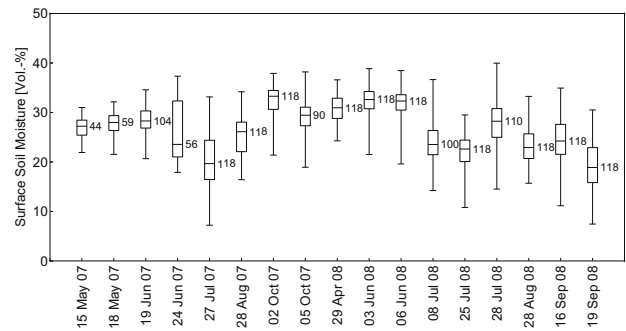


Fig. 3. Box-Whisker-Plot for the arable test site of all dates of measurements; the bottom and top of the box show the lower and upper quartiles, the band near the middle of the box is the median, the ends of the whiskers represent the measured minimum and maximum surface soil moisture; the number to the right of each box indicates the number of sampling locations for each date; data sets without gaps ($n=118$) were used for the EOF analysis.

Both analyses, for the grassland and the arable test site, resulted in only one significant temporal EOF/EC pair (Figs. 4b and 6b). The temporal EOF1 of the grassland test site explains 92% of the temporal variance and all values are positive. It shows a pattern similar to the spatial EOF1. Smaller and negative values occur in the northern part of the test site. However, the pattern is more irregular and patchy (Fig. 8a) as compared to the spatial EOF. The temporal EC1 has a maximum value on 27 May 2008 and a minimum value on 29 April 2008 (Fig. 8b). The temporal EOF1 of the arable test site explains about 72.5% of the temporal anomalies of the data set (Fig. 6b) and has all positive values with maximum values in field F3 in the eastern part of the test site (Fig. 9a). The associated EC1 has the highest positive value on 2 October 2007 and the lowest negative value on 10 September 2008 (Fig. 9b).

The interpretation of the results from spatial and temporal EOF analyses requires the consideration of the sign of the EOF values and the sign of the associated EC values, because the soil moisture variability explained by this EOF/EC pair (anomalies) is computed by multiplying EOF and EC.

5.4 Correlation analysis

The spatial patterns computed from the EOF analysis were correlated with different parameters for the grassland (Table 1) and the arable test sites (Table 2). These parameters were derived from topography, soil, vegetation and land management data and allow relating the patterns found in the EOF analysis to the driving processes. Only significant correlations of the EOF patterns with the parameters are presented here. The spatial patterns determined for the grassland test site show the highest Pearson correlation coefficient with elevation and the soil property gleyic/non gleyic. By distinguishing between gleyic and non gleyic soils, an ordinal scale

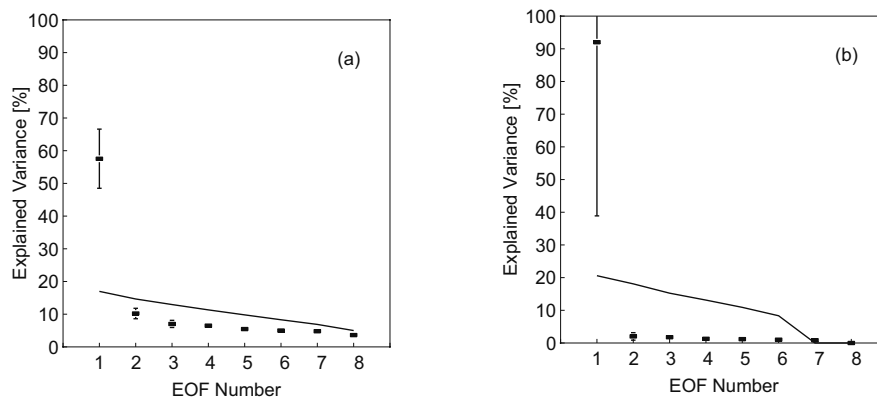


Fig. 4. Variance spectrum of the spatial (a) and temporal (b) analysis in the grassland test site. Error bars indicate the 95% confidence interval according to Eq. (6); the solid line represents the significance limit calculated by Monte Carlo simulation.

was defined for use in the correlation analysis. The highest correlation for the temporal pattern was with SOC, percentage of sand in the topsoil (0–10 cm) and soil type. In the arable test site, the first spatial pattern was highly correlated with elevation and soil parameters, particularly the percentage of stone cover and field capacity (Table 2). The correlations of the parameters with the temporal EOF1 pattern were smaller but also highly significant. The second spatial pattern (EOF2) cannot be correlated with any of the tested parameters. The temporal course of the EC1 values of the spatial analysis in both test sites shows a high correlation coefficient with the average soil moisture ($r=0.73$ for grassland, $r=-0.71$ for arable land). The temporal course of the EC1 patterns for the temporal analysis shows a perfect correlation to the mean soil moisture for both test sites (Table 3). The different signs of the Pearson correlation coefficients are due to the different signs of the EOF values. Several parameters used to explain the EOFs are correlated (e.g. field capacity, % sand, % silt and % clay) and point to the same hydrological process.

6 Discussion

6.1 Spatial analysis

The analysis performed on the spatial variability in the grassland test site shows that the main soil moisture pattern (spatial EOF1) is strongly related to soil properties and explains about 57.5% of the spatial soil moisture variation. The highly significant correlations with the soil property gleyic / non gleyic ($r=0.7$), soil texture (e.g. % sand 0–10 cm: $r=-0.42$), and SOC ($r=0.47$ for 0–10 cm and $r=0.37$ for 10–30 cm) indicate a clear link to infiltration (locally controlled vertical process). The impermeable Stagnosol layer resulted in a higher amount of organic matter and also in a very high porosity in the topsoil at these points. The pattern is also linked to catchment topography. The correlations to pa-

Table 1. Pearson correlation coefficients between EOFs and topographic and soil parameters for the grassland test site; Curvature H/V, % Clay 0–10 cm, 10–30 cm and % SOC 30–60 cm were additionally tested but not significant; *EV* is the variance explained by the EOF.

Grassland	spatial EOF1 (57.5% EV)	temporal EOF1 (92% EV)
Elevation [m]	−0.57(**)	0.27(**)
Flow Accumulation	0.32(**)	−0.24(*)
ln (Flow Accumulation)	0.45(**)	−0.23(*)
Slope [°]	0.46(**)	not significant
1/Slope [°]	−0.32(**)	not significant
Wetness Index	0.34(**)	not significant
Soil Parameter gleyic/ non gleyic	0.70(**)	−0.34(**)
Sand [%]		
0–10 cm	−0.42(**)	0.33(**)
10–30 cm	−0.4(**)	0.27(**)
30–60 cm	−0.4(**)	0.26(*)
Silt [%]		
0–10 cm	0.41(**)	−0.30(**)
10–30 cm	0.35(**)	−0.22(*)
30–60 cm	0.41(**)	−0.24(*)
Clay [%]		
30–60 cm	not significant	0.21(*)
SOC [%]		
0–10 cm	0.47(**)	−0.44(**)
10–30 cm	0.37(**)	−0.25(*)

* Correlation is significant at the 0.05 level (2-tailed test).

** Correlation is significant at the 0.01 level (2-tailed test).

rameters such as elevation ($r=-0.57$), natural logarithm of flow accumulation ($r=0.45$), slope ($r=0.46$) and Wetness Index ($r=0.34$) indicate that the spatial pattern is related to landscape position, which is affected by two processes: the

Table 2. Pearson correlation coefficients between EOFs and topographic and soil parameters for the arable test site; *EV* is the variance explained by the EOF.

Arable land	spatial EOF1 (38.4% <i>EV</i>)	spatial EOF2 (28.2% <i>EV</i>)	temporal EOF1 (72% <i>EV</i>)
Elevation [m]	−0.73(**)	not significant	0.47(**)
Surface stone cover [%]	−0.79(**)	not significant	0.48(**)
Field capacity [%]	0.75(**)	not significant	−0.41(**)

** Correlation is significant at the 0.01 level (2-tailed test)

position within the landscape determines (i) the redistribution of water through surface runoff and subsurface drainage and (ii) the amount of solar radiation received at this position, which affects the amount of evapotranspiration.

Perry and Niemann (2007) applied an EOF analysis to the widely studied soil moisture dataset of 459 locations at 13 campaigns from the 10.5 ha Tarrawarra grassland catchment (Western and Grayson, 1998; Western et al., 1998, 2001, 1999a, b). The first EOF in their study explained 55% of the spatial variability of soil moisture. Similar to our results, a clear dependence on hillslope and valley topography was determined which was most prominent during wet periods. Our EOF analysis yielded one significant spatial EOF explaining 57.5% of the variance. Due to the smaller size of our dataset, the spatial EOF2 (10% explained variance) is statistically degenerated, whereas the second EOF in the study done by Perry and Niemann (2007) explained 9% of the spatial variability and could be related to the exposition (or PSRI; Potential Solar Radiation Index). Yoo and Kim (2004) investigated the characteristics of spatial and temporal variability of soil moisture and the relative roles of various affecting factors with the data of the SGP97 Little Washita field site (Famiglietti et al., 1999). Their first EOF accounted for more than 70% of the variability for interstorm periods and more than 60% for the whole dataset. The most important factors are topography related to a decreasing role after rainfall stops and an increasing role of soil- and land-use-related factors. Jawson and Niemann (2007) decomposed remotely sensed soil moisture data from the SGP97 field campaign with an EOF analysis and found a single pattern explaining 61% of the observed spatial variability. The physical characteristic most related to the EOF pattern seemed to be soil texture (percent sand and percent clay). In contrast to the findings of Yoo and Kim (2004), topographic characteristics were relatively unimportant and even less relevant for dry conditions. Jawson and Niemann (2007) attributed this to the fact that topographic characteristics may influence soil moisture patterns mainly through lateral flow. However, lateral flow was not observed at the scale of this study.

In summary it can be stated that our findings are in agreement with the previously mentioned studies that about 55% to 70% of surface soil moisture variability can be explained

Table 3. Pearson correlation coefficients between ECs and the soil moisture average from each measuring campaign.

	Soil Moisture Average [%]
Grassland spatial EC1	0.73(**)
Grassland temporal EC1	−1.00(**)
Arable land spatial EC1	−0.71(**)
Arable land spatial EC2	not significant
Arable land temporal EC1	1.00(**)

**Correlation is significant at the 0.01 level (2-tailed test).

by stable patterns and is correlated to soil parameters and topography. On the other hand, our result for the grassland test site indicates that 42.5% of the spatial variability changes in time and can therefore not be explained by a stable spatial pattern. This portion of the overall variance is mainly due to differences in management (grazing, cutting and fertilizing) of the different fields. Also random noise due to measurement errors contributed to the unexplained variance. In the EOF analysis of spatial patterns, the impact of temporally variable factors, which do not affect the whole area uniformly, results in noise, decreases the amount of the variance explained by the significant EOFs or decreases the number of significant EOFs. In addition, a difficulty in interpreting the results for the grassland test site is the not exactly known location and functionality of old drainage pipes in field F6. While the low values of field F6 might indicate that the drainage tiles are still functioning, a clear relationship with this effect cannot be established. The existence of functioning drainage tiles should yield a stable spatial pattern.

The spatial EC1 is positively correlated with the average soil moisture of the measuring days, meaning that EOF1 reflects more the structure of soil moisture during wet days than during dry days. As expected, during wet periods, lateral redistribution of water over longer distances is possible and the effect of the impermeable soil layer of the soil type (Stagnosol) on surface soil moisture is more pronounced. This leads, in combination with the higher amount of organic

matter and higher porosity in the topsoil of the Stagnosol area of the test site, to very high topsoil moisture values (up to 75 Vol.-%). The impact of the Stagnosols decreases as the soil dries with increasing evapotranspiration. Prior findings of Perry and Niemann (2007), indicating a pronounced decrease of the weight of the spatial EOF1 pattern on very dry and very wet conditions, cannot be confirmed by our dataset. Potential causes of this discrepancy might be stronger seasonality in the Tarrawarra catchment and the lack of dry conditions during the measurements in our grassland test site. Also, the first EOF in the Tarrawarra test site is primarily related to landscape position and the associated lateral redistribution of water and subordinately to evapotranspiration, while our first EOF is rather related to soil properties than landscape position.

Most of the previous studies at a comparable spatial scale to our study focussed on test sites with little management impacts. Our study also investigated spatial anomalies in an arable test site. Our results show, that the first spatial EOF in the arable test site is still related to soil properties, namely surface stone cover ($r=-0.79$) and field capacity ($r=0.75$) and explains 38.4% of the variance. However, the second EOF indicates effects originating from different seasonality in tillage operations of the different fields. The spatial patterns of the first EOF can be explained from the effects of an old river terrace which crops out in the eastern part of the test site approximately at an elevation of 107 m (see Fig. 1) and causes a high amount of coarse alluvial deposits in the adjacent fields (F1/3/4), especially on field F3. Both parameters, stone cover and field capacity, point at the importance of spatial differences of soil properties in relation to soil moisture dynamics. The highly significant correlation with elevation ($r=-0.73$) must be seen as an artefact from the cross correlation of the presence of outcrop of the old river terrace and its position in the elevation gradient. The correlation between the spatial EC1 and the average soil moisture ($r=0.71$) shows that the influence of the EOF1 pattern associated with soil properties is more pronounced on dry dates. Due to the lower porosity in the eastern part of the test site, soil moisture decreases more rapidly after precipitation.

The spatial EOF2 shows no significant correlation with any of the tested parameters. However, the variation of the spatial EOF2 values is quite small within the individual fields (coefficient of variation (CV) between -5.2 and 0.6%) while it is pronounced between different fields (CV: -43.5%), which indicates that the EOF2 pattern is dominated by a different seasonality in tillage operations in different fields. The importance of tillage operations on soil moisture can be shown for soil moisture dates with similar patterns to the spatial EOF2 values (27 July 2007 between the adjacent fields F5 and F6; 19 September 2008 between the adjacent fields F1 and F2). On both dates, the wetter field of the two was harvested while the drier field was also ploughed the week before the measurements. Because of the higher porosity after ploughing, soil moisture decreased in-

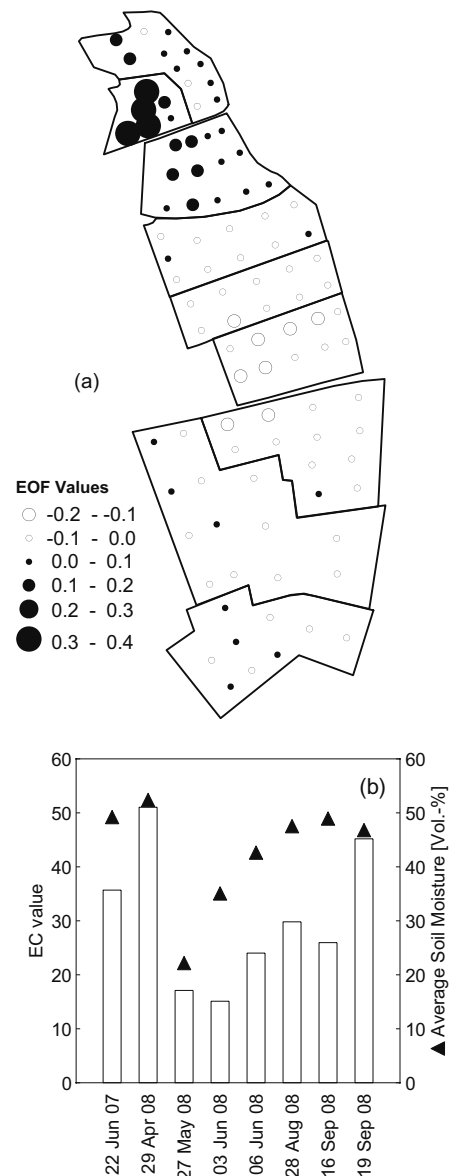


Fig. 5. EOF1 (a) and EC1 (b) patterns of the spatial analysis in the grassland test site; the triangles in (b) represent the average soil moisture on the different days.

ducing a steep gradient at the field boundaries. The highest positive and negative values of the spatial EC2 can be found on days with low average soil moisture, when some field were ploughed just before the measurements (27 July 2007, 16 September 2008 and 19 September 2008). Due to multiple vegetation periods being covered in our multi-annual dataset, there is no spatial stability with regards to land management effects. This is reflected in the negative and positive values of the spatial EC2 in our measurements, indicating a reversing management pattern. Thus, we can identify the influence of the land management by tillage (i.e. the increase of pore volume after ploughing and differences in evaporation)

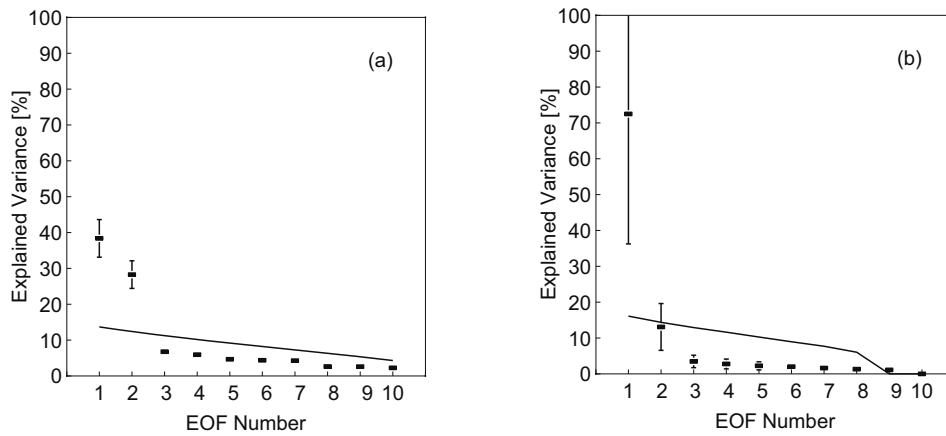


Fig. 6. Variance spectrum of the spatial (a) and temporal (b) analysis in the arable test site. Error bars indicate the 95% confidence interval according to Eq. (6); the solid line represents the significance limit calculated by Monte Carlo simulation.

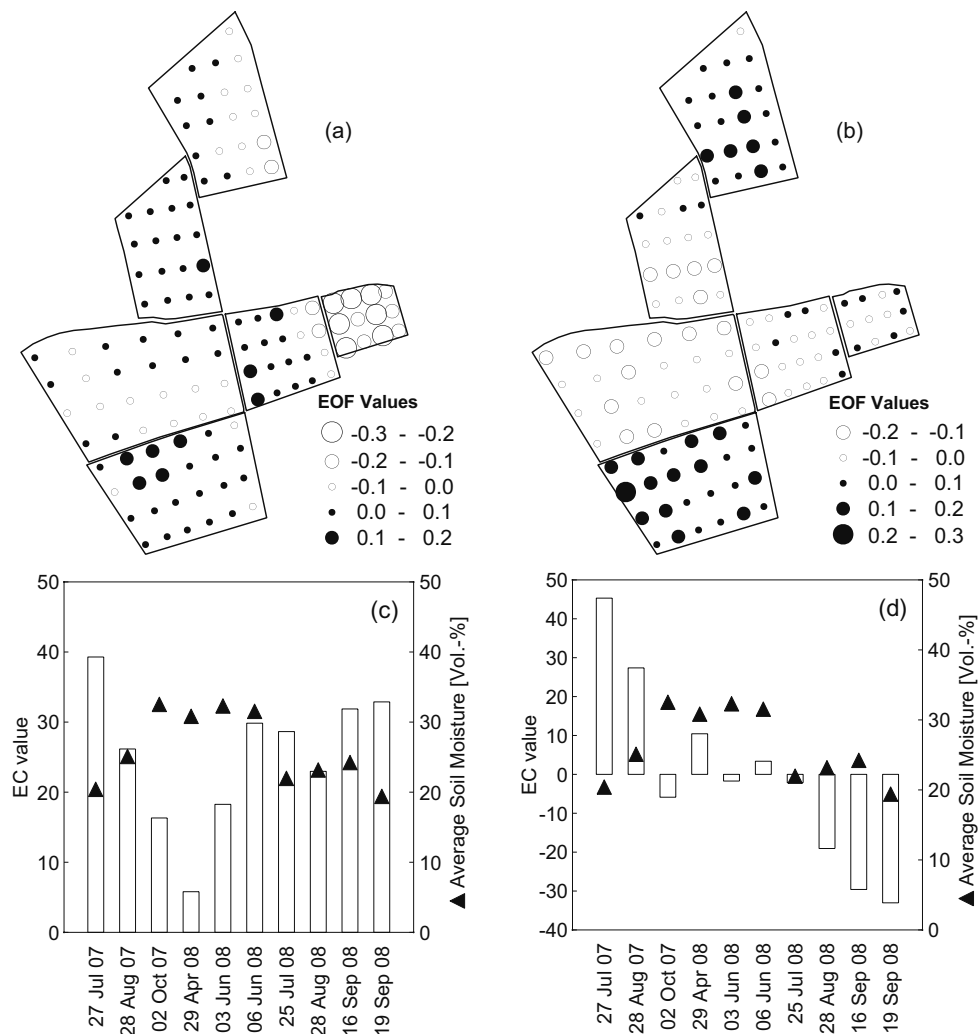


Fig. 7. EOF1 (a), EOF2 (b), EC1 (c) and EC2 (d) patterns of the spatial analysis in the arable test site; the triangles in (c) and (d) represent the average soil moisture on the different days.

and different crop rotation or vegetation heights, resulting in differences of transpiration. These results from the spatial analysis show that it is possible to apply EOF analyses on managed agricultural fields or regions. The structure of our dataset with alternating management patterns in the two consecutive years of measurements allows to detect not only the stable pattern (connected with soil parameters), but also the non stable pattern of different land management options on the different fields.

6.2 Temporal analysis

The temporal analysis identifies locations with large temporal variability. These locations are identified by high absolute numbers in Fig. 8a. Both temporal EC1s have a perfect correlation with the average soil moisture on the days of the measurements, substantiating the control of these patterns by wet and dry periods. The existence of only one dominant mode of temporal variability in each test site, with all negative EOF1 values in the grassland test site and all positive EOF1 values in the arable test site, indicates a consistent reaction of the soil moisture values on dry and wet periods in the same direction on each test site. Both test sites are small enough to assume homogeneous precipitation across the fields over the time of measurements. The comparatively high value of explained variance (13.1%) of the temporal EOF2 in the arable test site might indicate the influence of land management. The temporal EOF1 in the grassland test site explains 92% of the temporal variance. This is related to soil properties (e.g. % SOC: $r=-0.44$; Soil Type: $r=-0.34$; % Sand: $r=0.33$) and catchment topography (e.g. Elevation: $r=0.27$). Therefore, the highest soil moisture variability during dry and wet periods in the grassland test site is located in its low-lying parts. Here also high SOC contents in the topsoil can be found. These high topsoil SOC contents are associated with areas where higher soil moisture content prevails over longer time periods resulting from and indicated by the Stagnosols. In the arable test site, the points with the highest temporal EOF1 values are correlated with surface stone cover ($r=0.48$) and field capacity ($r=-0.41$), implying that soil moisture varies more on locations with low porosity. At these locations higher thermal conductivity and lower water holding capacity, caused by higher content of the coarse fraction in the soil, lead to a higher temporal variance of soil moisture.

7 Conclusions

Empirical Orthogonal Function analysis was used to detect the stable spatial and temporal patterns of surface soil moisture. A subsequent correlation analysis was used to identify the dominant parameters and underlying processes controlling the stable (significant) spatial and temporal patterns of surface soil moisture under different soil moisture states. In

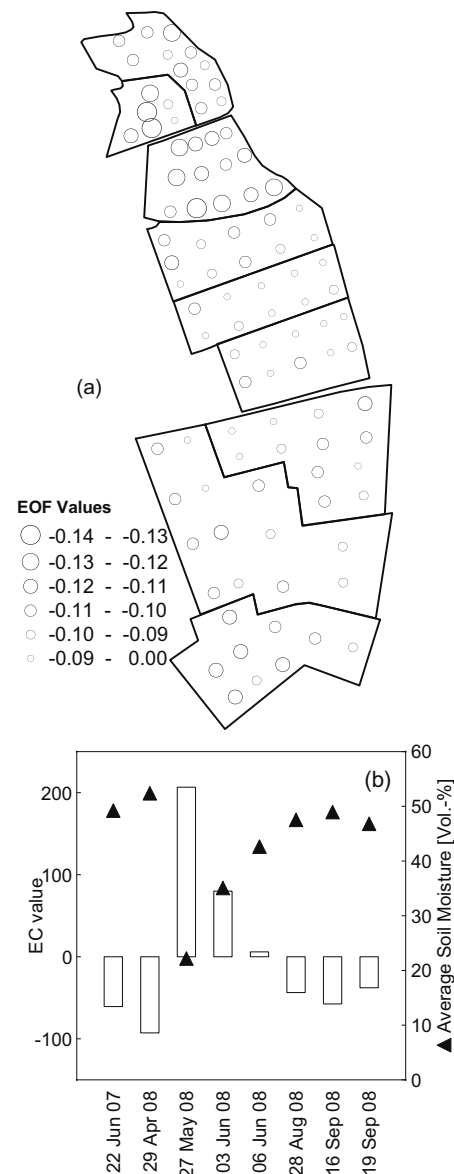


Fig. 8. EOF1 (a) and EC1 (b) patterns of the temporal analysis in the grassland test site; the triangles in (b) represent the average soil moisture on the different days.

the grassland test site (Rollesbroich), one significant spatial pattern, explaining 57.5% of the spatial soil moisture variability, was determined. This pattern is related to soil properties (soil type) and topography. Its dominance is largest during or shortly after wet periods, because under wet conditions, the lateral redistribution of water and the varying infiltration by different soil types becomes more important. Another significant spatial pattern accounting for the differences in land management (grazing, cutting, fertilizing) could not be identified for the grassland site. The highest soil moisture variability was in the lower parts of the test site at locations with a high percentage of SOC and influenced by the soil

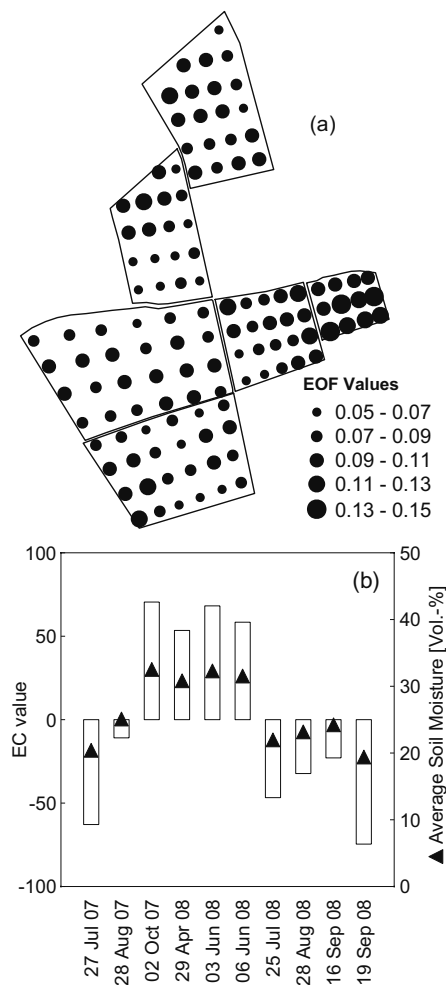


Fig. 9. EOF1 (a) and EC1 (b) patterns of the temporal analysis in the arable test site; the triangles in (b) represent the average soil moisture on the different days.

type in that area. In the arable test site (Selhausen), two significant patterns controlling the major part of the spatial variability were determined. The first pattern (spatial EOF1), accounting for 38.4% of the variance, is strongly related to soil properties (surface stone cover and field capacity). The impact of this pattern is more pronounced during dry periods, indicating a compensating effect of precipitation. The second pattern (spatial EOF2) explains 28.3% of the variance and can be assigned to different land management patterns, influencing soil properties and increased evaporation due to tillage as well as transpiration, due to different crops and different dates of sowing and fertilization. More than 66% of the spatial variability of surface soil moisture in the arable test site can be explained by these two patterns associated with soil properties and land management. The highest temporal variability of soil moisture during the dry and wet periods can be found on locations with low porosity. The struc-

ture of our dataset with alternating management patterns in the arable test site in two consecutive years of measurements allows detecting not only the stable pattern (connected with soil parameters), but also the non stable pattern of different land management options on different fields.

In general, a combination of EOF and correlation analysis provides an objective method to identify the dominant parameters controlling spatio-temporal patterns of surface soil moisture, without being affected by single random processes. This is even possible in intensively managed agricultural areas. Moreover, this combination has the capability to quantify the proportion of influence of different parameters on soil moisture patterns under different soil moisture states.

Acknowledgements. We gratefully acknowledge financial support by the SFB/TR 32 “Pattern in Soil-Vegetation-Atmosphere Systems: Monitoring, Modelling, and Data Assimilation” funded by the Deutsche Forschungsgemeinschaft (DFG). We thank L. Bornemann from the Institute of Crop Science and Resource Conservation in Bonn for the soil analysis using mid-infrared-spectroscopy. Special thanks also go to our students for helping with the field measurements and to the farmers in Selhausen and Rollesbroich for granting access to their fields. The authors thank the editor and the four anonymous referees for their helpful comments.

Edited by: N. Verhoest

References

- Beven, K. J. and Kirkby, M. J.: A physically based, variable contributing area model of basin hydrology, *Hydrological Sciences Bulletin*, 24, 43–69, 1979.
- Björnsson, H. and Venegas, S. A.: A manual for EOF and SVD analyses of climate data, McGill University, Montreal, 52 pp., 1997.
- Bornemann, L., Welp, G., Brodowski, S., Rodionov, A., and Amelung, W.: Rapid assessment of black carbon in soil organic matter using mid-infrared spectroscopy, *Org. Geochem.*, 39, 1537–1544, 2008.
- Burt, T. P. and Butcher, D. P.: Topographic Controls of Soil-Moisture Distributions, *J. Soil. Sci.*, 36, 469–486, 1985.
- Famiglietti, J. S., Devereaux, J. A., Laymon, C. A., Tsegaye, T., Houser, P. R., Jackson, T. J., Graham, S. T., Rodell, M., and van Oevelen, P. J.: Ground-based investigation of soil moisture variability within remote sensing footprints during the Southern Great Plains 1997 (SGP97) Hydrology Experiment, *Water Resour. Res.*, 35, 1839–1851, 1999.
- Grayson, R. B., Western, A. W., Chiew, F. H. S., and Blöschl, G.: Preferred states in spatial soil moisture patterns: Local and non-local controls, *Water Resour. Res.*, 33, 2897–2908, 1997.
- Green, T. R. and Erskine, R. H.: Measurement, scaling, and topographic analyses of spatial crop yield and soil water content, *Hydrol. Process.*, 18, 1447–1465, 2004.
- Hannachi, A., Jolliffe, I. T., and Stephenson, D. B.: Empirical orthogonal functions and related techniques in atmospheric science: A review, *Int. J. Climatol.*, 27, 1119–1152, 2007.

- Hawley, M. E., Jackson, T. J., and McCuen, R. H.: Surface Soil-Moisture Variation on Small Agricultural Watersheds, *J. Hydrol.*, 62, 179–200, 1983.
- Herbst, M. and Diekkrüger, B.: Modelling the spatial variability of soil moisture in a micro-scale catchment and comparison with field data using geostatistics, *Phys. Chem. Earth*, 28, 239–245, 10.1016/s1474-7065(03)00033-0, 2003.
- Herbst, M., Diekkrüger, B., and Vanderborght, J.: Numerical experiments on the sensitivity of runoff generation to the spatial variation of soil hydraulic properties, *J. Hydrol.*, 326, 43–58, 2006.
- Jawson, S. D., and Niemann, J. D.: Spatial patterns from EOF analysis of soil moisture at a large scale and their dependence on soil, land-use, and topographic properties, *Adv. Water Resour.*, 30, 366–381, 2007.
- Jaynes, D. B., Kaspar, T. C., Colvin, T. S., and James, D. E.: Cluster analysis of spatiotemporal corn yield patterns in an Iowa field, *Agron. J.*, 95, 574–586, 2003.
- Jolliffe, I. T.: *Principal Component Analysis*, 2nd edn., Springer, New York, USA, 487 pp., 2002.
- Kim, G. and Barros, A. P.: Space-time characterization of soil moisture from passive microwave remotely sensed imagery and ancillary data, *Remote Sens. Environ.*, 81, 393–403, 2002.
- Kitanidis, P. K. and Bras, R. L.: Real-Time Forecasting with A Conceptual Hydrologic Model. I. Analysis of Uncertainty, *Water Resour. Res.*, 16, 1025–1033, 1980.
- Koyama, C. N., Korres, W., Fiener, P., and Schneider, K.: Variability of Surface Soil Moisture Observed from Multi-temporal C-band SAR and Field Data, *Vadose Zone J.*, V09–0165, in press, 2010.
- Lorenz, E. N.: *Empirical Orthogonal Functions and Statistical Weather Prediction*, Department of Meteorology, MIT, 49, 1956.
- Moore, I. D., Burch, G. J., and Mackenzie, D. H.: Topographic Effects on the Distribution of Surface Soil-Water and the Location of Ephemeral Gullies, *T. Asae*, 31, 1098–1107, 1988.
- Moran, P. A. P.: Notes on continuous stochastic phenomena, *Biometrika*, 37, 17–23, 1950.
- North, G. R., Bell, T. L., Cahalan, R. F., and Moeng, F. J.: Sampling Errors in the Estimation of Empirical Orthogonal Functions, *Mon. Weather Rev.*, 110, 699–706, 1982.
- Ntelekos, A. A., Georgakakos, K. P., and Krajewski, W. F.: On the uncertainties of flash flood guidance: Toward probabilistic forecasting of flash floods, *J. Hydrometeorol.*, 7, 896–915, 2006.
- Oppelt, N. M., Schneider, K., and Mauser, W.: Mesoscale soil moisture patterns derived from ERS data, *Proc. SPIE*, 3499, 41–51, doi:10.1117/12.332775, 1998.
- Owe, M. and Van de Griend, A. A.: Comparison of Soil Moisture Penetration Depths for Several Bare Soils at Two Microwave Frequencies and Implications for Remote Sensing, *Water Resour. Res.*, 34(9), 2319–2327, doi:10.1029/98wr01469, 1998.
- Perry, M. A. and Niemann, J. D.: Analysis and estimation of soil moisture at the catchment scale using EOFs, *J. Hydrol.*, 334, 388–404, 2007.
- Preisendorfer, R. W.: *Principal Component Analysis in Meteorology and Oceanography*, Developments in Atmospheric Science, Elsevier, Amsterdam, 425 pp., 1988.
- Schneider, K.: Assimilating remote sensing data into a land-surface process model, *Int. J. Remote Sens.*, 24, 2959–2980, 2003.
- Vachaud, G., Desilans, A. P., Balabanis, P., and Vauclin, M.: Temporal Stability of Spatially Measured Soil-Water Probability Density-Function, *Soil Sci. Soc. Am. J.*, 49, 822–828, 1985.
- Vereecken, H., Kamai, T., Harter, T., Kasteel, R., Hopmans, J., and Vanderborght, J.: Explaining soil moisture variability as a function of mean soil moisture: A stochastic unsaturated flow perspective, *Geophys. Res. Lett.*, 34, L22402, doi:10.1029/2007gl031813, 2007.
- Western, A. W. and Grayson, R. B.: The Tarrawarra data set: Soil moisture patterns, soil characteristics, and hydrological flux measurements, *Water Resour. Res.*, 34, 2765–2768, 1998.
- Western, A. W., Blöschl, G., and Grayson, R. B.: Geostatistical characterisation of soil moisture patterns in the Tarrawarra catchment, *J. Hydrol.*, 205, 20–37, 1998.
- Western, A. W., Grayson, R. B., and Green, T. R.: The Tarrawarra project: high resolution spatial measurement, modelling and analysis of soil moisture and hydrological response, *Hydrol. Process.*, 13, 633–652, 1999a.
- Western, A. W., Grayson, R. B., Blöschl, G., Willgoose, G. R., and McMahon, T. A.: Observed spatial organization of soil moisture and its relation to terrain indices, *Water Resour. Res.*, 35, 797–810, 1999b.
- Western, A. W., Blöschl, G., and Grayson, R. B.: Toward capturing hydrologically significant connectivity in spatial patterns, *Water Resour. Res.*, 37, 83–97, 2001.
- Western, A. W., Zhou, S. L., Grayson, R. B., McMahon, T. A., Blöschl, G., and Wilson, D. J.: Spatial correlation of soil moisture in small catchments and its relationship to dominant spatial hydrological processes, *J. Hydrol.*, 286, 113–134, 2004.
- Yoo, C. and Kim, S.: EOF analysis of surface soil moisture field variability, *Adv. Water Resour.*, 27, 831–842, 2004.
- Zaslavsky, D. and Sinai, G.: *Surface Hydrology 1, Explanation of Phenomena*, *J. Hydr. Eng. Div.-ASCE*, 107, 1–16, 1981.

4. Analysis of surface soil moisture patterns based on radar remote sensing

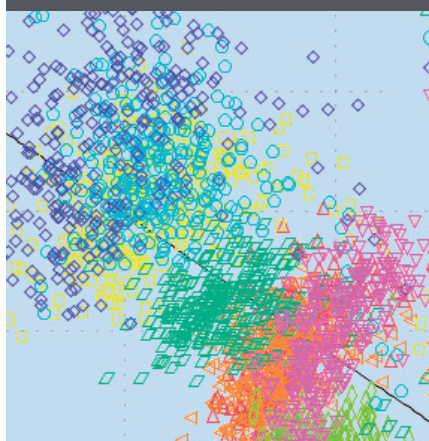
Journal article (published):

Koyama, C.N., Korres, W., Fiener, P., Schneider, K., 2010. Variability of Surface Soil Moisture Observed from Multitemporal C-Band Synthetic Aperture Radar and Field Data. *Vadose Zone Journal*, 9(4): 1014-1024.

Permission to reprint:

The permission to reprint of the above-named article within this dissertation thesis was granted by Lisa Al-Amoodi, managing editor of the *Vadose Zone Journal*, on 29.10.2012 via email. Original page numbers are used.

Christian N. Koyama
Wolfgang Korres
Peter Fiener
Karl Schneider*



The relationship between the spatial variability of surface soil moisture and the mean surface moisture content is investigated at different scales (field to catchment scale) using in situ measurements and synthetic aperture radar retrievals. We show that the spatial variability strongly depends on scale as well as on soil moisture status.

Dep. of Geography, Univ. of Cologne, Albertus-Magnus-Platz, 50923 Cologne, Germany.
*Corresponding author (karl.schneider@uni-koeln.de).

Vadose Zone J. 9:1014–1024
doi:10.2136/vzj2009.0165
Received 18 Nov. 2009.
Published online 7 Sept. 2010.

© Soil Science Society of America
5585 Guilford Rd. Madison, WI 53711 USA.
All rights reserved. No part of this periodical may be reproduced or transmitted in any form or by any means, electronic or mechanical, including photocopying, recording, or any information storage and retrieval system, without permission in writing from the publisher.

Variability of Surface Soil Moisture Observed from Multitemporal C-Band Synthetic Aperture Radar and Field Data

The study aimed to analyze the spatial variability of surface soil moisture at different spatial scales based on field measurements and remote sensing estimates. Multitemporal Envisat satellite Advanced Synthetic Aperture Radar (ASAR) data were used to derive the surface soil moisture utilizing an empirical C-band retrieval algorithm. Eight wide-swath (WS) images with a spatial resolution of 150 m acquired between February and October 2008 were used to determine the surface soil moisture contents. The accuracy of the surface soil moisture retrievals was evaluated by comparison with in situ measurements. This comparison yielded a root mean square error of 5% (v/v). Based on our in situ measurements as well as remote sensing results, the relationship of the coefficient of variation of the spatial soil moisture patterns and the mean soil moisture was analyzed at different spatial scales ranging from the catchment scale to the field scale. Our results show that the coefficient of variation decreases at all scales with increasing soil moisture. The gain of this relationship decreases with scale, however, indicating that at a given soil moisture state, the spatial variation at the large scale of whole catchments is larger than at the field scale. Knowledge of the spatial variability of the surface soil moisture is important to better understand energy exchange processes and water fluxes at the land surface as well as their scaling properties.

Abbreviations: ASAR, Advanced Synthetic Aperture Radar; SAR, synthetic aperture radar; WS, wide swath.

Soil moisture and its distribution in space and time plays a critical role in the surface energy balance at the soil–atmosphere interface; it is a key variable influencing the partitioning of solar energy into latent and sensible heat flux as well as the partitioning of precipitation into runoff and percolation. In situ measurements of soil moisture are time and cost intensive. Due to their large spatial variability, estimation of spatial patterns of soil moisture from field measurements is rather difficult and not feasible for large-scale analyses. Although hydrologic models have shown their capability to derive spatial soil moisture patterns, their application is a challenging task, requiring a multitude of input data (such as soil properties, i.e., hydraulic characteristics and permeability, along with meteorologic and climatologic data). Neither the full spatial variability of these environmental parameters nor the full details of the processes are typically known, thus modeled spatial patterns tend to reduce spatial variability. Therefore, as well as due to the need for independent validation, direct and repeatable soil moisture measurements covering large spatial scales obtained from remote sensing instruments is becoming increasingly necessary and now, with the advent of new sensor generations, feasible.

The sensitivity of the radar backscattering coefficient (σ^0) to soil moisture at low microwave frequencies is well described in the literature (Boisvert et al., 1997; Loew et al., 2003; Quesney et al., 2000). Numerous research activities performed within the last three decades have demonstrated that sensors operating in the low-frequency portion of the microwave electromagnetic spectrum (especially the P and L bands) are suitable for measuring the surface moisture content. The penetration depth of the radar beam depends on soil characteristics and moisture state. It is typically in the order of some tenths of the wavelength up to half a wavelength. While the combination of different frequencies, polarizations, and incidence angles provide best results (e.g., Dubois et al., 1995; Wang et al., 1997; Romshoo et al., 2000), these data are today only available from airborne sensors. The P band is not available from current satellite sensors and full polarimetric space-borne L-band data are available only from PALSAR aboard the Advanced Land Observing Satellite (ALOS). Space-borne systems do not offer the repetition rate, spatial resolution, frequency, and polarimetric

characteristics needed for continuous high-resolution soil moisture monitoring. Current and future satellite-based synthetic aperture radar (SAR) systems such as ALOS-2 (Japanese Aerospace Exploration Agency), SENTINAL-1 (European Space Agency), DESDynI (NASA Jet Propulsion Laboratory), etc., are, and will be in the foreseeable future, limited to a single frequency band. Nonetheless, considerable effort has been successfully devoted to research on the retrieval of soil moisture from C-band data, which is operational today on Earth Observation platforms such as ERS-2, RADARSAT-1, ENVISAT, and RADARSAT-2. Besides being sensitive to soil moisture, however, the radar backscatter signal at the C-band (4–8 GHz) is significantly influenced by vegetation and surface roughness. Thus the estimation of spatial soil moisture patterns with a suitable accuracy for many applications requires the use of correction procedures for vegetation and roughness effects (Calvet et al., 1995; Cognard et al., 1995; Le Hégarat-Masclé et al., 2002; Baghdadi et al., 2002; Loew et al., 2006; Bryant et al., 2007).

For bare soils, the relationship between the SAR backscattering coefficient (σ^0), surface roughness, and surface soil moisture has been well investigated (Autret et al., 1989; Calvet et al., 1995; Boisvert et al., 1997; Le Toan et al., 2002; Baghdadi et al., 2002). It is based on the large contrast of the dielectric constant (ϵ') of dry soil (~ 3) and water (~ 80). The dielectric constant directly affects the backscatter intensity. Physically based backscatter models are available for bare soil conditions (Oh et al., 1992; Fung, 1994; Dubois et al., 1995; Baghdadi and Zribi, 2006). In general, these scattering models calculate σ^0 as a function of sensor configuration and soil surface state, allowing the inversion of near-surface volumetric water content; however, these physically based models require either detailed knowledge of the spatial patterns of soil parameters (e.g., surface roughness) or multiple radar channels or polarizations to isolate the effects of the surface dielectric constant and surface roughness. A suitable parameterization of these models, especially for larger areas, is therefore often not possible (Romshoo et al., 2000; van Zyl and Kim, 2001). Empirical and semiempirical algorithms have shown their potential to derive soil moisture from single-frequency SAR data (Oh et al., 1992; Rombach and Mauser, 1997). Their applicability might be limited to the region where they were developed, however, and thus must be validated if transferred to a different area. A comprehensive overview of existing theoretical, semiempirical, and empirical inversion approaches was given by Verhoest et al. (2008).

A key issue with regard to soil moisture is to understand the spatial patterns at different scales, the scaling behavior, and the processes that lead to spatial patterns. Several studies have investigated the spatial variability of soil moisture based on remotely sensed as well as ground-based measurements. Reynolds (1970) classified the controls into static (e.g., topography and soil texture) or dynamic (e.g., rainfall and varying vegetation cover) parameters. The lower boundary of the wilting point and the upper boundary of soil saturation provide physical limits for variations in water content for a given soil texture. Thus, one can assume that the relationship between the spatial

variance in soil moisture and the average moisture content shows a decrease in variance at low as well as at high soil moisture values.

Measurements provided by Famiglietti et al. (1998), for instance, support this assumption. They monitored time series of soil moisture along a 200-m hillslope transect and found that the magnitude of the spatial variability across the transect decreased with decreasing mean moisture values. Owe et al. (1982), as well as Albertson and Montaldo (2003), found the trend of variability to depend on the mean soil moisture state. Comparable findings were also published by other groups (e.g., Bell et al., 1980; Western and Grayson, 1998; Choi and Jacobs, 2007). Nevertheless, studies with contradictory observations can be found. Hawley et al. (1983), as well as Charpentier and Groffman (1992), did not find a relationship between mean soil moisture and soil moisture variability. Other researchers found increasing moisture variability with decreasing mean soil moisture (e.g., Famiglietti et al., 1999; Hupet and Vanclooster, 2002; Oldak et al., 2002). These observations indicate that in a complex landscape, the spatial variability is a result of the interactions of many different parameters and processes. Moreover, observations have been made that show that the dependency of the soil moisture variability on the mean soil moisture varies with spatial scale (Rodríguez-Iturbe et al., 1995; Crow and Wood, 1999). Teuling and Troch (2005) showed that both soil and vegetation controls can cause either the creation or destruction of spatial variance. Vereecken et al. (2007) conducted a re-examination of recent experimental work (e.g., Choi and Jacobs, 2007; Choi et al., 2007) showing that the spatial variance increases when drying occurs from a very wet state. Spatial variability peaks at moisture values in the mid range between maximum and minimum values and decreases accordingly with further drying.

The primary aim of the study was to analyze the spatial variability of surface soil moisture based on remote sensing and field measurements at different spatial scales. To this end, we derived a time series of surface soil moisture patterns from ASAR data of the European Earth Observation satellite ENVISAT using an empirical soil moisture retrieval algorithm by Loew et al. (2006). The algorithm was validated with independent ground-truth measurements. Based on these data, the dependence of spatial soil moisture variability on the soil moisture state was analyzed for different spatial scales ranging from the field to the catchment scale.

◆ Materials and Methods

Study Site

The research area of the SFB/TR32, namely the catchment of the River Rur, is located in the western part of Germany, covering a total area of 2364 km² with about 10% belonging to Belgium (140 km²) and the Netherlands (100 km²). The area is divided into two major landscape units: (i) a fertile loess plain in the north dominated by agriculture, and (ii) a low mountain range in the south characterized by forest and grassland patches (Fig. 1).

Field measurements were performed at two test sites within the catchment. The test site Rollesbroich (50°37'25" N, 6°18'16" E) represents typical grassland within the rolling topography of the Eifel. This test site is characterized by a mean elevation of ~510 m above sea level, slopes from 0 to 10° and mean annual precipitation of 1200 mm. The dominant soils are Inceptisols, Alfisols, and Aqualfs developed in silt loam, according to the U.S. Soil Taxonomy. Due to the dense root network of the grass cover, the amount of soil organic matter in the topsoil (<5 cm) is up to 8% (w/w) (Korres et al., 2009). Thus, low bulk densities (0.57–0.83 g cm⁻³) prevail. The test site Selhausen (50°52'10" N, 6°27'4" E) represents an intensively used agricultural area of the Belgium–Germany loess belt (subsequently referred to as fertile loess plain). Crops are grown on virtually flat terrain (slopes 0–4°, mean elevation ~100 m above sea level, mean annual precipitation 705 mm). The major soils are Alfisols and Inceptisols with a silt loam texture.

Ground-truth measurements were taken on 15 sampling fields at the two test sites. The measurements were performed on different land cover types (sugarbeet [*Beta vulgaris* L.], winter wheat [*Triticum aestivum* L.], and grassland vegetation dominated by a ryegrass society, particularly perennial ryegrass [*Lolium perenne* L.] and smooth meadow grass [*Poa pratensis* L.]). The size of the individual sampling fields varied between 2 and 10 ha. The surface soil moisture measurements were arranged in a grid with a sampling point spacing of 30 to 60 m, with 12 to 24 points per field. According to the length of the rods of the hand-held frequency domain reflectometry probes (ThetaProbe ML2x, Delta-T Devices, Cambridge, UK), the measured surface soil moisture was an average value for the topmost 6 cm. To minimize sampling errors and to yield a representative value for each sampling location, each sampling location was represented by the mean of six individual measurements taken within a radius of 40 cm of the sampling location. Obvious measurement errors, which might occur for instance by incomplete contact with the substrate, were excluded from further analysis. At the grassland test site, distributed field measurements were performed during Envisat overflights on 29 April, 3 June, and 16 September. At the arable land test site, distributed surface soil moisture measurements were performed during Envisat overflights on 29 April, 3 June, 8 July, 27 July, and 16 September. In addition, we used measurements from six continuous soil moisture stations installed at the test sites. At these stations, soil water content was monitored with FDR probes installed at 10- and 30-cm depth for grassland, sugarbeet, and winter wheat. A transect along the slope at the Rollesbroich site was observed with a time domain reflectometry (TDR) station (TDR-100/SDMX50, Campbell Scientific, Logan, UT).

Envisat Advanced Synthetic Aperture Radar Data

Envisat ASAR operates at C-band with a center frequency of 5.331 GHz and can perform multiple acquisition modes. The platform revolves around the Earth on a sun-synchronous polar orbit with a nominal reference mean altitude of 800 km and 98.55°

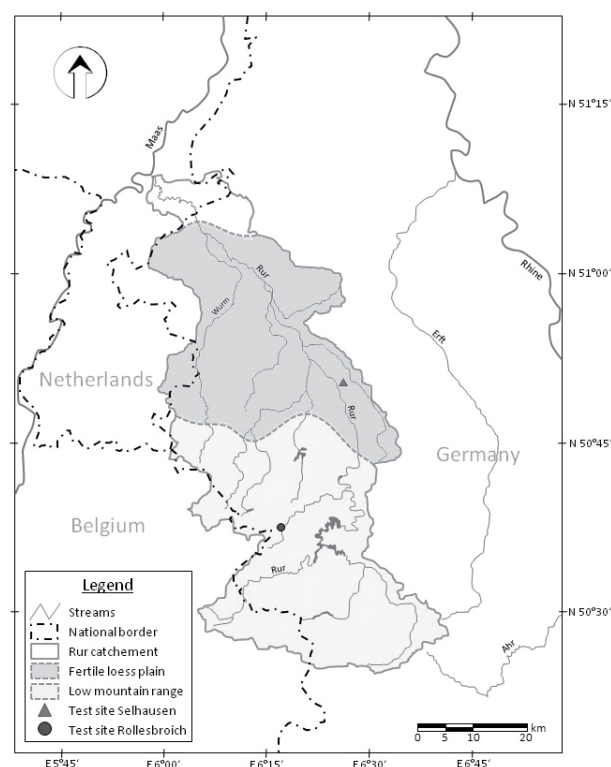


Fig. 1. River Rur catchment with the two major landscape units (gray shaded) and locations of the test sites for in situ soil moisture measurements in Selhausen and Rollesbroich.

inclination. The SAR data used in the present study are eight WS images with a resolution of approximately 150 m and a swath width of 400 km. All images are from 2008, starting on 19 February and ending on 21 October. Because every scene was acquired on the same orbit, the time lag between the single-mode images equals the orbital repeat cycle of 35 d. An overview of the eight ASAR images used is given in Table 1. We used Level 1 ASAR wide-swath single-look complex (ASA_WSS_1P) data, which represent single-look, complex, slant-range, digital images generated from Level 0 data.

Table 1. Overview of the Advanced Synthetic Aperture Radar (ASAR) wide-swath, single-look (WSS), vertically co-polarized data acquired on descending orbits in 2008 used for this study.

Date	Start time	LIA near range†	LIA far range‡	LIA mid range§
h				
19 Feb.	0959:09	28.8	30.5	27.1
25 Mar.	0959:10	28.7	30.4	27.0
29 Apr.	0959:07	28.8	30.5	27.1
3 June	0959:09	28.8	30.5	27.1
8 July	0958:49	28.9	30.6	27.2
12 Aug.	0959:10	28.8	30.5	27.1
16 Sept.	0958:45	28.8	30.5	27.1
21 Oct.	0959:08	28.9	30.6	27.2

† The local incidence angle (LIA) of the very eastern part of the catchment, which is closest to the sensor in range direction.

‡ The LIA of the very western part of the catchment, representing the location farthest from the sensor in range direction.

§ The LIA of the median of the catchment.

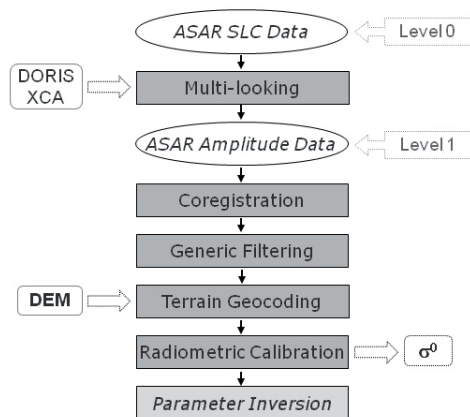


Fig. 2. Basic processing chain for Envisat satellite Advanced Synthetic Aperture Radar (ASAR) wide-swath, single-look complex (SLC) data, with input from external calibration (XCA) data and a digital elevation model (DEM) and output of the radar backscattering coefficient (σ^0).

All images were vertically co-polarized and were acquired on descending orbits.

Advanced Synthetic Aperture Radar Data Processing

There is no standard processing chain for SAR data. Principally, the processing depends on how the data were acquired (SAR system and acquisition mode). Additionally, the type of product that is envisaged determines how intermediate SAR products (i.e., terrain geocoded backscattering coefficient data) will be further processed. All image processing performed in this study used ENVI (ITT Visual Information Solutions, Boulder, CO) and the add-on module SARscape (sarmap, Purasca, Switzerland). Figure 2 outlines the image processing steps.

After header analysis, full resolution extraction is performed to produce single-look complex (SLC) images. Wide-swath data must be multi-looked separately for each of its five subswaths to produce the slant range intensity image with square resolution cells. The resolution of the WS SLC is 150 m. Auxiliary orbit and calibration information for each ASAR image are used to yield the most accurate multi-looked intensity images (Rosich and Meadows, 2004). The DORIS (Doppler Orbitography and Radiopositioning Integrated by Satellite) data provide precise orbital information for Envisat ASAR; two different versions are available. We used the verified orbits (VOR) because they provide the most precise location information; however, VOR data are not available until 1 mo after the actual satellite acquisition at the earliest. In addition, the most recent external calibration data (XCA) files were used to assure the best radiometric accuracy (ESA, 2007). These ancillary ASAR data are also used in the following processing steps.

To render the application of a multitemporal speckle filter and to assure completely identical geometries, the multi-look images were subsequently co-registered. This step requires spatial registration to correct for relative translational shift and rotational and scale

differences. Co-registration can be described as the process of superimposing, in the slant range geometry, two or more SAR images having the same acquisition geometry (Meijering and Unser, 2004).

Speckle, a typical feature of SAR images, was reduced in a two-step approach. A first step to reduce the speckle is inherently performed as part of the multi-lookup procedure through averaging the range or azimuth resolution cells to produce the spatial resolution of the WS images. According to De Grandi et al. (1997), multitemporal speckle filtering should be applied whenever two or more images of the same scene taken at different times are available. By exploiting the varying temporal correlation of speckle between images, this filtering process significantly reduces the noise. Hence, we used a multitemporal De Grandi filter for despeckling of the images (De Grandi et al., 1997).

After despeckling, the images were geocoded and radiometrically calibrated to σ^0 . The SAR images were orthorectified using a high-resolution (10-m) airborne laser scanner digital elevation model (Sciland, 2008). Local terrain slopes and aspects with respect to the incident wave result in significant radiometric as well as geometric distortions in the recorded backscatter amplitude (Meier et al., 1993). Also, the effects of variations in the scattering area must be accounted for (Ulander, 1996; Small et al., 2004). These terrain effects were corrected, including an incidence angle correction, before calculating the surface soil moisture using SARscape.

Empirical Soil Moisture Retrieval Model

The inversion approach for Envisat ASAR data was developed with the aim to provide soil moisture maps for mesoscale catchments in an operational manner. The algorithm is based on an empirical inversion scheme initially developed for C-band SAR data from the European Remote Sensing satellite mission (Rombach and Mauser, 1997). The approach calculates the real part of the complex dielectric constant ϵ' as a function of land use. Thus the algorithm requires a detailed land use map as well as additional soil texture information for the inversion of ϵ' to soil moisture by means of a dielectric mixing model. The model has proven its applicability in different studies showing that surface soil moisture contents can be derived with a RMSE of 4 to 7% (v/v) and that it is also usable for mesoscale C-band SAR data (Schneider and Oppelt, 1998; Mauser, 2000; Loew et al., 2003). An advantage of this empirical retrieval approach is that it requires very few model parameters to derive surface soil moisture values. The soil moisture retrieval model has been developed and validated for a range of land cover types, in particular cereal, root crops, bare soils, harvested fields, and grassland. Soil moisture is derived from the remotely measured backscatter in a two-step approach. First, ϵ' is derived from the SAR backscattering coefficient σ^0 and ancillary land use information. In a second step, the conversion of ϵ' to volumetric soil moisture (m_v) contents is calculated on the basis of a soil texture map using the dielectric mixing model proposed by Hallikainen et al. (1985).

The measured backscattering coefficient is converted to the relative dielectric constant by

$$\epsilon' = a + b\sigma^0 [\text{dB}] + c\sigma^0 [\text{dB}]^2 \quad [1]$$

where a , b , and c are empirical land-use-dependant model parameters, as shown in Table 2.

In contrast to the constant vegetation influence for the field crops, a significant impact of biomass on the backscattering coefficient was observed for grassland (Rombach and Mauser, 1997). This finding was supported by Dubois et al. (1995), who observed significant differences in backscatter intensities between grassland fields with the same soil moisture content attributable to varying amounts of biomass. Rombach and Mauser (1997) proposed the use of an attenuation factor Ω , which is related to the dry biomass of the grassland vegetation M_{DRY} (kg/m^2) as

$$\Omega = \alpha - \beta\sqrt{M_{\text{DRY}}} \quad [2]$$

where α and β are specific parameters, given in Table 2 for intensively and extensively used grassland (Loew et al., 2006). It should be mentioned that the actual physical scattering mechanisms and attenuation properties due to interactions between aboveground biomass, thatch, and the underlying mineral soil constitutes a major problem for the estimation of soil moisture under grassland vegetation from C-band SAR (Martin et al., 1989; Saatchi et al., 1994; Wang et al., 1997). The applicability of an empirical inversion algorithm to a different region and sensor system must be validated with independent measurements. In the present study, this validation was carried out on the basis of a large number of field measurements.

Analysis of Soil Moisture Variability

To analyze the soil moisture variability at different spatial scales, field and remote sensing data with different aggregation levels were used in a three-step approach:

1. In a first step, the ASAR soil moisture retrievals were analyzed at the scale of the entire Rur catchment and at the scales of the two major landscape units. At these scales, differences in soil moisture variability should result from variations in soil, topography (especially in the low mountain range area), land cover type, and potential variations in the spatial distribution of antecedent rainfall
2. In a next step, we analyzed 1.5- by 1.5-km boxes (10 by 10 pixels) of the ASAR-derived soil moisture (the number of boxes per image was 293). This analysis was restricted to the fertile loess plain because the effects of topography on rainfall, soil type, and soil moisture, as well as small-scale patterns in land cover type, should be reduced as far as possible. The mean soil moisture and variance for the 1.5- by 1.5-km boxes were calculated by shifting a nonoverlapping, moving, 10- by 10-pixel window over the ASAR images. Because not all of the pixels in the image (e.g., built-up areas, forests, and water) represent a soil moisture value, only those boxes that had at least 30% of the

Table 2. Land-use-dependent coefficients for the inversion of the radar backscattering coefficient (σ^0) to the dielectric constant (ϵ') using Eq. [1] and biomass correction coefficients for Eq. [2] at an incidence angle of 23° (Loew et al., 2006).

Land use	Model parameters			
	a	b	C	R^2
Bare soil	34.20	4.42	0.15	0.90
Cereal	42.77	4.91	0.16	0.88
Harvested fields	45.71	5.87	0.20	0.81
Grassland	40.94	5.33	0.18	0.92
Root crops	42.05	4.42	0.15	0.84
Biomass correction	a	b		
Meadow, extensive use	0.9765	0.7278		
Meadow, intensive use	1.0350	0.5934		

pixels classified were included in the analysis. At this spatial scale, soil moisture differences should be dominated by differences in land cover type, while differences due to varying soil texture should be small and homogenous antecedent rainfall is still a reasonable assumption.

3. For a field-scale evaluation, the field measurements at Selhausen were analyzed on the basis of individual fields (0.02–0.10 km^2) to address the within-field soil moisture variability because differences in soil texture were small and homogenous antecedent rainfall per field could be assumed.

At all spatial scales, the soil moisture variability was compared with the mean soil moisture content. To avoid interdependency between both statistical moments, coefficients of variation instead of standard deviations were used to represent variability.

Results and Discussion

Soil Moisture Retrievals

Eight WS images were processed for 2008. As an example, Fig. 3 shows the spatial patterns and frequency distribution of the soil moisture map for 25 March. Areas where the land cover did not allow the calculation of the surface soil moisture (e.g., built-up areas, forests, and water) remain unspecified in the soil moisture maps. The soil moisture frequency distribution of the derived pattern is shown in the histogram. The histogram shows a bimodal soil moisture distribution averaging 34.5% (v/v), with a range of 25 to 47.5% (v/v); the first and second peaks are centered at 31.5 and 38% (v/v), respectively. While the soil moisture map shows quite similar soil moisture values within the major landscapes units, it can be seen that the low mountain range part is wetter than most areas of the fertile loess plain. Within a period of 2 d before the satellite overpass, the catchment received precipitation amounts ranging from 2.2 to 8.5 mm. The image covers 97% of the Rur catchment area. The southeastern part of the catchment (approximately 70 km^2) is not covered due to missing land use information.

To evaluate the applicability and quality of the derived soil moisture inversion algorithm, we compared the surface soil moisture values calculated from the ASAR data with in situ ground-truth measurements.

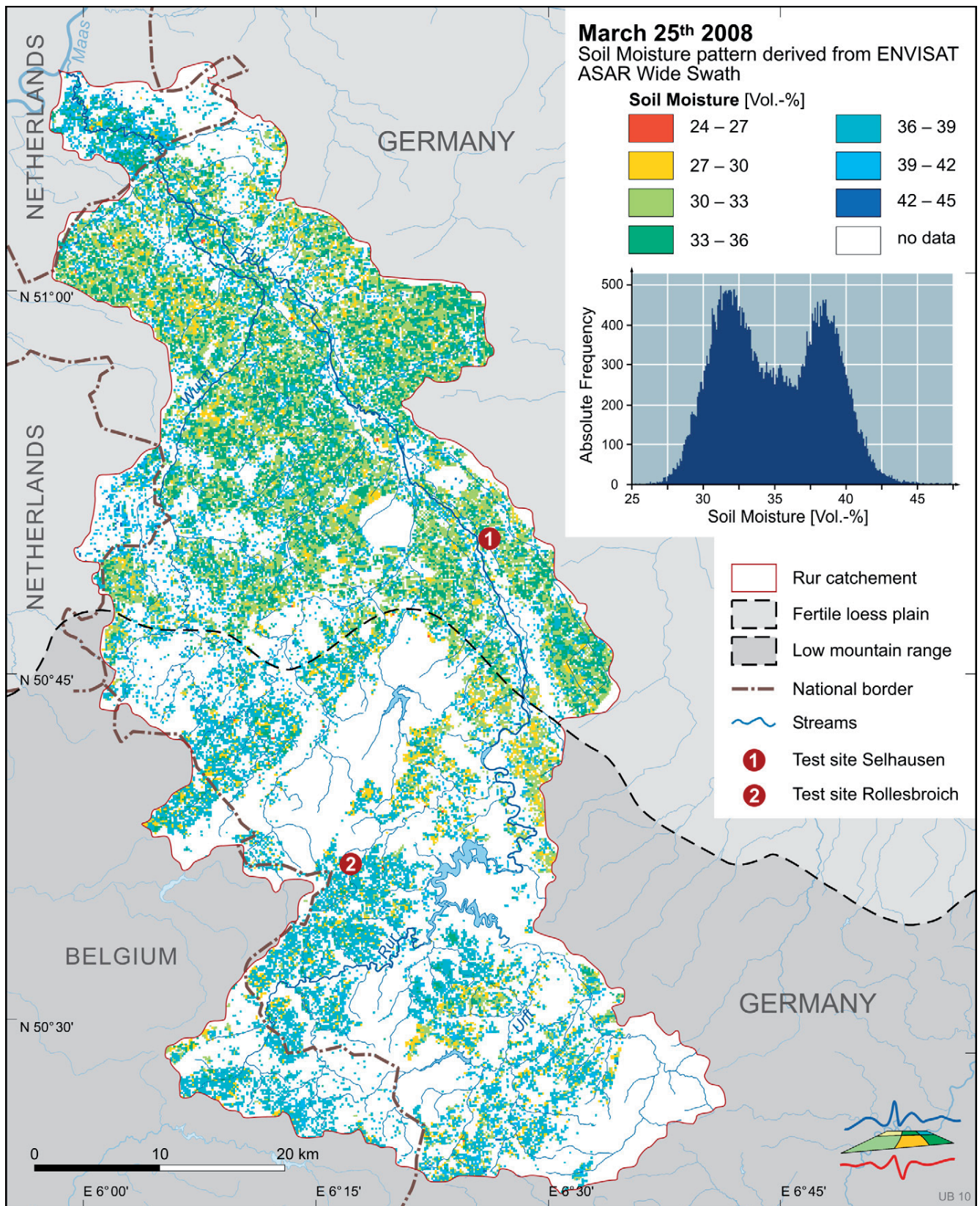


Fig. 3. Envisat satellite Advanced Synthetic Aperture Radar (ASAR) derived soil moisture pattern of the River Rur catchment from 25 Mar. 2008.

The soil moisture estimates were determined on a pixel-by-pixel basis from the space-borne microwave measurements in the C-band using the empirical algorithm discussed above. Because the coefficients of these equations were based on previous research (Rombach and Mauser, 1997), ground-truth data and remote sensing estimates were independent of each other. Because ASAR WS pixels provide an average value for a 150- by 150-m surface, comparison of remote sensing and ground measurement was done on the basis of individual fields and for all available dates with ground-truth data.

Figure 4 shows the comparison of measured and retrieved soil moisture values for all eight maps. Triangles indicate the average values measured for the different fields. According to the individual size, each field is represented by 10 to 24 measurement locations, each covered by six samples. In addition, measurements taken at our continuous-measurement sites are shown as circles. Because the continuous measurements represent only the given measurement location instead of an areal average, larger differences in the point measurements and the spatial mean covered by the remote sensing data may exist. Nevertheless, the measurements taken at the continuous-measurement sites match the values derived from remote sensing very well.

Comparison of the field average ground-truth data with ASAR-derived soil moisture values yielded a RMSE of 5% (v/v). While field measurements and remote sensing estimates agreed well in the mid and low soil moisture range, at high soil moisture states the ASAR retrievals significantly underestimated the field measurements. Very high soil moisture values in excess of 45% (v/v) were measured only under grassland, where the handheld probes integrated the wet thatch and the mineral soil parts. The thatch layer of the grass cover and the organic topsoil layer provided a large storage capacity for water, which exceeded the porosity of the mineral soils and thereby dominated the soil moisture measurement. The empirical inversion algorithm did not appropriately account for this effect. In addition, the soil texture map did not reflect the large water retention characteristic of the organic upper layer of this land use–soil combination. For dry conditions, the soil moisture estimates for grassland as well as for arable land agreed well with the field measurements. This indicates that for dry conditions, the measured water content of the soil is mainly determined by the properties of the mineral soil rather than the thatch layer.

The soil moisture conditions of the arable land of the loess plain were generally well represented by the ASAR estimates. Because the inversion algorithms were developed mainly for mineral soils, they performed well here. If field-measured soil moisture values >45% (v/v) are excluded from the comparison and thereby the effect of the organic topsoil layer reduced, a RMSE of 4.3% (v/v) is achieved. Loew et al. (2006) pointed out that the empirical model is based on a limited set of observations, representing a span of 18 and 45% (v/v) and thus might be less accurate beyond this range.

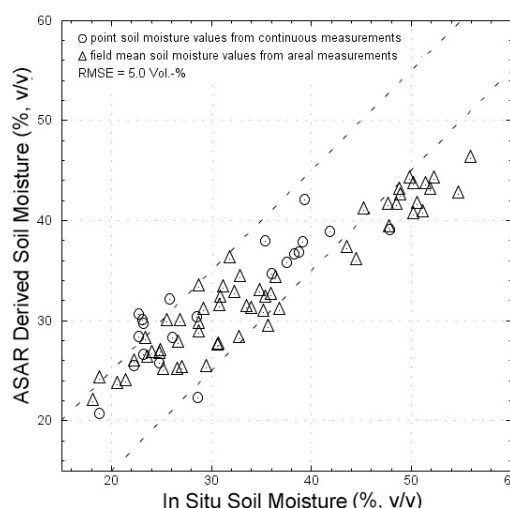


Fig. 4. Comparison between measured and Advanced Synthetic Aperture Radar (ASAR) derived surface soil moisture. Field soil moisture values are averages from 10 to 24 individual measurement locations. Dashed lines indicate the $\pm 5\%$ (v/v) margins.

Nevertheless, one has to be aware of different sources of uncertainty in the estimation of surface soil moistures from ASAR data, which can arise from the following:

1. Image calibration errors, which range between 0.5 and 1.0 dB for the ASAR products (ESA, 2007). Insufficient speckle reduction can add a stochastic component to σ^0 . Both error sources were assumed to be small because accurate ancillary data and state-of-the-art image processing were used.
2. Imprecise land use information and land use specific conversion, which can result in a false inversion of σ^0 to ϵ' .
3. Unknown or imprecise biomass information for grassland pixels. Spatial variability in biomass results in spatial variability of the attenuation factor. We used field measurements to determine the biomass of the grassland. While these measurements provided accurate data for our sample fields, they might not be accurate everywhere in the catchment.
4. Unknown or imprecise soil texture information, which can result in a false conversion of ϵ' to volumetric soil moisture by means of dielectric mixing models.

Analysis of Soil Moisture Variability

The relationship between the mean soil moisture and the CV calculated for the whole Rur watershed using all ASAR soil moisture images is shown in Fig. 5. The CV decreased linearly with increasing mean soil moisture. A decreasing soil moisture variability with increasing soil moisture has been described in the literature (e.g., Famiglietti et al., 1999; Hupet and Vanclooster, 2002; Choi et al., 2007) and should be expected, particularly when areas with homogeneous soil textures approach saturation.

As described above, the watershed consists of two distinctively different regions: the flat loess plain and the mountainous Eifel region. Land use and soil textures as well as their spatial variability are

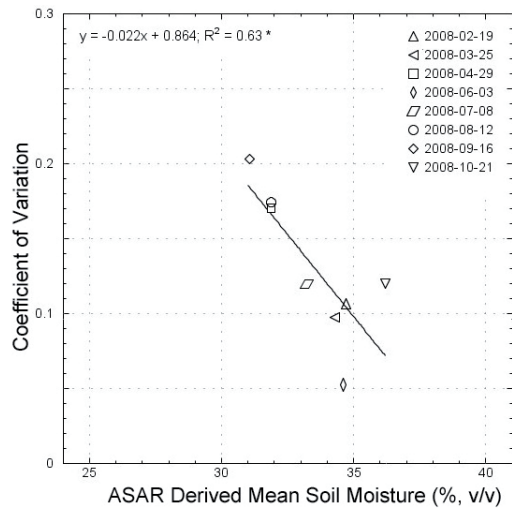


Fig. 5. Relationship between Advanced Synthetic Aperture Radar (ASAR) derived mean soil moisture and the CV for the entire River Rur catchment.

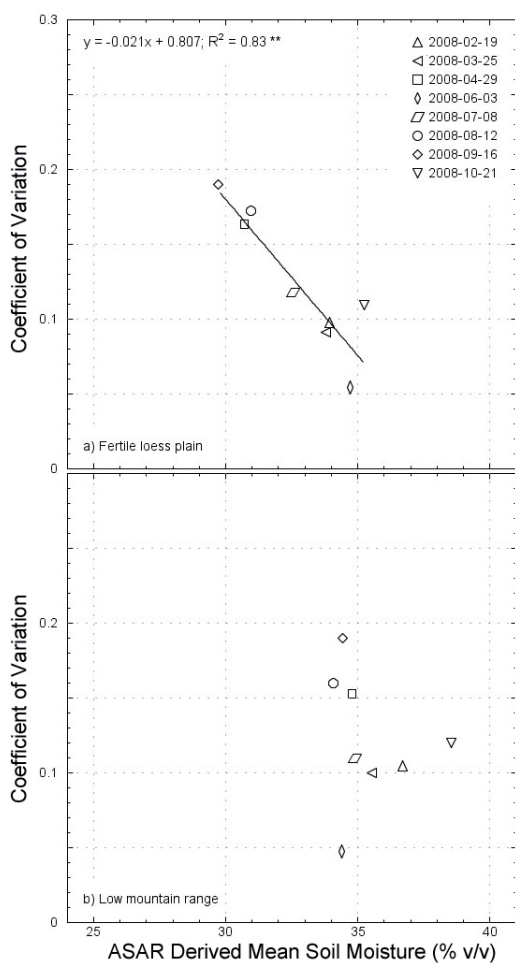


Fig. 6. Relationship between Advanced Synthetic Aperture Radar (ASAR) derived soil moisture and the CV for (a) the fertile loess plain, and (b) the low mountain range region.

significantly different in both regions. While in the Eifel region the topography results in large spatial heterogeneity, particularly with respect to soil texture, the loess plain exhibits more or less uniform soil textures but differs strongly with respect to different types of arable land use. These differences in landscape properties may result in a different relationship between average soil moisture and soil moisture variability. Consequently, we analyzed this relationship separately for both regions (Fig. 6).

The correlation for the loess plain (Fig. 6a) yielded a very strong negative relationship ($R^2 = 0.83$) between the mean soil moisture and the spatial moisture variability as expressed by the CV. The slope of the relationship is very close to the slope for the whole catchment. In contrast, the relationship for the Eifel area does not show a clear trend (Fig. 6b). Even at high soil moisture levels, the spatial variability was high. While the soil texture in the loess plain is rather uniform, the soil textures in the Eifel vary considerably, from mineral soils saturating at moisture values between 45 and 50% (v/v) to organic soil or soils with an organic topsoil layer with surface soil moisture values in excess of 60% (v/v). Thus, even at or close to saturation, the Eifel soils showed large spatial variability. Moreover, the hilly topography of the Eifel also caused larger spatial variation in precipitation.

Figure 7 shows the relationship of the CV and the mean surface soil moisture based on 10- by 10-pixel boxes for the fertile loess plain. The different acquisition dates of the images are color coded to allow assessment of the variability with a given scene. The slope of the regression line in Fig. 7 is significantly smaller than the respective slope for the whole area (Fig. 6a). While the soil moisture varied considerably within the 10 by 10 box for all soil moisture values, the decrease in the CV with increasing soil moisture described above is still obvious. In addition, the upper limit of the soil moisture variability decreased significantly with increasing soil moisture and the lower limit of the soil moisture variability within the 10 by 10 boxes was considerably larger at lower soil moistures than at soil moistures in excess of 32% (v/v).

Figure 8 shows the relationship between the mean field surface soil moisture measured during our field campaigns and the CV within the individual fields. It can be seen that the CV decreased again with increasing mean soil moisture. For the soil moisture range from 15 to 34% (v/v), the linear regression resulted in a coefficient of determination of 0.59 and a slope of -0.0063 on the winter wheat fields, and a coefficient of determination of 0.76 and a slope of -0.0065 on the sugarbeet fields. At the field scale, the slope of the regression line is significantly smaller than the slope for the mesoscale (10- by 10-pixel boxes) or the regional scale. Thus, while the level of spatial variation shows a comparable range of values at all spatial scales, the decrease in the soil moisture variability with increasing soil moisture was smaller at the local scale than at the large scale.

Choi and Jacobs (2007) also used an exponential fit as an efficient way to explain soil moisture variability patterns as a function of mean

soil moisture. An exponential fit $CV = A \exp(B\theta)$ between mean soil moisture and CV yields a tighter coefficient of determination of 0.60 with $A = 0.521$ and $B = -0.059$, and of 0.81 with $A = 0.591$ and $B = -0.073$ for the winter wheat and sugarbeet fields, respectively. The parameter A describes the relative variability range and B indicates the variability change as related to mean soil moisture. Hence, parameter A is related to the maximum relative variability while parameter B is related to the slope of the relative variability. The parameters A and B , as observed from our in situ field measurements, are consistent with the observations of surface soil moisture variability from the Small Explorer (SMEX), as reported by Choi et al. (2007).

The negative correlations between soil moisture variability and mean soil moisture content found in our study are consistent with previous studies of Famiglietti et al. (1999), Hupet and Vanclooster (2002), and Choi and Jacobs (2007). Nonetheless, it should be noted that some studies also found positive relationships between the mean surface soil moisture content and the soil moisture variability (Famiglietti et al., 1998; Western and Grayson, 1998). These studies postulated that variability peaked under wet conditions because soil heterogeneity would be maximized after precipitation events. While we concur that spatially heterogeneous precipitation, particularly when investigating large areas, results in increased heterogeneity if soil saturation is not reached, our findings indicate that for areas with homogeneous soil textures, the soil moisture variability decreases with increasing soil moisture. In regions with large differences in soil texture and thus soil porosity and maximum soil moisture values at saturation, however, this relationship might not hold and may result in a large soil moisture variability even at high soil moistures, as evidenced by the data for the Eifel. According to Famiglietti et al. (1998), the combined effects of soil texture, hysteresis effects, vegetation, topography, and sampling scale may lead to different relationships between spatial variability and soil moisture.

Figure 9 provides a comprehensive overview of the relationship of spatial soil moisture variability and soil moisture values for different spatial scales. As can be seen, the gain of the relationship between soil moisture value and CV decreases with scale. Hence, at a given soil moisture level, we observed the highest variability at the scale of the entire Rur catchment and the smallest variability at the field scale. We attribute this to the fact that the drivers of variations in surface soil moisture contents are much more variable at the larger scale. If we consider precipitation as the dominant driving process for spatial variance on days with high mean soil moisture values, the variability in surface soil water contents increases with increasing scale because the amounts of rainfall, with annual means of ~600 mm in the fertile loess plain and >1200 mm in the low mountain range, vary significantly across the whole Rur catchment. At smaller scales, on the other hand, these fluctuations in precipitation decrease and contribute only small amounts of variance. On days with dry conditions, i.e., low mean soil moisture values, variance is more likely driven by processes associated with evapotranspiration. Thus, soil moisture

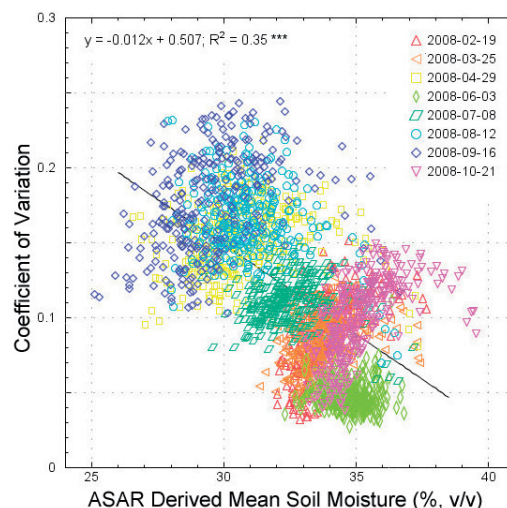


Fig. 7. Relationship between Advanced Synthetic Aperture Radar (ASAR) derived soil moisture and the CV for (a) the fertile loess plain pixels taking into account all dates and land cover classes.

variability also increases with increasing scale due to the fact that spatial heterogeneities of factors like soil clay content, vegetation (including agricultural management), and topographic conditions become larger the larger the scale.

As microwave remote sensing using the C-band only provides information about the top surface layer of a soil volume, it is unclear if these relationships also hold for deeper soil layers. Thus, care should be taken in extrapolating statistics from surface measurements (e.g., SAR) to the entire root zone. Choi and Jacobs (2007) found that surface soil moisture had the least negative relationship (slope closest to zero) between CV and mean soil moisture in comparison to deeper soil layers. According to them, these small variability patterns for the surface layer are affected by the high

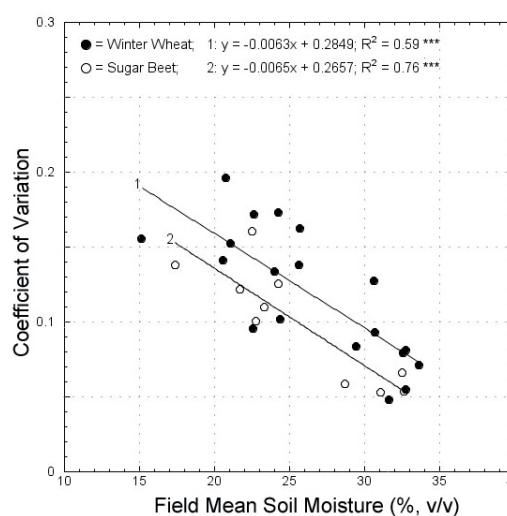


Fig. 8. Relationship between field mean soil moisture and the CV from in situ measurements at the Rollesbroich and Selhausen test sites.

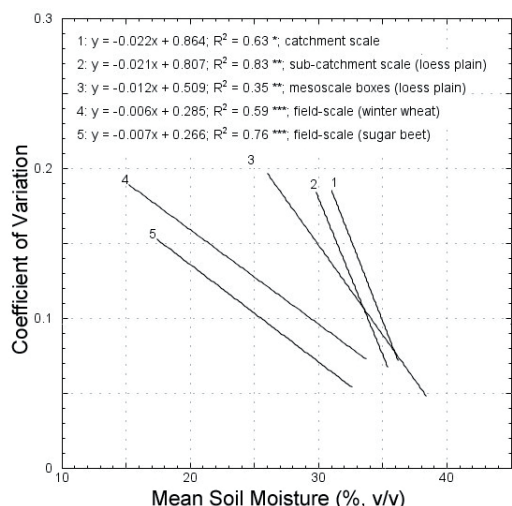


Fig. 9. Overview of the scale-dependent relationships between the CV and the mean surface soil moisture.

variation in mean soil moisture at the surface. Several other studies found less variability at deeper depths compared with surface soil moisture observations (Famiglietti et al., 1999; Hupet and Vanlooster, 2002; Albertson and Montaldo, 2003).

Conclusions

An empirical retrieval algorithm of surface soil moisture from Envisat ASAR data in the C-band was applied successfully within the Rur catchment. We validated the model to derive soil moisture values for a catchment in central Europe yielding a RMSE of 5.0% (v/v). The main advantage of the inversion scheme is that it requires very few parameters in comparison with other retrieval approaches. With regard to the operational use of any parameter inversion model for either optical or microwave remote sensing data, the availability of input parameters is of great importance. The highest deviations from in situ values of the derived soil moisture were recorded on wet meadows and a mature sugarbeet field. The model parameters could be further improved using empirical data measured under these conditions; however, any improvement of the algorithm will rely on a better assessment of the vegetation influence on the C-band backscattering mechanisms, taking into account dynamic vegetation effects.

The variability of mean surface soil moisture was investigated at different scales using in situ measurements and eight ASAR-derived soil moisture patterns. By analyzing the relationships between the spatial variance and the mean soil moisture state at the scales of the entire catchment (~2400 km²), the two major landscape units (~1000 km²), boxes (2.25 km²), and individual fields (~0.1 km²), we found that the CVs decreased with decreasing sampling scale for all data sets. The different slopes of the linear correlations, ranging from -0.0063 at the field scale to -0.022 at the catchment scale, indicate that small-scale and large-scale variances depend differently on mean soil moisture content.

Acknowledgments

We gratefully acknowledge financial support by the SFB/TR-32 "Patterns in Soil-Vegetation-Atmosphere Systems: Monitoring, Modeling, and Data Assimilation" funded by the German Research Foundation (DFG). In addition, we thank the European Space Agency (ESA) for the provision of Envisat ASAR data through their PI program (AOALO.3570).

References

- Albertson, J., and N. Montaldo. 2003. Temporal dynamics of soil moisture variability: 1. Theoretical basis. *Water Resour. Res.* 39(10):1274, doi:10.1029/2002WR001616.
- Autret, M., R. Bernard, and D. Vidal-Madjar. 1989. Theoretical study of the sensitivity of the microwave backscattering coefficient to the soil surface parameters. *Int. J. Remote Sens.* 10:171-179.
- Baghdadi, N., C. King, A. Chanzy, and J.P. Wigneron. 2002. An empirical calibration of the integral equation model based on SAR data, soil moisture, and surface roughness measurements over bare soils. *Int. J. Remote Sens.* 23:4325-4340.
- Baghdadi, N., and M. Zribi. 2006. Evaluation of radar backscatter models IEM, OH and Dubois using experimental observations. *Int. J. Remote Sens.* 27:3831-3852.
- Bell, K.R., B.J. Blanchard, T.J. Schumge, and M.W. Witzak. 1980. Analysis of surface moisture variations within large-field sites. *Water Resour. Res.* 16:796-810.
- Boisvert, J.B., Q.H.J. Gwyn, A. Chanza, D.J. Major, B. Brisco, and R.J. Brown. 1997. Effect of soil surface moisture gradients on modelling radar backscattering from bare fields. *Int. J. Remote Sens.* 18:153-170.
- Bryant, R., M.S. Moran, D.P. Thoma, C.D. Holfield, S. Skirvin, and M.M. Rahman. 2007. Measuring surface roughness to parameterize radar backscatter models for retrieval of surface soil moisture. *IEEE Geosci. Remote Sens. Lett.* 4:137-141.
- Calvet, J.-C., J.-P. Wigneron, A. Chanzy, S. Raju, and L. Laguerre. 1995. Microwave dielectric properties of a silt-loam at high-frequencies. *IEEE Trans. Geosci. Remote Sens.* 33:634-642.
- Charpentier, M., and P. Groffman. 1992. Soil moisture variability within remote sensing pixels. *J. Geophys. Res.* 97:18,987-18,995.
- Choi, M., and J.M. Jacobs. 2007. Soil moisture variability of root zone profiles within SMEX02 remote sensing footprints. *Adv. Water Resour.* 30:883-896.
- Choi, M., J.M. Jacobs, and M.H. Cosh. 2007. Scaled spatial variability of soil moisture fields. *Geophys. Res. Lett.* 34:L01401, doi:10.1029/2006GL028247.
- Cognard, A.L., C. Loumagne, M. Normand, P. Olivier, C. Ottlé, D. Vidal-Madjar, S. Louahala, and A. Vidal. 1995. Evaluation of the ERS-1/synthetic aperture radar capacity to estimate surface soil moisture: Two year results over the Naizin watershed. *Water Resour. Res.* 31:975-982.
- Crow, W.T., and E.F. Wood. 1999. Multi-scale dynamics of soil moisture variability observed during SGP'97. *Geophys. Res. Lett.* 26:3485-3488.
- De Grandi, G.F., M. Leysen, J.S. Lee, and D. Schuler. 1997. Radar reflectivity estimation using multiple SAR scenes of the same target: Techniques and applications. p. 1047-1050. *In* IGARSS '97: Remote Sensing, A Scientific Vision for Sustainable Development, Singapore. 3-8 Aug. 1997. Vol. 2. IEEE, New York.
- Dubois, P.C., J.J. van Zyl, and T. Engman. 1995. Measuring soil moisture with imaging radar. *IEEE Trans. Geosci. Remote Sens.* 33:915-926.
- European Space Agency. 2007. ASAR product handbook issue 2.2. ESA, Paris.
- Famiglietti, J., J. Devereaux, C. Laymon, T. Tsegaye, P. Houser, T. Jackson, S. Graham, M. Rodell, and P. Oevelen. 1999. Ground-based investigation of soil moisture variability within remote sensing footprints during the Southern Great Plains 1997 (SGP97) hydrology experiment. *Water Resour. Res.* 35:1839-1851.
- Famiglietti, J., J. Rudnicki, and M. Rodell. 1998. Variability in surface moisture content along a hillslope transect: Rattlesnake Hill, Texas. *J. Hydrol.* 210:259-281.
- Fung, A.K. 1994. Microwave scattering and emission models and their applications. Artech House, Boston.
- Hallikainen, M.T., F.T. Ulaby, M.C. Dobson, M.A. El-Rayes, and L.-K. Wu. 1985. Microwave dielectric behavior of wet soil: I. Empirical models and experimental observations. *IEEE Trans. Geosci. Remote Sens.* 23:25-34.
- Hawley, M., T. Jackson, and R. McCuen. 1983. Surface soil moisture variation on small agricultural watersheds. *J. Hydrol.* 62:179-200.
- Hupet, F., and M. Vanlooster. 2002. Intraseasonal dynamics of soil moisture variability within a small agricultural maize crop field. *J. Hydrol.* 261:86-101.
- Korres, W., C.N. Koyama, P. Fiener, and K. Schneider. 2009. Analysis of surface soil moisture patterns in agricultural landscapes using empirical orthogonal functions. *Hydrol. Earth Syst. Sci. Discuss.* 6:5565-5601.

- Le Hégarat-Masclé, S., M. Zribi, F. Alem, A. Weisse, and C. Loumagne. 2002. Soil moisture estimation from ERS/SAR data: Toward an operational methodology. *IEEE Trans. Geosci. Remote Sens.* 40:2647–2658.
- Le Toan, T., M. Davidson, F. Mattia, P. Borderies, I. Chenerie, and T. Manninen. 2002. Improved observation and modeling of bare soil surface for soil moisture retrieval. p. 20–24. *In* Retrieval of Bio- and Geophysical Parameters from SAR Data for Land Applications: Proc. Int. Symp., 3rd, Sheffield, UK, 11–14 Sept. 2001. ESA SP-475. Eur. Space Agency, Paris.
- Loew, A., R. Ludwig, and W. Mauser. 2003. Mesoscale soil moisture estimation from SAR data using subscale land use information. p. 1396–1398. *In* IGARSS '03 Proc., Toulouse, France. 21–25 July 2003. Vol. 2. IEEE, New York.
- Loew, A., R. Ludwig, and W. Mauser. 2006. Derivation of surface soil moisture from Envisat ASAR wide swath and image mode data in agricultural areas. *IEEE Trans. Geosci. Remote Sens.* 44:889–899.
- Martin, R.D., G. Asrar, and E.T. Kanemasu. 1989. C-band scatterometer measurements of a tallgrass prairie. *Remote Sens. Environ.* 29:281–292.
- Mauser, W. 2000. Comparison of ERS SAR data derived soil moisture distributions with SVAT model results. *In* Proc. ERS-Envisat Symp.: Looking Down to Earth in the New Millennium, Gothenburg, Sweden [CD-ROM]. ESA-SP461. Eur. Space Agency, Paris.
- Meier, E., U. Frei, and D. Nuesch. 1993. Precise terrain corrected geocoded maps. p. 173–185. *In* G. Schreier (ed.) SAR processing: Data and systems. Wichmann, Karlsruhe, Germany.
- Meijering, E., and M. Unser. 2004. A Note on cubic convolution. *IEEE Trans. Image Process.* 12:477–479.
- Oh, Y., K. Sarabandi, and F.T. Ulaby. 1992. An empirical model and an inversion technique for radar scattering from bare soil surfaces. *IEEE Trans. Geosci. Remote Sens.* 30:370–381.
- Oldak, A., T.J. Jackson, and Y. Pachepsky. 2002. Using GIS in passive microwave soil moisture mapping and geostatistical analysis. *Int. J. Geogr. Inf. Sci.* 16:681–698.
- Owe, M., E. Jones, and T. Schmutge. 1982. Soil moisture variation patterns observed in Hand County, South Dakota. *Water Resour. Bull.* 16:949–954.
- Quesney, A., S. Le Hégarat-Masclé, O. Taconet, D. Vidal-Madjar, J.-P. Wigneron, C. Loumagne, and M. Normand. 2000. Estimation of watershed soil moisture index from ERS/SAR data. *Remote Sens. Environ.* 72:915–926.
- Reynolds, S.G. 1970. The gravimetric method of soil moisture determination: III. An examination of factors influencing soil moisture variability. *J. Hydrol.* 11:188–200.
- Rodriguez-Iturbe, I., G.V. Vogel, R. Rigon, D. Entkhabi, F. Castelli, and A. Rinaldo. 1995. On the spatial organization of soil moisture fields. *Geophys. Res. Lett.* 22:2757–2760.
- Rombach, M., and W. Mauser. 1997. Multi-annual analysis of ERS surface soil moisture measurements of different land uses. p. 703–708. *In* Space at the Service of the Environment: Proc. ERS Symp., 3rd, Florence, Italy. ESA SP414. Eur. Space Agency, Paris.
- Romshoo, S.A., T. Nakaegawa, T. Oki, and K. Musiaka. 2000. Estimation of soil moisture using spaceborne SAR data and scattering models. *In* Proc. Remote Sens. Soc. Japan Conf., 28th, Tsukuba. 19–21 May 2000. Remote Sens. Soc. of Japan, Tokyo.
- Rosich, B., and P. Meadows. 2004. Absolute calibration of ASAR Level 1 products generated with PF-ASAR. ESA ESRIN, Frascati, Italy.
- Saatchi, S.S., D.M. Le Vine, and R.H. Lang. 1994. Microwave backscattering and emission model for grass canopies. *IEEE Trans. Geosci. Remote Sens.* 32:177–186.
- Schneider, K., and N. Oppelt. 1998. Determination of mesoscale soil moisture patterns with ERS data. pp. 1831–1833. *In* IGARSS '98: IEEE Int. Geosci. and Remote Sens. Symp., Seattle, WA. 6–10 July 1998. IEEE, New York.
- Scilands. 2008. Dokumentation zur Aufbereitung eines DGM10 für das Rur-Gebiet. Scilands GmbH, Göttingen, Germany.
- Small, D., M. Jehle, E. Meier, and D. Nuesch. 2004. Robust radiometric terrain correction for SAR image comparison. p. 929–932. *In* Proc. EUSAR 2004: Eur. Conf. on Synthetic Aperture Radar, 5th, Ulm, Germany. 25–27 May 2004. VDE Verlag, Berlin.
- Teuling, A.J., and P.A. Troch. 2005. Improved understanding of soil moisture variability dynamics. *Geophys. Res. Lett.* 32:L05404, doi:10.1029/2004GL021935.
- Ulander, L.M. 1996. Radiometric slope correction of synthetic aperture radar images. *IEEE Trans. Geosci. Remote Sens.* 34:1115–1122.
- van Zyl, J.J., and Y.J. Kim. 2001. A quantitative comparison of soil moisture inversion algorithms. p. 37–39. *In* Scanning the Present and Resolving the Future: Proc. IEEE 2001 Int. Geosci. and Remote Sens. Symp., Sydney, Australia. 9–13 July 2001. IEEE, New York.
- Vereecken, H., T. Kamai, T. Harter, R. Kasteel, J. Hopmans, and J. Vanderborght. 2007. Explaining soil moisture variability as a function of mean soil moisture: A stochastic unsaturated flow perspective. *Geophys. Res. Lett.* 34:L22402, doi:10.1029/2007GL031813.
- Verhoest, N.E.C., H. Lievens, W. Wagner, J. Álvarez-Mozos, M.S. Moran, and F. Mattia. 2008. On the soil roughness parameterization problem in soil moisture retrieval of bare surfaces from synthetic aperture radar. *Sensors* 8:4213–4248.
- Wang, J., A. Hsu, J.C. Shi, P. O'Neil, and T. Engman. 1997. Estimating surface soil moisture from SIR-C measurements over Little Washita River watershed. *Remote Sens. Environ.* 59:308–320.
- Western, A., and R. Grayson. 1998. The Tarrawara data set: Soil moisture patterns, soil characteristics, and hydrological flux measurements. *Water Resour. Res.* 34:2765–2768.

5. Analysis of surface soil moisture patterns based on ecohydrological modeling

Journal article (in review):

Korres, W., Reichenau T.G., Schneider, K., 2012. Patterns and scaling properties of surface soil moisture in an agricultural landscape: An ecohydrological modeling study. *Journal of Hydrology*, submitted 23.10.2012, in review since 05.11.2012.

Original page numbers of the manuscript are used.

**PATTERNS AND SCALING PROPERTIES OF SURFACE SOIL
MOISTURE IN AN AGRICULTURAL LANDSCAPE:
AN ECOHYDROLOGICAL MODELING STUDY**

W. Korres¹, T. G. Reichenau¹ and K. Schneider^{1}*

¹Hydrogeography and Climatology Research Group, Institute of Geography,

University of Cologne, D-50923 Köln, Germany

**Corresponding author. Tel.: +49 221 470 4331; fax: +49 221 470 5124;
E-mail address: karl.schneider@uni-koeln.de*

Abstract

Soil moisture is a key variable in hydrology, meteorology and agriculture. Soil moisture, and surface soil moisture in particular, is highly variable in space and time. Its spatial and temporal patterns in agricultural landscapes are affected by multiple natural (precipitation, soil, topography, etc.) and agricultural (soil management, fertilization, etc.) factors, making it difficult to identify unequivocal cause and effect relationships between soil moisture and its driving variables. The goal of this study is to characterize and analyze the spatial and temporal patterns of surface soil moisture (top 20 cm) in an intensively used agricultural landscape namely the northern part of Rur catchment (1100 km²) located in Western Germany and to determine the dominant factors and underlying processes controlling these patterns. A second goal is to analyze the scaling behavior of surface soil moisture patterns in order to investigate how spatial scale affects spatial patterns. To achieve these goals, a dynamically coupled, process-based and spatially distributed ecohydrological model was used to analyze the key processes, their interactions and feedbacks. At first, the model was validated for two growing seasons for the three main crops in the investigation area: Winter wheat, sugar beet, and

maize. This yielded RMSE values for surface soil moisture between 1.8 and 7.8 Vol.-% and index of agreement values for the total aboveground biomass of 0.96 or higher and values ranging from 0.81 to 0.98 for green LAI. Large deviations of measured and modeled soil moisture can be explained by a change of the infiltration properties towards the end of the growing season, especially in maize fields. The validated model was used to generate daily surface soil moisture maps, serving as a basis for an autocorrelation analysis of spatial patterns and scale. Outside of the growing season, surface soil moisture patterns at all spatial scales depend mainly upon soil properties. Within the main growing season, larger scale patterns that are induced by soil properties are superimposed by the small scale land use pattern and the resulting small scale variability of evapotranspiration. However, this influence decreases at larger spatial scales. Most precipitation events cause temporarily higher surface soil moisture autocorrelation lengths at all spatial scales for a short time even beyond the autocorrelation lengths induced by soil properties. The relation of daily spatial variance to the spatial scale of the analysis fits a power law scaling function, with negative values of the scaling factor β , indicating a decrease in spatial variability with increasing spatial resolution. High evapotranspiration rates cause an increase in the small scale soil moisture variability, thus leading to large negative values of the scaling factor β . Utilizing a multiple regression analysis, we found that 53 % of the variance of the scaling factor β can be explained by an independent LAI parameter and by the antecedent precipitation.

Keywords: Catchment hydrology; Soil moisture; Ecohydrological crop model; Pattern; Scale; Autocorrelation

1. Introduction

Soil moisture is a key variable in hydrology, meteorology and agriculture. Particularly surface soil moisture plays a critical role in partitioning precipitation into infiltration and runoff (Western et al., 1999b) and of solar energy into latent and sensible heat fluxes (Entekhabi and Rodriguez-Iturbe, 1994). Soil moisture, and surface soil moisture in particular, is highly variable in space and time. Many factors control its spatial patterns and temporal dynamics, such as topography, soil properties, aspect, land use, management, vegetation, precipitation, solar radiation and specific contributing area (Famiglietti et al., 1998; Hawley et

al., 1983; Hebrard et al., 2006; Korres et al., 2010; Rodriguez-Iturbe et al., 2006; Svetlitchnyi et al., 2003; Western et al., 1998; Western et al., 1999a). Reynolds (1970) distinguished between static (e.g., soil texture, topography) and dynamic (e.g., precipitation, vegetation) controlling factors. Many of these factors are interrelated and most of these factors vary spatially and/or temporally, making it difficult to identify unequivocal cause and effect relationships between soil moisture and its driving variables.

In situ measurements of soil moisture are very time consuming and costly, particularly at larger scales. Therefore, great efforts were undertaken to derive spatially distributed soil moisture maps from remote sensing and/or modeling. Many studies have analyzed the spatial structure of soil moisture and their scaling properties using point measurements (e.g., Famiglietti et al., 1998; Western et al., 1998), remotely sensed images (e.g., Kim and Barros, 2002; Koyama et al., 2010; Rodriguez-Iturbe et al., 1995) and model generated maps (e.g., Manfreda et al., 2007; Peters-Lidard et al., 2001). Controversial findings of the relationship between soil moisture variability and mean soil moisture have been reported. Some studies found an increase of spatial variability with decreasing mean soil moisture (Choi and Jacobs, 2011; Famiglietti et al., 1999; Koyama et al., 2010), others found opposite trends (Famiglietti et al., 1998; Western and Grayson, 1998) or were unable to detect a trend (Hawley et al., 1983). Teuling and Troch (2005) showed that both, soil properties and vegetation dynamics, can act to either create or to destroy spatial variability. Rodriguez-Iturbe et al. (1995) and Manfreda et al. (2007) showed that soil moisture variability is not only depending on mean soil moisture, but also varies with the spatial scale of the analysis.

Autocorrelation length is often used to analyze the spatial structure of soil moisture fields. For a small grassland catchment, Western et al. (1998) found shorter autocorrelation lengths on wet days, related to the smaller spatial scale of lateral redistribution, in contrast to longer autocorrelation lengths on dry dates, connected to the larger scale of evapotranspiration as the dominant driver. At the field scale (mainly on wheat fields) in a semi-arid climate, Green and Erskine (2004) found a spatial structure of surface soil moisture, but no clear connection of the autocorrelation length to dry or wet soil moisture conditions. Western et al. (2004) compared soil moisture autocorrelation lengths of soil moisture and terrain attributes, indicating the important role of topography at one test site and the variation of soil properties at other test sites. But these studies focused on small catchments, mostly with homogeneous vegetation, therefore the influence of the interacting factors topography, vegetation, soil and meteorology on soil moisture patterns were not investigated.

The main objective of this study is to characterize and analyze the spatial and temporal patterns of surface soil moisture in an intensively used agricultural landscape and to determine the dominant factors and underlying processes controlling these patterns. A second goal is to analyze the scaling behavior of soil moisture patterns in order to investigate how spatial scale affects the spatial patterns. This is of particular interest for downscaling or aggregation purposes in order to prevent systematic biases in modeled water and energy fluxes. To achieve these goals, a dynamically coupled, process-based and spatially distributed ecohydrological model was used to analyze the key processes, their interactions and feedbacks leading to spatial and temporal soil moisture patterns as well as to assess the impact of topography, soil, precipitation and vegetation on these patterns. This model includes a hydrological process model, a plant growth model and a nitrogen turnover model to generate a time series of soil moisture maps for agricultural areas. These maps were subsequently used to derive autocorrelation properties and scaling behavior.

2. Materials and methods

2.1. The DANUBIA simulation system

The DANUBIA simulation system is a component and raster-based modeling tool designed for coupling models of different complexity and temporal resolution. The model framework controls the temporal course of the simulation as well as the dynamic exchange of data at runtime, thus enabling numerous dynamic feedback effects of the various model components. In its complete structure, DANUBIA consists of 17 components, representing natural as well as socio-economic processes (Barth et al., 2004; Barthel et al., 2012). For the current study, only the ecohydrological components regarding plant growth, soil nitrogen transformation, hydrology, and energy balance were used. These components model fluxes of water, nitrogen and carbon in the soil-vegetation-atmosphere system using physically-based process descriptions. The relevant processes are computed at hourly or daily time steps.

A complete description of the model is beyond the scope of this paper and we refer to previous publications of the components involved, namely Mauser and Bach (2009), Klar et al. (2008), Lenz-Wiedemann et al. (2010) and Muerth and Mauser (2012). Thus, we limit our model description here to the fundamental background needed to understand the model setup.

2.1.1. Hydrology and energy balance component

Vertical water fluxes are modeled using a modified Eagleson approach (Eagleson, 1978). The modification particularly pertains to describing water fluxes in soil by a user defined number of soil layers. Percolation of the upper soil layer is interpreted as effective precipitation for the downward layer. Here we used four soil layers (0-5, 5-20, 20-60, 60-200 cm). The uppermost layer is needed to properly model the water available for evaporation from the soil surface. For other processes (e.g., transpiration, plant water uptake, nitrogen turnover and transfer) only three layers are distinguished. Thus, an aggregated top layer is used for these processes by calculating the weighted mean soil moisture of the 0-5 and the 5-20 cm layer.

Volumetric soil moisture and matrix potential is calculated according to the one-dimensional, concentration dependent diffusivity equation (Philip, 1960). Eagleson (1978) presented an analytical solution of the Philips equation for simplified boundary conditions to model the key processes of soil water movement, namely infiltration, exfiltration, percolation and capillary rise. Each layer is assumed to have homogeneous soil characteristics, described by a set of parameters (e.g., thickness, soil texture, bulk density, organic matter content). Based on these soil parameters, hydraulic parameters are calculated using pedo-transfer functions (Brooks and Corey, 1966; Rawls and Brakensiek, 1985; Wösten et al., 1999). Evaporation from interception storage and from the uppermost soil layer is described by a Penman-Monteith approach. For further details, see Mauser and Bach (2009) and Klar et al. (2008).

2.1.2. Plant growth component

The crop growth model simulates water, carbon, and nitrogen fluxes within the crops as well as the energy balance at leaf level. It models photosynthesis, respiration, soil layer-specific water and nitrogen uptake, dynamic allocation of carbon and nitrogen to four plant organs (root, stem, leaf, harvest organ), as well as phenological development and senescence. Resulting from the interplay of these processes, transpiration is a function of available energy, stomatal conductance (controlled by soil moisture and CO₂), and leaf area (emerging from carbon and nitrogen dynamics). The main concepts and algorithms are adopted from the models GECROS (Yin and van Laar, 2005) and CERES (Jones and Kiniry, 1986) with extensions from Streck et al. (2003a; 2003b) for modeling phenological development. For further details, see Lenz-Wiedemann et al. (2010).

2.1.3. Soil nitrogen component

The soil nitrogen transformation model (Klar et al., 2008) is based on algorithms from the CERES maize model (Jones and Kiniry, 1986). The modeled nitrogen transformation processes are mineralization from two organic carbon pools (easily decomposable fresh organic matter and stable humus pool), immobilization, nitrification, denitrification, urea hydrolysis, and nitrate leaching.

2.2. Model validation

Prior to using the model for the analysis of surface soil moisture patterns, the model was thoroughly validated. The model was parameterized using field measurements (e.g., soil texture), data from maps or literature. A site specific calibration of the model was not performed.

2.2.1. Test site and field data

Field measurements for model validation were carried out at the Selhausen test site (50°52'10''N / 6° 27'4''E, Fig. 1) located in the Rur catchment (Western Germany, see section 2.3.1) for winter wheat, sugar beet, and maize in the growing seasons 2007 / 2008 and 2008 / 2009. The meteorological measurement station and all test fields are located within a 500 meter radius of each other.

Continuous soil moisture measurements were taken in 10 cm depth at two different locations at each of the three test fields with FDR soil moisture stations (Delta-T Devices Ltd., Cambridge, UK). The two measurement locations on each field were 5 m apart. The absolute accuracy of measurements is ± 3 Vol.-% with a relative accuracy of ± 1 % (manufacturer specification, for probe calibration information see Korres et al., 2010). Layer specific soil properties (soil texture, bulk density) for three soil layers (0-30, 30-60, 60-90 cm) were measured according to the sieve-pipette method after DIN 19683-2 (1997) at 20 locations on the winter wheat field in 2007. The measured soil is classified as silt loam with 12 % clay, 71 % silt and 17 % sand for the upper soil layer (mean values from these 20 measurements). The second layer yielded the following clay, silt and sand fractions: 17 %, 68 %, 15 % and the lower soil layer 19 %, 66 %, 15 %. According to the digital soil map provided by the Geological Survey of North Rhine-Westphalia (scaled 1:50000), all measurement fields have the same soil texture. Thus, the measured mean values were used for all model validation runs with the exception of the maize 2008 field, since here the outcrop of

an old river terrace of the river Rhine leads to a high amount of gravel on this particular field. Therefore on this field, the layer specific coarse material content was estimated to 35, 15, and 10 Vol.-%, respectively.

Soil organic carbon and nitrogen (ammonium and nitrate) content was measured in the same depths at the start of each growing season on all fields to provide field specific initial values for the model. Organic carbon and total nitrogen content were determined with an elemental analyzer (CNS Elementaranalysator Vario EL, Elementar Analysensysteme GmbH, Hanau, Germany), ammonium and nitrate with a reflectometer (RQflex plus Reflektrometer, Merk, Darmstadt, Germany).

Organ specific fresh and dry biomass and nitrogen content, leaf area index (LAI), phenological stage, plant height and plant density were determined biweekly on up to 14 dates throughout the growing season. Organ specific biomass samples for stem, leaf, and the harvested organ were taken at three locations within each field. After drying of an organ-specific representative aliquot for 24h at a temperature of 105 °C, average dry biomass was determined. LAI was measured using the LI-3000A Area Meter (LI-COR Bioscience, Lincoln, NE, USA).

Hourly meteorological data (global radiation, precipitation, air temperature, wind speed, air pressure and humidity) were measured at an eddy covariance station (Campbell Scientific, Inc., Logan, USA) located within the winter wheat field. Short data gaps were filled with data from the meteorological tower at the Forschungszentrum Jülich (50°54'37''N / 6°24'34''E, distance to Selhausen test fields: 5.1 km). Cloud cover data was taken from the weather station Aachen (German National Weather Service, 50°47'58''N / 6°1'30''E, distance to Selhausen test fields: 31.1 km). Precipitation measurements were corrected according to Richter (1995). Due to the close proximity of all test fields to the meteorological station in the winter wheat field, these meteorological measurements were used in all validation runs.

2.2.2. Model parameterization and model validation runs

For model validation, the model was run in point mode (no spatial distribution) for each crop and year. Initial conditions and agricultural management were set as indicated in Table 1. Soil moisture at the beginning of the model period is assumed to be at field capacity. The model runs start at the first of October of the previous year to make sure that the modeled soil moisture is independent of the initial conditions. Soil parameters were set as described in

section 2.2.1. The plant growth model was parameterized according to Lenz-Wiedemann et al. (2010) except for parameters from the phenology model, which were adjusted to field observations of the first year (Table 1).

Modeled surface soil moisture, biomass, and LAI were validated against field measurements using three evaluation criteria, the root mean squared error (RMSE), the mean absolute error (MAE) and the normalized measure “index of agreement” (Willmott, 1981). The IA is calculated as:

$$IA = 1 - \frac{\sum_{i=1}^n (M_i - O_i)^2}{\sum_{i=1}^n [|M_i - \bar{O}| + |O_i - \bar{O}|]} \quad (1)$$

where M_i and O_i are simulated and observed values, respectively. \bar{O} is the mean of the observed values and n is the number of data points. A perfect fit between modeled and observed values would result in an IA value of 1.

2.3. Patterns of surface soil moisture

2.3.1. The Rur catchment

The catchment of the river Rur is located in the western part of Germany, covering a total area of 2364 km² with about 140 km² belonging to Belgium and 100 km² to the Netherlands (Fig. 1). The catchment is divided into two major landscape units. The southern part is a low mountain range with forest and grassland characterized by a rolling topography, a mean elevation of about 510 m above sea level, slopes up to 10° and a mean annual precipitation of about 1200 mm. Our study focuses on the northern part of the Rur catchment (1100 km²), since 46 % of the area is farmland. The area is located in the Belgium-Germany loess belt, where crops are grown on a virtually flat terrain (slopes less than 4°). The main crops are winter cereals (mainly winter wheat), sugar beet and maize.

Table 1. Initial biomass after sowing, management dates and parameters of the phenology model (R_{max} , see Lenz-Wiedemann, 2010).

Crop and year (of harvest)	Initial biomass (g m ⁻²)	Sowing / harvesting date (DOY)	Fertilizer date (DOY)	Fertilizer amount (kg N ha ⁻¹)		$R_{max, V1}$ (d ⁻¹)	$R_{max, V2}$ (d ⁻¹)	$R_{max, R}$ (d ⁻¹)
				mineral	organic			
Sugar beet 2008	14.25	114 / 265	115	80	0.033	0.033	0.012	
Sugar beet 2009	14.25	98 / 288	135	80	0.033	0.033	0.012	
Winter wheat 2008	11.875	323 / 219	122	60	0.026	0.035	0.021	
Winter wheat 2009	11.875	291 / 209	59	80	0.026	0.035	0.021	
Maize 2008	4.225	123 / 277	109	36	0.039	0.039	0.034	
Maize 2009	4.225	126 / 262	141	80	0.039	0.039	0.034	
			77	60	0.026	0.035	0.021	
			104	36				
			139	70				
			124	170				
			127	175				
			251	20				

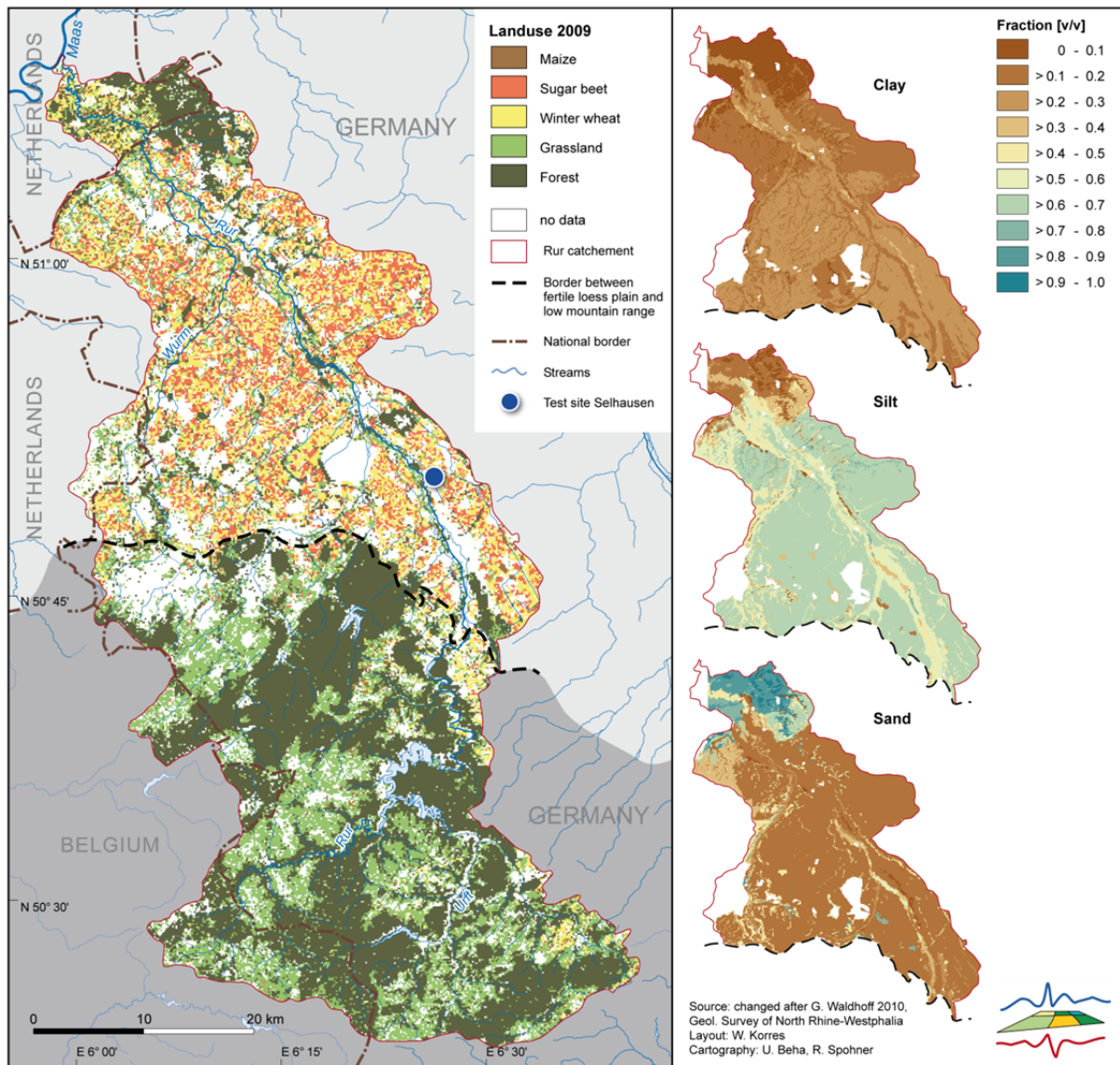


Fig. 1. The Rur catchment with the land use map of 2009, separated into the fertile loess plain in the north and the low mountain range in the south. On the right side, soil texture maps of the top 20 cm of the investigation area are depicted.

The fertile loess plain has a mean elevation of about 100 m above sea level and a mean annual precipitation of about 700 mm. The major soils are Haplic Luvisols and Cumulic Anthrosols near the drainage lines, both with silt loam textures. Soils with a loamy sand texture (Fimic Anthrosols and Dystric Cambisols) are located on the northern edge of the loess plain. Soils close to the Rur are Gleysols and Fluvisols with silty loam and loamy sand textures. Thus, this investigation area is particularly suitable to analyze the effects of vegetation and land use dynamics as well as agricultural management upon soil moisture patterns.

2.3.2. Distributed model runs for northern part of the Rur catchment

Spatially distributed model runs for the year 2009 with a spatial resolution of 150 m were carried out to produce surface soil moisture data for the pattern analysis. Soil properties were derived from a digital soil map (scaled 1:50000, Geological Survey of North Rhine-Westphalia) for each pixel and soil layer. Land use information (Fig. 1) was gathered from a multitemporal land use classification (Waldhoff, 2010). In the investigation area, 20299 pixels are classified as cropland (54 % winter cereals, parameterized as winter wheat, 41 % sugar beet, 5 % maize). For spatially distributed model runs, meteorological data from 19 stations of the German National Weather Service within or in direct proximity (< 20 km) to the Rur catchment were used to derive the necessary meteorological model input. The measurements were spatially interpolated using the method described by Mauser and Bach (2009). Prior to interpolation, precipitation data was corrected according to Richter (1995). Data on agricultural cultivation as recorded at the Selhausen test site for 2009 (Table 1) was applied throughout the investigation area.

To analyze the respective impact of the spatial patterns of meteorological parameters, land use, and soil properties upon the surface soil moisture patterns, additional model runs were performed using homogeneous inputs for i) meteorology, using measurements at Selhausen for the whole investigation area, ii) land use, assuming all agricultural pixels to be winter wheat and iii) soil texture, using the soil texture of the validation model runs throughout the investigation area.

2.3.3. Pattern analysis

Modeled patterns of daily surface soil moisture on arable land were analyzed in terms of structure, scaling properties and their temporal variation.

Structure analysis

For the analysis of the structure of surface soil moisture patterns, a global spatial autocorrelation coefficient (SAC) was calculated for different step widths. At a step width of 1, each pixel is paired with its direct neighbors in all 8 directions (Fig. 2). Pairs with no data values (e.g., due to a non-agricultural land use class) were discarded. The SAC was then calculated as the Pearson correlation coefficient over values of all remaining pairs. For larger step widths, only pairs in the directions of the queen's move in chess were used (Fig. 2). Values of SAC were only calculated for sets of pairs containing a minimum of 100 data pairs,

which was the case for all evaluated step widths up to 260. In addition to the analysis of daily soil moisture patterns, the SAC was calculated for spatially distributed soil properties (soil texture and soil hydraulic conductivity).

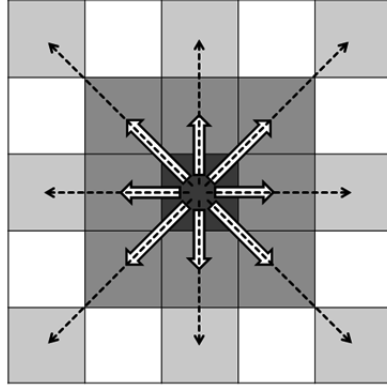


Fig. 2. Exemplary illustration of the pairing for the spatial autocorrelation coefficient for two step widths. For step width 1, the center pixel in dark grey is paired with its direct neighbors (bold white arrows). For step width 2, the center pixel is again paired with pixels in all eight directions, but the distance from the center pixel is extended by one pixel (dashed black arrows). This is done for every pixel and up to a step width of 260.

Scaling analysis

Starting from the model's spatial resolution of 150 m, which is referred to as grain size 1, the scaling behavior of surface soil moisture patterns was analyzed by aggregating the pixels to an increasingly coarser grain size of 2 (2 x 2 pixels), 3 (3 x 3 pixels), and so forth up to grain size 37. According to Qi and Wu (1996), aggregation starts in the upper left corner of the grid. Aggregated pixels were assigned the mean value of the original pixels. Aggregated pixels were discarded if the totaled area of winter wheat, sugar beet, and maize occupied less than 30 % of the pixel area.

The scaling behavior of surface soil moisture can be quantified by the slope of a power law relationship computed from the spatial variance (Rodriguez-Iturbe et al., 1995):

$$\sigma_{\lambda}^2 = \left(\frac{\lambda}{\lambda_0}\right)^{\beta} \sigma_{\lambda_0}^2 \quad (2)$$

where λ_0 is the reference scale, λ is the grain size, σ^2 the soil moisture's variance at scale λ , and β is the scaling factor of the scaling function. β was derived by least square fitting to pairs of λ and σ_{λ}^2 from grain size 2 to 37, setting λ_0 to grain size 1. A small value of β corresponds to a high spatial correlation in the data (a perfect correlation across all computed scales

provides a slope value of 0 while no correlation results in a value of -1 (Manfreda et al., 2007; Whittle, 1962).

To further investigate the spatial patterns at different spatial scales, the SAC with a step width of 1 was calculated for grain sizes 2 to 37 (corresponding to a pixel size of 0.3 km x 0.3 km to 5.55 km x 5.55 km). In both analyses, larger grain sizes were not analyzed because the number of valid pairs for the calculation of SAC was below 100.

3. Results and discussion

During the growing season, soil moisture dynamics is strongly influenced by the water uptake of the vegetation. In turn, water demand of the vegetation strongly depends upon vegetation type and development state. Thus it is important, that vegetation dynamics are adequately modeled regarding temporal dynamics as well as spatial patterns. Therefore prior to discussing the results of the model validation for surface soil moisture, we present the validation for the plant growth model.

3.1. Model validation

3.1.1. Biomass and LAI

An overview about the temporal course of key plant parameters (biomass and LAI) for different crops and years is provided in Fig. 3. While the green LAI and the total biomass are of prime importance in the given context, the plant growth model also provides organ specific data for leaf, stem, root and grain. The latter parameters are summarized in Table 2.

Table 2. Results of the model validation for the crop growth model. Indices are the Root Mean Square Error (RMSE), the Mean Absolute Error (MAE), and the Index of Agreement (IA). Aboveground biomass is defined here as the sum of living leaf, stem, and harvest organ dry biomass.

Crop and year (of harvest)	Winter wheat 2008			Winter wheat 2009			Sugar beet 2008			Sugar beet 2009			Maize 2008			Maize 2009		
	RMSE	MAE	IA	RMSE	MAE	IA	RMSE	MAE	IA	RMSE	MAE	IA	RMSE	MAE	IA	RMSE	MAE	IA
plant variables																		
Green LAI	0.49	0.40	0.98	0.96	0.74	0.96	1.25	1.05	0.84	1.91	1.40	0.81	0.41	0.34	0.85	0.58	0.46	0.95
Living leaf (g m ⁻²)	96	85	0.75	41	30	0.96	301	248	0.65	144	109	0.90	70	63	0.63	72	58	0.85
Stem (g m ⁻²)	99	84	0.95	239	125	0.90							141	115	0.91	183	106	0.91
Harvest organ (g m ⁻²)	101	74	0.99	318	235	0.90	237	198	0.98				117	76	0.99	120	68	0.99
Aboveground biomass (g m ⁻²)	278	156	0.96	188	130	0.98	348	217	0.97				194	122	0.98	328	166	0.96

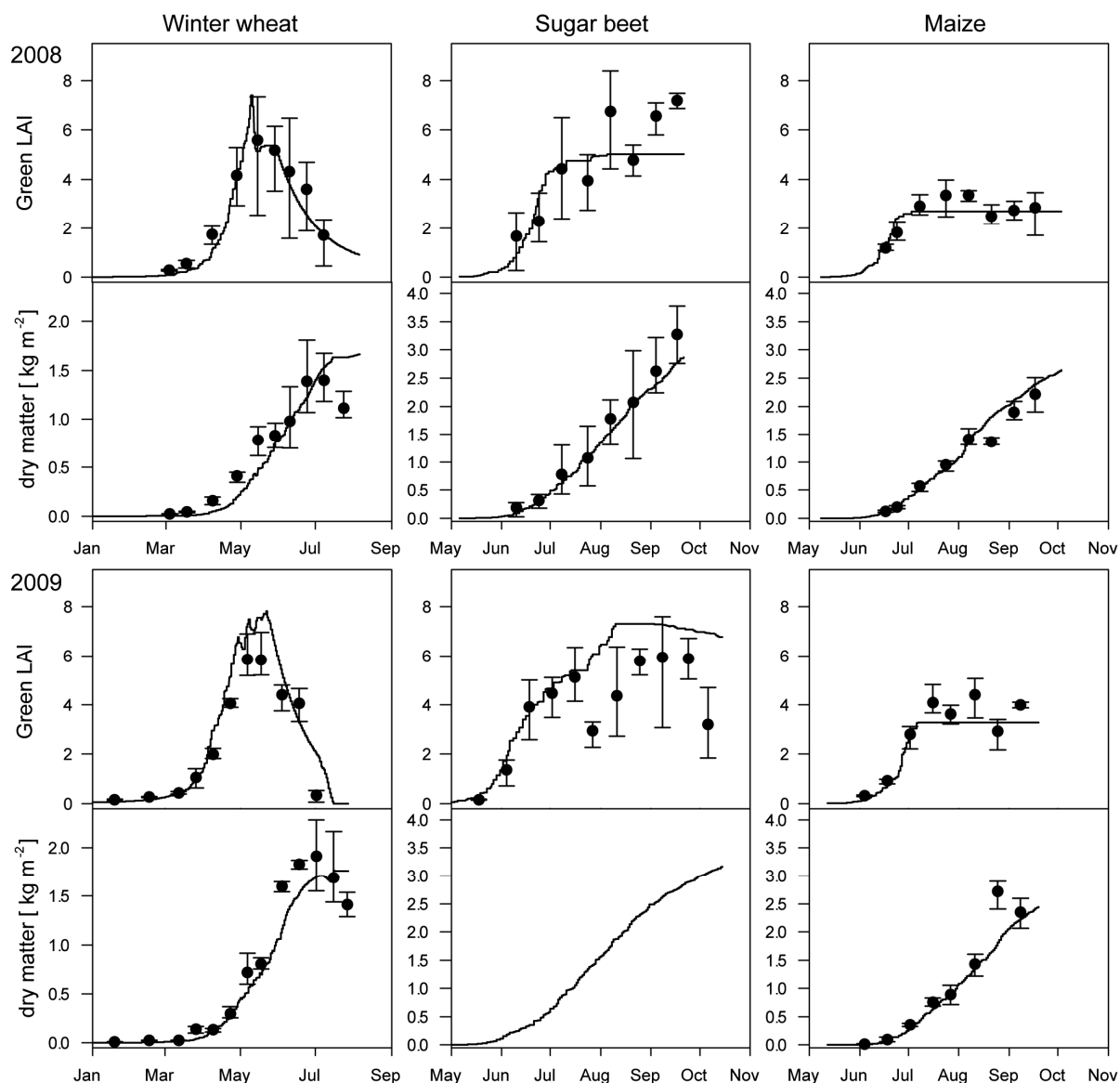


Fig. 3. Green LAI and aboveground biomass (living leaf, stem and harvest organ dry biomass) for winter wheat, sugar beet and maize for the years (of harvest) 2008 and 2009. Measured values (field means) are depicted as dots, bars represent the span of the measurements and modeled values are displayed as lines. Field measurements of the sugar beet biomass in 2009 were not available.

Fig. 3 shows a very good agreement of the measured and modeled dry matter biomass and LAI. Typically, the model results are within the range of the field measurements denoted by the vertical bars (Fig. 3). Moreover, the model results are very close to observed mean values, despite the large within-field variability especially in the case of the green LAI for sugar beet and winter wheat. The biomass buildup for winter wheat was slightly delayed in 2008, while the LAI was modeled quite accurately. In the case of sugar beet, deviations of modeled and measured green LAI are evident from mid-July onwards in both years with a tendency to overestimate in 2008 and underestimate in 2009. Biomass was reproduced very

well in 2008. Validation data of dry biomass for sugar beet in 2009 were not available. The modeled biomass and LAI of maize agrees very well with the measurements.

Table 2 provides an overview about the performance of the plant growth model. For all test fields, the index of agreement (IA) for the total aboveground biomass yields values of 0.96 or higher, which indicate very good agreement between model and measurement. Green LAI is also modeled quite well with IA-values that range from 0.81 to 0.98. Moreover the results of the different organs are modeled well, providing evidence that not only the bulk model parameters, but also the processes leading to these results are modeled suitably well.

Leaf area is a limiting factor for transpiration and carbon uptake. Both processes are directly coupled due to common stomatal conductance. The buildup of biomass in turn depends on carbon uptake. Therefore, model performance with respect to green LAI and biomass supports our confidence in the modeled transpiration amounts.

Thus, we are confident that the model performance is sufficiently accurate to adequately simulate key impacts of plant growth dynamics upon the temporal course and spatial dynamics of soil moisture.

3.1.2. Soil moisture: Detailed example

A comparison of modeled and measured soil moisture is presented in Fig. 4 for the example of sugar beet 2008. Since the model was started on the first of October of the previous year, the model results are independent of the assumed initial soil moisture conditions. Due to tillage of the fields, the soil moisture probes were installed in mid-June. Thus no earlier measurements are available. To show the spatial variability of the soil moisture measurements, the measurements of both sampling locations per field are depicted in the figures (Fig. 4 and Fig. 5). The statistical indices cited in the text and in Table 3 refer to the average of these two measurements.

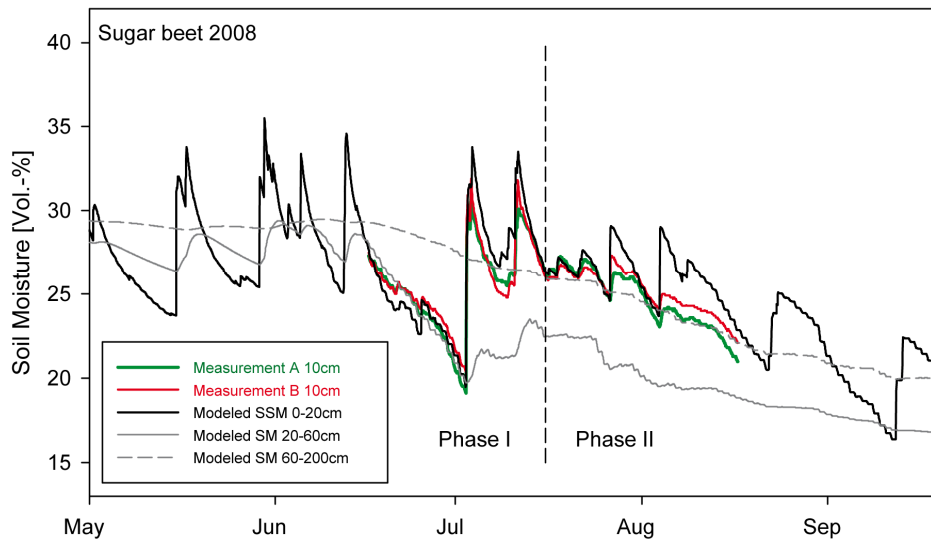


Fig. 4. Modeled and measured surface soil moisture (SSM) and soil moisture (SM) for the sugar beet field 2008.

The modeled soil moisture in the uppermost layer (Fig. 4) shows distinct peaks related to precipitation events followed by characteristic decreases due to evapotranspiration from the soil surface and percolation into the next soil layer when modeled soil moisture exceeds field capacity (28.6 Vol.-%). The deeper soil layers show a damped temporal course of the soil moisture. In June, the sugar beet roots reach the lowest soil layer. This is when the modeled soil moisture in the deepest layer starts to decline. A significant recharge of the lowest soil layer was not modeled during the vegetation period. Thus precipitation during the vegetation period is entirely used for evapotranspiration and to a lesser degree for surface runoff.

The model results for the uppermost soil layer agree very well with the measurements at both measurement locations, particularly until mid-July. Thereafter, the model overestimates soil moisture especially immediately after precipitation events but approximates observations in the drying phases. In contrast to the preceding precipitation events where infiltration was only slightly overestimated, in phase II the model simulates an infiltration which is more than twice as high as indicated by measured soil moisture particularly during the precipitation event on 26 July 2008. Starting with that event, modeled soil moisture deviates significantly from observations. During phase I, which we defined as the time prior 16 July 2008, the RMSE is 1.3 Vol.-%, thereafter (phase II) it increases to 2.0 Vol.-%, respectively (Table 3).

Table 3. Results of the model validation for surface soil moisture. Indices are the Root Mean Square Error (RMSE), the Mean Absolute Error (MAE), and the Index of Agreement (IA). Phase I + II denotes the indices for the validation over the whole measurement period. The phase change is defined on 16 July (DOY 198) for the year 2008 and 9 July (DOY 190) for the year 2009 and divides the validation period.

Crop and year (of harvest)	Winter wheat 2008			Winter wheat 2009			Sugar beet 2008			Sugar beet 2009			Maize 2008			Maize 2009		
	RMSE	MAE	IA	RMSE	MAE	IA	RMSE	MAE	IA	RMSE	MAE	IA	RMSE	MAE	IA	RMSE	MAE	IA
Phase I + II	2.1	1.6	0.92	2.6	2.0	0.77	1.8	1.4	0.91	1.3	1.0	0.95	6.4	5.6	0.54	7.8	6.7	0.57
Phase I							1.3	1.0	0.95	2.5	2.0	0.67	3.0	2.8	0.78	2.5	2.3	0.75
Phase II							2.0	1.5	0.87				7.2	6.6	0.47	9.8	9.5	0.31

This change in model behavior can be attributed to a change in soil surface properties affecting the infiltration properties. Possible processes leading to the changes at the soil surface might be clogging of the pores by siltation or crust formation. However, these processes might have occurred particularly on loess soils as a result of the strong precipitation event on 10 July 2008 and the following drying period. The model is not calibrated and model parameters are derived from measured soil texture and pedo-transfer functions. It appears, that at the beginning of the year, this parameterization results in a suitable representation of the infiltration process, while the infiltration process appears to be retarded in the second half of the year. As the soil properties are derived from pedo-transfer functions, a change in surface properties is not represented by the model. To test the assumption of a change of the soil surface conditions, we ran the model for sugar beet 2008 assuming a reduced infiltration capacity of 1.8 mm h^{-1} instead of the original values between 6 and 8 mm h^{-1} . This change resulted in an improvement of the RMSE from 2.0 Vol.-% to 1.7 Vol.-% for phase II, while the overall RMSE for the whole period improved from 1.8 Vol.-% to 1.6 Vol.-%. A similar effect can be observed for maize 2008 (starting on the same date) and maize 2009 after 6 July 2009. For winter wheat, this effect was not observed (Fig. 5).

3.1.3. Soil moisture: overview

The modeled and measured course of surface soil moisture for all crops for 2008 and 2009 is shown in Fig. 5. For sugar beet 2008 as well as for winter wheat 2008, measured values are reproduced well with RMSE values of 1.8 and 2.1 Vol.-%, respectively (compare Table 3 and Fig. 5). In the case of winter wheat 2009, RMSE is slightly higher with a value 2.6 Vol.-% which is mainly due to overestimation after 27 June 2009. After establishment of canopy closure ($\text{LAI} > 2$) by sugar beet and maize, these differences decrease and the CV declines to values of around 14 % in mid-July. The second increase of the CV that starts in mid-August and peaks at 23 % in the beginning of October is again caused by the different phenological development of wheat and sugar beet / maize. In the case of maize 2008, the model slightly overestimates the measured soil moisture. This may be related to the very high percentage of coarse material in the soil of the maize field 2008 (outcrop of gravel from a former river terrace) causing also relatively low observed surface soil moisture between 6 and 24 Vol.-% compared to the other validation examples.

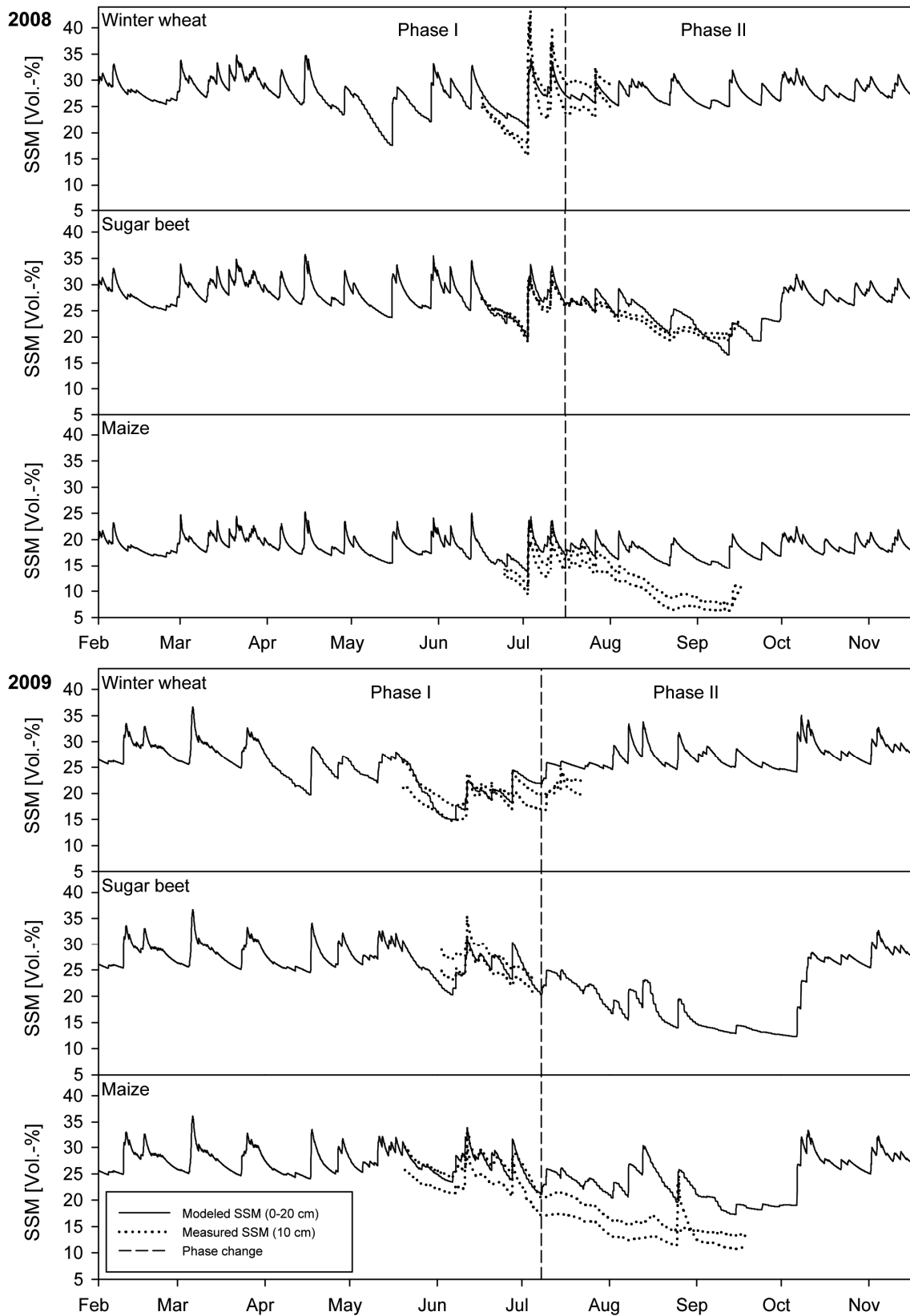


Fig. 5. Modeled and measured surface soil moisture (SSM) for winter wheat, sugar beet and maize for the years (of harvest) 2008 and 2009. The dashed line indicates the change from phase I to phase II.

For both years, the modeled surface soil moisture and the measurements agree well during the first part of the year (phase I). After 16 July 2008 and after 9 July 2009 (beginning of phase II), model results for sugar beet and maize systematically deviate from the measurements: The amplitude of the modeled surface soil moisture is henceforth significantly larger than the observed data. As indicated above in the detailed example of the sugar beet 2008, this behavior hints towards a change in soil surface properties for root crops. Calibrating the infiltration capacity for maize, comparable to the sugar beet 2008, the RMSE improved during phase II from 7.2 Vol.-% in 2008 to 3.3 Vol.-% and from 9.8 Vol.-% in 2009 to 1.7 Vol.-% yielding an overall RMSE for the whole period of 3.2 Vol.-% in 2008 and 2.1 Vol.-% in 2009. After harvesting of sugar beet and maize, which occurred in 2008 in early October, while sugar beet in 2009 was not harvested until 15 October 2009, the temporal course of the surface soil moisture is very similar in all crops.

The RMSE between modeled and observed surface soil moisture for both years and all crops ranges from 1.8 to 7.8 Vol.-% (see Table 2). Considering only phase I for root crops, the RMSE shows values between 1.3 and 3.0 Vol.-% which indicates a) the good performance of the model and b) that obviously a change in infiltration conditions occurred for root crop fields and that this effect should be taken into account. As shown above, modeled surface soil moisture has a much lower RMSE at the beginning of the measurements. Therefore, it can be assumed that the RMSE for the whole year is lower than in the validation period. However, an appropriate model to account for the observed change in infiltration conditions is not available.

All results presented above were derived using measured soil parameters from the test site Selhausen. For spatially distributed model runs, a digital soil map provided by the Geological Survey of North Rhine-Westphalia was used. The soil map provides generalized information of the soil texture, thus resulting in a larger uncertainty of the soil parameters as compared to the soil parameterization based on field measurements of the soil texture. Using data from the digital soil map instead of the measured soil data to estimate the model parameters for the test fields in Selhausen yielded an average RMSE of 5.5 Vol.-% and thus an increase by 2.1 Vol.-%. The maize 2008 field was disregarded in this analysis, since it is an exceptional case due to its high gravel content and since it is atypical for most of the agricultural area. In general, utilizing the model parameterization based upon the soil map resulted in an overestimation of the soil moisture. This is due to the higher percentage of

clay in the soil texture from the soil map, which results in higher field capacities by approx. 5 Vol.-% as compared to the measured soil texture.

The validation shows that the model simulates plant growth, plant water uptake, and surface soil moisture with sufficient accuracy and thus provides suitable base data for the analysis of surface soil moisture patterns. However, discrepancies between modeled and observed soil moisture, especially in phase II of the growing season should to be taken into account in further analyses, since these were not corrected in the spatially distributed model runs, since a model to account for these abrupt changes in infiltration properties is currently not available.

3.2. Soil moisture patterns in the Rur catchment

3.2.1. Model results

Fig. 6 shows the temporal course of the spatial mean soil moisture along with the precipitation and evaporation for the investigation area for 2009. The mean surface soil moisture calculated from the 20299 pixels is highly responsive to precipitation events. The average spatial mean soil moisture during the main growing season (defined from DOY 103, when LAI of the winter wheat reaches 2, to DOY 288, when sugar beet is harvested) is 26.4 Vol.-% (Min.: 21.0 Vol.-%, Max.: 32.6 Vol.-%) and 28.9 Vol.-% (Min.: 25.0 Vol.-%, Max.: 33.8 Vol.-%) for the rest of the year. The difference in the average soil moisture is mainly due to evapotranspiration. The spatial coefficient of variation (CV, Fig. 6) describes the (mean-) normalized variability of soil moisture and increases during the course of dry periods, while precipitation events lead to a reduction of the CV. Very low CV values are observed in winter and spring until the end of March and in late fall and winter with values around 12 %. A period of high CV starts in April with a peak (22 %) in the beginning of June, due to the strong spatial variability of water uptake related to the differences in phenological development of winter wheat and sugar beet / maize. Wheat is harvested earlier (DOY 209), thus the differences in evapotranspiration of bare soil (harvested winter wheat) and the later harvested crops (DOY 262 for maize and DOY 288 for sugar beet) together with the low precipitation amounts result in an increase of the CV until the end of September.

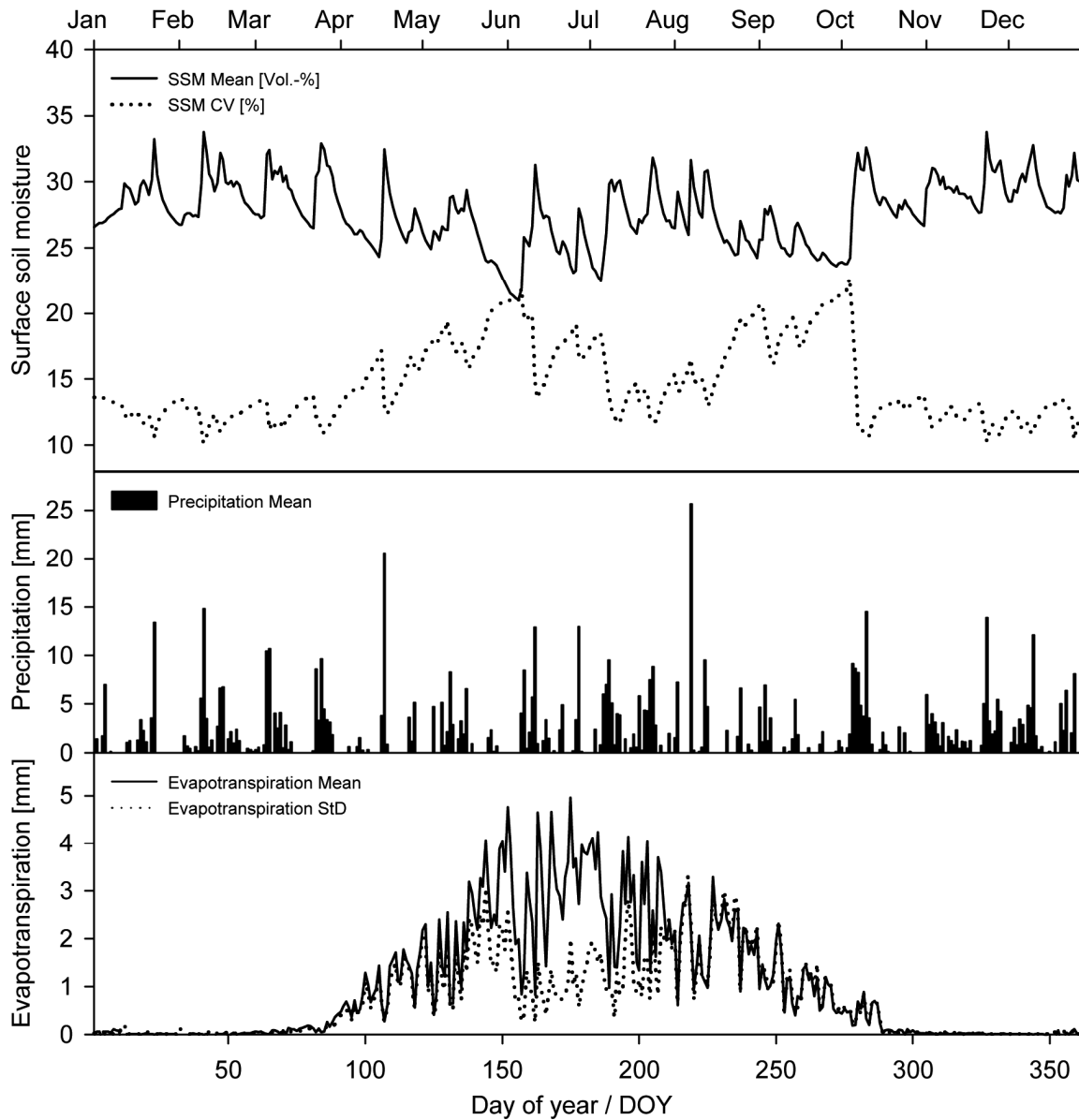


Fig. 6. Spatial mean surface soil moisture, precipitation and evapotranspiration over all 20299 pixels of the investigation area of the year 2009. In addition, the coefficient of variation (CV) of surface soil moisture and the standard deviation (StD) of evapotranspiration is depicted with dotted lines.

In general a highly significant negative exponential relationship between the CV and the mean surface soil moisture (msm) can be found (p-value: 0.01):

$$CV = 97.495 e^{-0.069 \text{ msm}} \quad (R^2 = 0.75) \quad (3)$$

In agreement with findings of other studies (Choi and Jacobs, 2007; Choi and Jacobs, 2011; Famiglietti et al., 1999; Koyama et al., 2010) the variability of surface soil moisture patterns increases with decreasing mean soil moisture. Some studies also found positive relationships between mean soil moisture and soil moisture variability. However, these

investigations were conducted on a hill slopes or at small catchments scale with homogeneous land use (grassland) and with significant slopes (Famiglietti et al., 1998; Western and Grayson, 1998). The combined effects of soil texture, vegetation, topography, and scale of analysis may lead to different relationships between spatial variability and mean soil moisture (Famiglietti et al., 1998).

The average CV over time (CV separately calculated for the whole year time series of every pixel and then averaged over all pixels) is highest for the second layer (layer 1: 11.0 %, layer 2: 14.0 % and layer 3: 11.4 %) due to the replenishing effect of precipitation in the top soil layer and the larger thickness and water storage capacity of the bottom layer. The dependence of the temporal soil moisture upon precipitation events and soil layer depth becomes evident by calculating the temporal CV for a 10 days moving window. The highest short time temporal variability was found for the uppermost soil layer (CV: 5.7 %), while layer 2 provides a CV-value of 2.6 % and layer 3 1.0 %.

The spatial distribution and variability of the modeled surface soil moisture is shown exemplarily for two days (Fig. 7): 29 January 2009 (DOY 29) and 21 August 2009 (DOY 233). For reasons of comparability, the dates were chosen with the condition that no precipitation occurred in the whole catchment on five consecutive prior days. DOY 29 shows a slightly higher mean value of 27.4 Vol.-% as compared to 25.6 Vol.-% on DOY 233. Both maps show very dry areas in the sandy north-western part and very wet areas mostly in proximity to the river Rur. The high values are due to soils with high organic content or high clay content. The general soil moisture patterns are determined by the pattern of the soil texture, particularly on DOY 29 (compare Fig. 1). While large scale soil moisture patterns relating to the soil texture are still discernible in summer, strong small scale variability can also be observed. The large small scale variability in late August is due to small scale land use patterns and the related differences of evapotranspiration, which range from low values of bare soil (harvested winter wheat) to high values for late season other crops (sugar beet, maize). The spatial CV (13.1 % for DOY 29, 17.2 % for DOY 233) supports this visual impression.

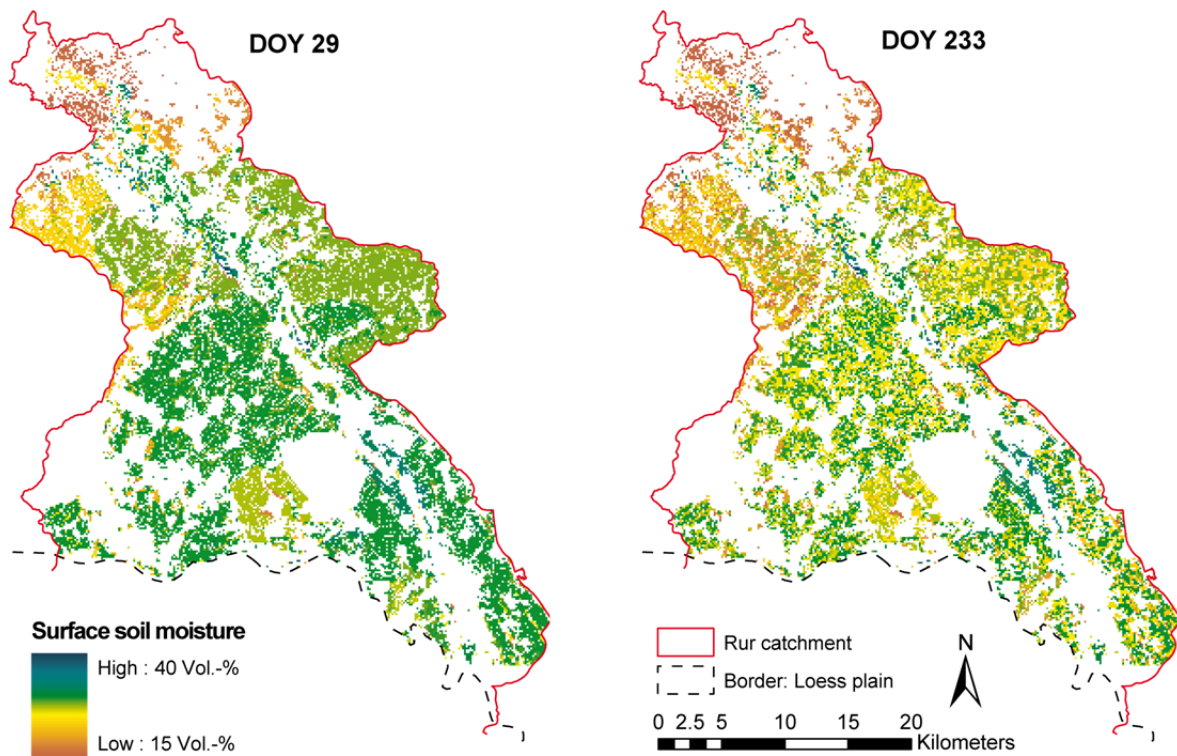


Fig. 7. Spatial distribution of surface soil moisture (top 20 cm) in the investigation area on 29 January (DOY 29) and 21 August 2009 (DOY 233).

3.2.2. *Spatial patterns*

The spatiotemporal patterns of surface soil moisture were analyzed using the spatial autocorrelation coefficient (SAC) for each day of 2009 at step widths (compare Fig. 2) ranging from 1 to 260 pixels (from 150 m distance to 39 km). In Fig. 8, SAC is shown as a color coded two-dimensional graph. The temporal change of autocorrelation is easily visible by tracing the same color code along the time axis. The step width at a certain value of SAC is the autocorrelation length. In order to relate the SAC of the surface soil moisture to influencing parameters, the SAC for soil texture and soil hydraulic conductivity (SHydCon), as well as time series of precipitation and evapotranspiration (mean and standard deviation) are presented. To separate the influences of land use, weather, and soil texture on surface soil moisture patterns, we conducted simulations of reduced complexity by respectively keeping one of these variables spatially homogeneous (Fig. 8 B, C, D).

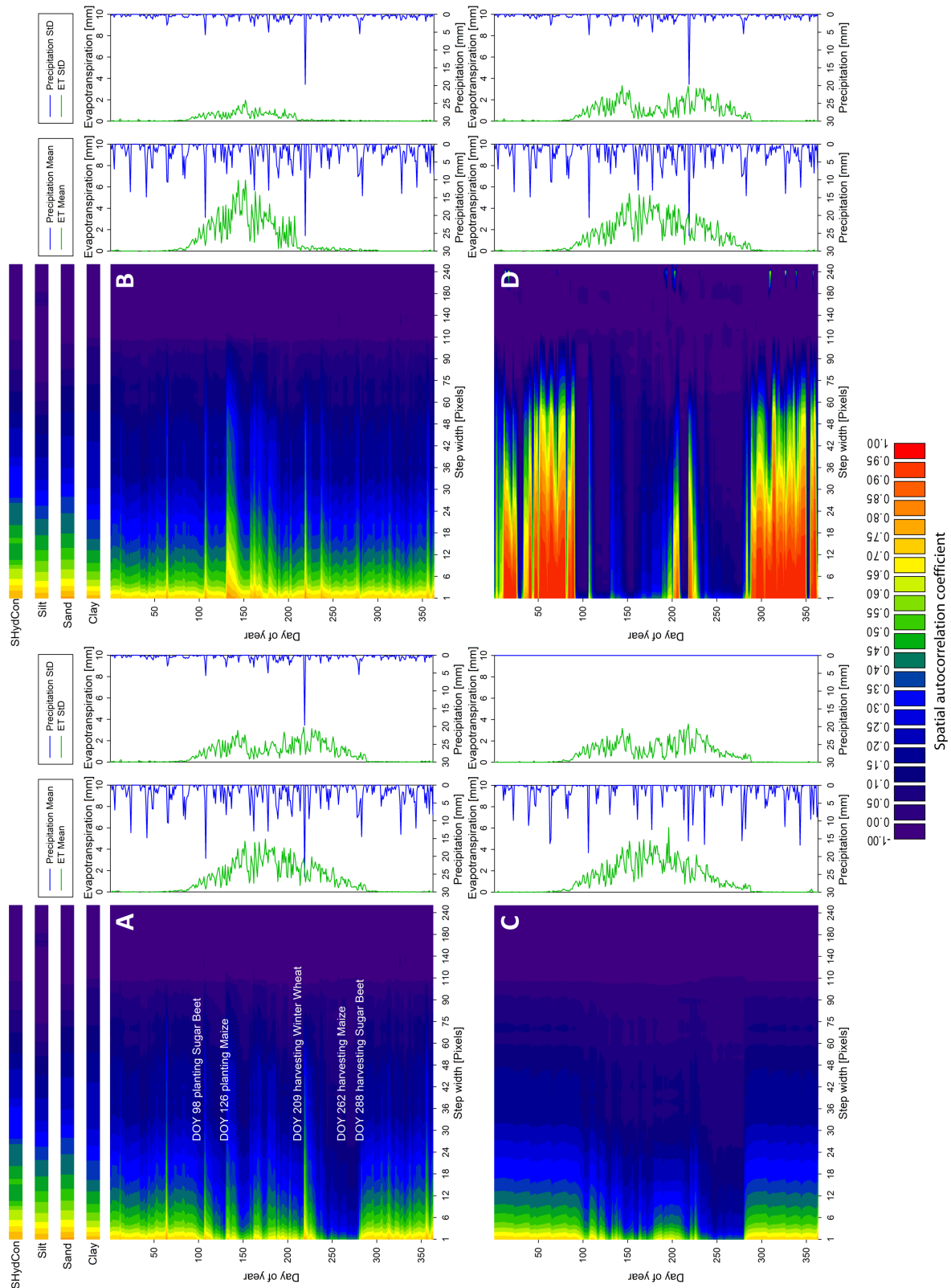


Fig. 8. Spatial autocorrelation coefficient (SAC) of surface soil moisture for different step widths for four different model runs: A) the reference run which represents the full complexity of the investigation area, B) a uniform land use model run, with winter wheat occupying all 20299 pixels, C) a uniform meteorology model run using the measured meteorological values at Selhausen throughout the investigation area, and D) a uniform soil model run assuming the soil properties from the Selhausen test site for each pixel in the investigation area. The temporally constant SAC of soil hydraulic conductivity (SHydCon) and soil texture (the same for all model runs) is depicted above and the course of precipitation and evapotranspiration (spatial mean and standard deviation of the investigation area) to the right of the corresponding model run.

The spatial autocorrelation for soil moisture was computed for: A) the reference run which represents the full complexity of the investigation area, B) a uniform land use model run, with winter wheat occupying all 20299 pixels, C) a uniform meteorology model run using the measured meteorological values at Selhausen throughout the investigation area, and D) a uniform soil model run assuming the soil properties from the Selhausen test site for each pixel in the investigation area. In general, SAC declines with increasing step width (Fig. 8) but the course of this decline and therefore the autocorrelation length changes throughout the year. For the first and last quarter of the year, where fields are fallow, all simulations - except for the homogeneous soil simulation - show similar autocorrelation lengths, resembling autocorrelation lengths for soil clay content. This indicates the dominating pattern generating role of the soil in the given period. On the other hand, differences between the reduced complexity simulations and the full simulation are noticeable: The homogeneous land use simulation (Fig. 8 B) lacks periods of very low SAC values, the homogeneous meteorology simulation (Fig. 8 C) lacks distinctive spikes after precipitation events, and the homogeneous soil simulation (Fig. 8 D) shows higher SAC values. These differences are now examined in more detail.

Considerable deviation between the full simulation (Fig. 8 A) and the homogeneous land use simulation (Fig. 8 B) starts around DOY 100 where SAC drops below 0.8 at a step width of 1. From this time on, significant evapotranspiration of winter wheat becomes noticeable, which in the full simulation increases spatial variability as the sugar beet and maize areas still lie fallow or are just planted. This also shows up in the standard deviation of evapotranspiration that is much smaller in the homogeneous land use simulation (Fig. 8 B). The spatial variability caused by differences in water uptake between the different crops is much larger than that resulting from weather or soil. After harvest of winter wheat on DOY 209, ongoing evapotranspiration of maize and sugar beet contrasted by fallow winter wheat area causes the very low autocorrelation lengths. These conditions persist until the soil-like patterns reemerge after all crops are harvested on DOY 288.

In contrast to the full simulation (Fig. 8 A), the homogeneous weather simulation (Fig. 8 C) does not show the short distinct increases of spatial autocorrelation after precipitation events. During these peaks, autocorrelation lengths rise beyond those for clay content. Without the spatial variability of precipitation, the soil is filled at similar rates of precipitation thus preserving or restoring the prevailing patterns induced by the soil. The large scale pattern of precipitation is superimposed on the otherwise prevailing patterns causing

increase of correlation lengths (compare Fig. 8 A, B). For some precipitation events, this increase is more pronounced, due to the changing spatial variability and amount of the precipitation and preceding soil moisture conditions. This effect is even stronger in the homogeneous land use simulation, where the pattern is not disturbed by the small scale spatial variability due to transpiration by different crops.

The high autocorrelation lengths in the homogeneous soil simulation (Fig. 8 D) occur outside the main growing season. Due to the absence of a soil induced pattern and no significant spatial variability of evapotranspiration, soil moisture patterns are predominantly determined by precipitation patterns. When no precipitation occurs, soil moisture is determined by field capacity removing all large scale variability and thus causing very low autocorrelation lengths (e.g., Fig. 8 D at about DOY 30 and 355). During the growing season, the high spatial variability of surface soil moisture due to the heterogeneous evapotranspiration persists even during precipitation events preventing high autocorrelation lengths as noticed outside the growing season. Only two precipitation events within the growing season result in noticeable autocorrelation lengths. At that time, soil moisture is close to field capacity, which is spatially invariant in the homogeneous soil simulation. Therefore large scale precipitation patterns instead of small scale evapotranspiration patterns determine the soil moisture patterns.

Model validation revealed an overestimation of surface soil moisture in the second phase of the growing season for sugar beet and especially for maize. The higher soil moisture makes sugar beet and maize pixels more similar to fallow pixels (former winter wheat pixels). It counteracts the small scale variability of surface soil moisture induced by differences between bare soil and the remaining crops at this time. Without the overestimation, the small scale differences between bare soil and sugar beet or maize were larger, leading to an increased degradation of the larger autocorrelation lengths.

In summary, it can be stated that in the beginning of the year at times when the overall soil moisture is high, the surface soil moisture patterns depend upon the soil properties (spatial differences of field capacity). In the main growing season, the larger scale pattern induced by soil properties is diminished by the small scale land use pattern and the resulting small scale variability of evapotranspiration. Due to their high autocorrelation lengths, precipitation events enlarge soil moisture autocorrelation lengths for a short time even beyond the range induced by soil properties. The strength of this effect depends upon the variability

and precipitation amount of the events and upon preceding soil moisture conditions. After the growing season, the patterns are again mainly determined by the soil properties.

3.2.3. *Scaling*

Spatial patterns of surface soil moisture have been shown to depend upon patterns of the controlling factors weather, soil properties, and land use. Over the course of the year, the small scale pattern of land use and the large scale pattern of precipitation superimpose on patterns of soil properties as the predominant factor for soil moisture patterns. This has been shown for the spatial resolution of the model run (150 m). In order to analyze these dependencies on coarser spatial scales, model results were gradually aggregated to lower spatial resolutions (higher grain sizes) and the autocorrelation analysis (with step width 1) was repeated for each level of aggregation. In Fig. 9, results are presented in a way similar to the presentation of the pattern analysis. For grain size 1, the data equals the data for step width 1 in Fig. 8. Starting from values around 0.75, SAC peaks at 0.84 at a grain size of 5 (Fig. 9 A). With increasing aggregation levels, SAC tends to decrease showing a course closely resembling that of soil texture. During most of the year, SAC drops below 0.6 at a grain size of 27. At several dates this course is interrupted by very short periods of elevated SAC (horizontal structures in Fig. 9 A). This can be assigned to precipitation events that also appeared in the pattern analysis. The large scale patterns of these events are superimposed on the soil patterns and cause higher autocorrelation even at high grain sizes. In the beginning of the growing season, SAC declines at low grain sizes (Fig. 9 A, after DOY 103). High spatial small scale variability of evapotranspiration strongly disturbs the prevailing patterns. The impact of the high spatial variability of evapotranspiration can be assessed by comparing the results to a homogeneous land use simulation (Fig. 9 B) where for example SAC at a grain size of 1 is reduced by a value of 0.3 at DOY 270. This difference decreases at higher grain sizes until it becomes less than 0.1 at a grain size of 9 and less than 0.05 at a grain size of 23. This behavior persists throughout the growing season and is interrupted by periods of strong rainfall, as described above.

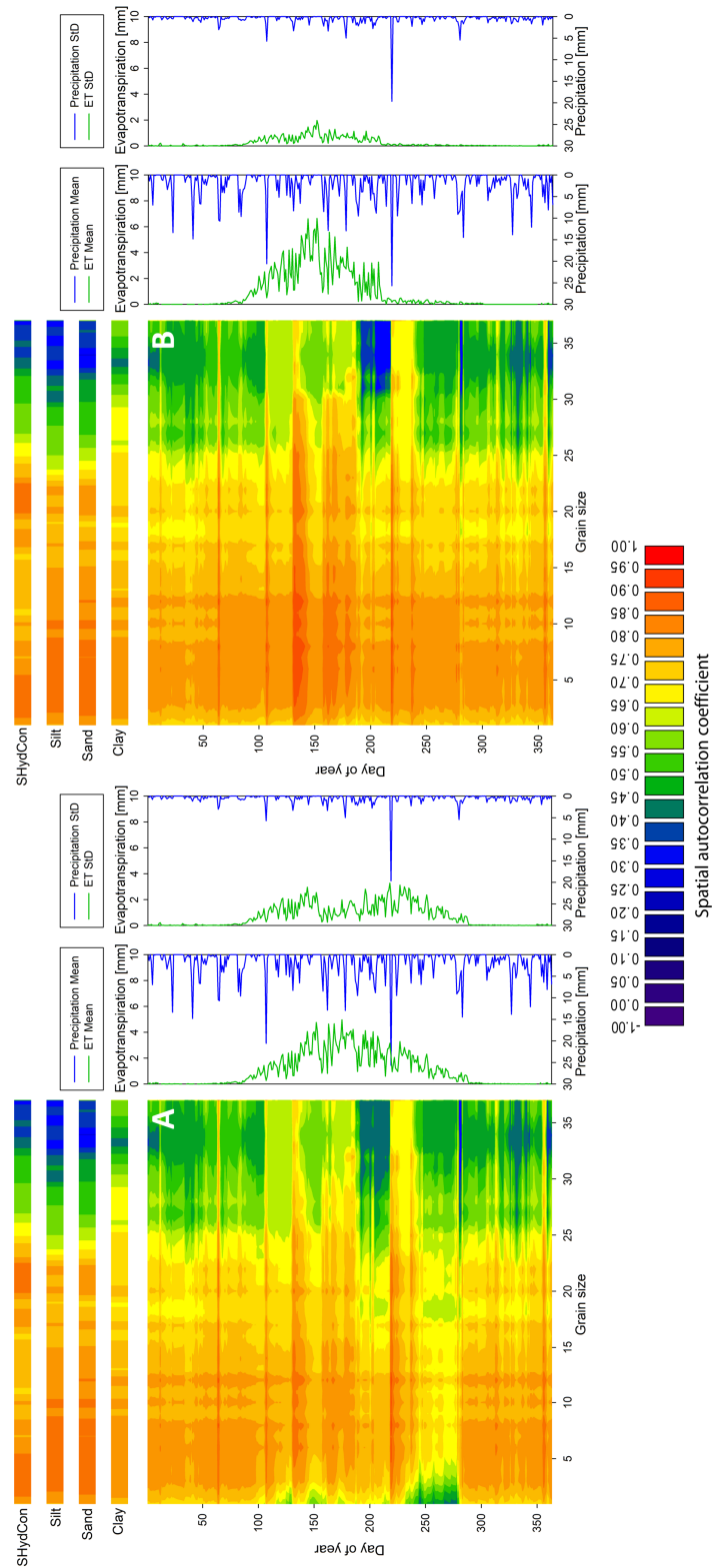


Fig. 9. Spatial autocorrelation coefficient (SAC) of surface soil moisture for different grain sizes for two different model runs: A) the reference run which represents the full complexity of the investigation area, B) a uniform land use model run, with winter wheat occupying all 20299 pixels. The temporally static SAC of soil hydraulic conductivity (SHydCon) and soil texture (the same for all model runs) is depicted above and the temporal course of precipitation and evapotranspiration (spatial mean and standard deviation of the whole investigation area) to the right of the corresponding model run.

In summary, surface soil moisture patterns are determined by soil patterns across the analyzed scales. Land use patterns disturb these patterns in times of high evapotranspiration, but disturbance decreases with coarser spatial resolution. Precipitation typically results in large scale patterns that are superimposed upon other patterns at all scales for a short time. These scaling properties are in part a result of the specific field sizes and management structures in the northern part of the Rur catchment and might not apply to areas with a significantly different agricultural field structure.

The scaling behavior of patterns is of importance when data are to be scaled down to finer resolutions. Downscaling can be accomplished for instance by relating the global spatial variance of surface soil moisture to the desired scale using a power law relationship (see 2.3.3). Fitting the power law function to grain sizes from 2 to 37 for each day of the year resulted in highly significant correlations with R^2 between 0.94 and 0.99. The value of the scaling factor β varies between -0.17 and -0.62 in the course of the year (Fig. 10) representing the changing scaling behavior of surface soil moisture patterns, which in the analysis above was shown to depend on varying influences of weather, soil, and land use.

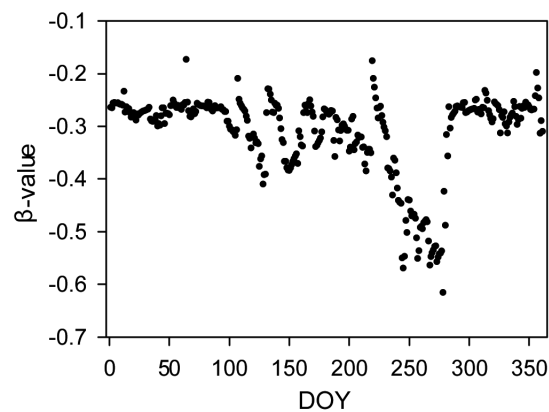


Fig. 10. Scaling factor β of the scaling function for every day of year (DOY) in 2009.

More negative values of β occur during periods of high small scale spatial variability. Large negative values denote a strong change of surface soil moisture variance with spatial scale, whereas less negative β -values indicate periods of little change of soil moisture variability with spatial scale. The annual course of β closely resembles the autocorrelation lengths found in the pattern analysis stressing a strong relationship between autocorrelation and scaling behavior of spatial variance as described by Whittle (1962). Outside the growing period, β -values found in the current study range from -0.17 to -0.31. This is similar to values

found by Rodriguez-Iturbe et al. (1995) and Manfreda et al. (2007). The computed β -values for temporal invariant soil parameters (e.g., -0.23 for clay content, -0.21 for sand content, all with $R^2 > 0.91$) suggests a controlling effect of the soil parameters on the scaling behavior particularly outside of the growing season. However within the growing season, the β -values are well below this range, indicating the strong impact of vegetation dynamics upon the scaling properties of surface soil moisture. As shown above, these low values are caused by the land use pattern and the resulting heterogeneous evapotranspiration particularly towards the end of the growing season. Large precipitation events reset the β -values to values around or even smaller than -0.25.

To be useable for downscaling, the value of β for a particular day has to be derivable from external variables. A linear equation was fitted to the time series of β and spatial mean surface soil moisture (msm, Vol.-%) resulting in the following highly significant (p-value: 0.01) relationship:

$$\beta = 0.0158 \text{ msm} - 0.7486 \quad (R^2 = 0.24) \quad (4)$$

The low R^2 value indicates only a weak tendency to less negative values of β at higher mean surface soil moisture, thus showing a limited usability in practical downscaling approaches. Comparable to our study, Manfreda et al. (2007) detected only weak trends over short time periods between mean surface soil moisture values and β , due to the highly variable influence of precipitation and evapotranspiration. A significant influence of drying and wetting cycles as in the study of Manfreda et al. (2007) could not be detected.

In order to better understand the main factors determining and predicting the scaling factor β we analyzed its dependency upon different independent variables. We found that both, the area averaged precipitation cumulated over the previous 20 days (sumPrecip, in mm) and a parameter (devLAI) which expresses the spatial variability of the LAI, yield significant correlations to the β -value. devLAI is the deviation of the LAI from the mean LAI of the investigation area. To calculate devLAI, we used the results of the validation model run from our test fields for the different crops. The mean LAI of the investigation area was calculated as area weighted average over the different crops. The area weights are taken from the land use classification. Equally, the deviation from the mean (devLAI) was calculated as an area weighted average. This procedure makes sure, that devLAI can be derived scale independently from generally available independent data. A linear regression analysis provided highly significant (p-value: 0.01) relationships between sumPrecip and β ($R^2 = 0.19$)

and devLAI and β ($R^2 = 0.38$). These results show that the plant related parameter (devLAI) has more predictive power for the scaling parameter β over the whole year than the mean soil moisture state. This indicates once again the importance of the plant controlled water fluxes to explain the soil moisture patterns. Combining these two parameters yields a highly significant (p-value: 0.01), multiple linear relationship:

$$\beta = 0.02 \text{ sumPrecip} - 0.032 \text{ devLAI} - 0.351 \quad (R^2 = 0.53) \quad (5)$$

Thus 53 % of the variance of the scaling factor β can be attributed to the spatial variability of the LAI and to the antecedent precipitation. A multiple regression analysis using devLAI and msm results in an R^2 value of 0.44.

4. Conclusions

A dynamically coupled, process-based and spatially distributed ecohydrological model was used to analyze the key processes, their interactions and feedbacks leading to spatial and temporal soil moisture patterns as well as to assess the impact of soil, precipitation, and vegetation on these patterns. Because of the strong influence of vegetation water uptake during the growing season in an agricultural landscape, the plant growth model was validated during two growing seasons for the three main crops in the investigation area: Winter wheat, sugar beet, and maize. The index of agreement for the total aboveground biomass yields values of 0.96 or higher and values ranging from 0.81 to 0.98 for green LAI supporting our confidence to adequately simulate the key impacts of plant growth dynamics upon the temporal course and spatial dynamics of soil moisture. The validation of surface soil moisture yields RMSE values that range from 1.8 to 7.8 Vol.-% for both years and all crops. However, a change in soil infiltration, which was clearly discernible in the field measurements, lead to significantly larger RMSE values for root crops at the end of the growing season. Considering only the first phase of the measurements for root crops, the RMSE shows values between 1.3 and 3.0 Vol.-%. Possible processes leading to the observed changes in soil infiltration might be clogging of the pores by siltation or crust formation. The validation shows that the model simulates plant growth, plant water uptake, and surface soil moisture with suitable accuracy and thus can provide a suitable base data for the analysis of surface soil moisture patterns and their scaling properties in the northern part of the Rur catchment.

In the northern part of the Rur catchment, the average spatial mean soil moisture during the main growing season is, as expected, lower (26.4 Vol.-%) as compared to 28.9 Vol.-% outside the main growing season of 2009. These differences are mainly due to evapotranspiration. A highly significant negative exponential relationship between the coefficient of variation and the mean surface soil moisture was found, meaning that the variability of surface soil moisture patterns increases with decreasing mean soil moisture. This indicates that evapotranspiration causes not only lower mean soil moisture but also increases spatial variability in our investigation area.

To analyze the patterns of surface soil moisture and their scaling properties, an autocorrelation analysis was conducted. At the beginning and the end of the year when the overall soil moisture is high, surface soil moisture patterns depend mainly on the soil properties (field capacity). This behavior was confirmed for all investigated scales with grain sizes between 1 and 37 (corresponding to pixel sizes from 0.15 km x 0.15 km to 5.55 km x 5.55 km). During the main growing season, the patterns resulting from soil properties were modified by the small scale land use pattern and the resulting small scale variability of evapotranspiration. With increasing spatial scales, land use related impacts decrease due to averaging of the small scale evapotranspiration variability. Due to their high autocorrelation lengths, precipitation events increase soil moisture autocorrelation at all spatial scales and even beyond the autocorrelation lengths resulting from the soil properties. The strength of this effect depends on the variability and amount of the precipitation and upon the preceding soil moisture conditions. Scaling properties found in this study depend further on the specific field sizes and management structures in the northern part of the Rur catchment. While the particular scaling properties may not apply to areas with a significantly different agricultural structure, the general finding of field size dominated spatial soil moisture patterns during the main growing period should also apply to other regions. The scale of our investigation was chosen to account for the small scale variability of surface soil moisture caused by heterogeneous land use.

Fitting the daily spatial variance of surface soil moisture to scale for grain sizes between 2 and 37 using a power law relationship yields daily values of the scaling factor β between -0.17 and -0.62. Large negative values of β occur during periods of high small scale spatial variability and denote a strong decrease of surface soil moisture variability with increasing scale, while less negative β -values indicate periods of reduced scale dependence. Large negative β -values occur mainly during dry periods in summer, which indicate again the

influence of small scale variability of evapotranspiration during the growing season. 53 % of the variance of the scaling factor β can be explained by an independent LAI parameter to account for the small scale variability of plant controlled water fluxes and a precipitation parameter to account for the temporal variability of the precipitation. This indicates a potential to assess the subscale surface soil moisture heterogeneity from coarse scale data. Understanding the subscale soil moisture heterogeneity is, for example, particularly relevant to better utilize coarse scale soil moisture data derived from SMOS or SMAP satellite measurements.

Acknowledgements

We gratefully acknowledge financial support by the SFB/TR 32 “*Pattern in Soil-Vegetation-Atmosphere Systems: Monitoring, Modelling, and Data Assimilation*” funded by the Deutsche Forschungsgemeinschaft (DFG). Special thanks go to our students for helping with the field measurements and to the farmers in Selhausen for granting access to their fields. Thanks also go to Karen Schneider for proof reading the manuscript.

References

- Barth, M., Hennicker, R., Kraus, A., Ludwig, M., 2004. DANUBIA: An integrative simulation system for global change research in the Upper Danube Basin. *Cybernet Syst*, 35(7-8): 639-666.
- Barthel, R. et al., 2012. Integrated Modeling of Global Change Impacts on Agriculture and Groundwater Resources. *Water Resour Manag*, 26(7): 1929-1951.
- Brooks, R.H., Corey, A.T., 1966. Properties of porous media affecting fluid flow. *Journal of Irrigation and Drainage Division, American Society of Civil Engineering* IR2: 61–88.
- Choi, M., Jacobs, J.M., 2007. Soil moisture variability of root zone profiles within SMEX02 remote sensing footprints. *Advances in Water Resources*, 30(4): 883-896.
- Choi, M., Jacobs, J.M., 2011. Spatial soil moisture scaling structure during Soil Moisture Experiment 2005. *Hydrological Processes*, 25(6): 926-932.
- DIN 19683-2, 1997. *Bodenuntersuchungsverfahren im Landwirtschaftlichen Wasserbau—Physikalische Laboruntersuchungen, Bestimmung der Korngrößenzusammensetzung nach Vorbehandlung mit Natriumpyrophosphat*. Beuth-Verlag GmbH, Berlin.
- Eagleson, P.S., 1978. *Climate, Soil, and Vegetation .3. Simplified Model of Soil-Moisture Movement in Liquid-Phase*. *Water Resources Research*, 14(5): 722-730.
- Entekhabi, D., Rodriguez-Iturbe, I., 1994. Analytical framework for the characterization of the space-time variability of soil moisture. *Advances in Water Resources*, 17(1–2): 35-45.
- Famiglietti, J.S. et al., 1999. Ground-based investigation of soil moisture variability within remote sensing footprints during the Southern Great Plains 1997 (SGP97) Hydrology Experiment. *Water Resources Research*, 35(6): 1839-1851.
- Famiglietti, J.S., Rudnicki, J.W., Rodell, M., 1998. Variability in surface moisture content along a hillslope transect: Rattlesnake Hill, Texas. *Journal of Hydrology*, 210(1-4): 259-281.

- Green, T.R., Erskine, R.H., 2004. Measurement, scaling, and topographic analyses of spatial crop yield and soil water content. *Hydrological Processes*, 18(8): 1447-1465.
- Hawley, M.E., Jackson, T.J., McCuen, R.H., 1983. Surface Soil-Moisture Variation on Small Agricultural Watersheds. *Journal of Hydrology*, 62(1-4): 179-200.
- Hebrard, O., Voltz, M., Andrieux, P., Moussa, R., 2006. Spatio-temporal distribution of soil surface moisture in a heterogeneously farmed Mediterranean catchment. *Journal of Hydrology*, 329(1-2): 110-121.
- Jones, C.A., Kiniry, J.R., 1986. *CERES-Maize: A simulation Model of Maize Growth and Development*. Texas A & M University Press, College Station, 194 pp.
- Kim, G., Barros, A.P., 2002. Space-time characterization of soil moisture from passive microwave remotely sensed imagery and ancillary data. *Remote Sensing of Environment*, 81(2-3): 393-403.
- Klar, C.W., Fiener, P., Neuhaus, P., Lenz-Wiedemann, V.I.S., Schneider, K., 2008. Modelling of soil nitrogen dynamics within the decision support system DANUBIA. *Ecol. Model.*, 217(1-2): 181-196.
- Korres, W., Koyama, C.N., Fiener, P., Schneider, K., 2010. Analysis of surface soil moisture patterns in agricultural landscapes using Empirical Orthogonal Functions. *Hydrol. Earth Syst. Sci.*, 14(5): 751-764.
- Koyama, C.N., Korres, W., Fiener, P., Schneider, K., 2010. Variability of Surface Soil Moisture Observed from Multitemporal C-Band Synthetic Aperture Radar and Field Data. *Vadose Zone Journal*, 9(4): 1014-1024.
- Lenz-Wiedemann, V.I.S., Klar, C.W., Schneider, K., 2010. Development and test of a crop growth model for application within a Global Change decision support system. *Ecol. Model.*, 221(2): 314-329.

- Manfreda, S., McCabe, M.F., Fiorentino, M., Rodríguez-Iturbe, I., Wood, E.F., 2007. Scaling characteristics of spatial patterns of soil moisture from distributed modelling. *Advances in Water Resources*, 30(10): 2145-2150.
- Mausser, W., Bach, H., 2009. PROMET - Large scale distributed hydrological modelling to study the impact of climate change on the water flows of mountain watersheds. *Journal of Hydrology*, 376(3-4): 362-377.
- Muerth, M., Mausser, W., 2012. Rigorous evaluation of a soil heat transfer model for mesoscale climate change impact studies. *Environ Modell Softw*, 35: 149-162.
- Peters-Lidard, C.D., Pan, F., Wood, E.F., 2001. A re-examination of modeled and measured soil moisture spatial variability and its implications for land surface modeling. *Advances in Water Resources*, 24(9-10): 1069-1083.
- Philip, J.R., 1960. General Method of Exact Solution of the Concentration-dependent Diffusion Equation. *Aust J Phys*, 13: 1-12.
- Rawls, W.J., Brakensiek, D.L., 1985. Predictions of soil water properties for hydrologic modelling, New York, pp. 293-299.
- Reynolds, S.G., 1970. The gravimetric method of soil moisture determination Part III An examination of factors influencing soil moisture variability. *Journal of Hydrology*, 11(3): 288-300.
- Richter, D., 1995. Ergebnisse methodischer Untersuchungen zur Korrektur des systematischen Meßfehlers des Hellmann-Niederschlagsmessers. *Berichte des Deutschen Wetterdienstes*, 194, Offenbach am Rhein, 93 pp.
- Rodriguez-Iturbe, I., Isham, V., Cox, D.R., Manfreda, S., Porporato, A., 2006. Space-time modeling of soil moisture: Stochastic rainfall forcing with heterogeneous vegetation. *Water Resources Research*, 42(6): W06D05.
- Rodriguez-Iturbe, I. et al., 1995. On the Spatial-Organization of Soil-Moisture Fields. *Geophysical Research Letters*, 22(20): 2757-2760.

- Streck, N.A., Weiss, A., Baenziger, P.S., 2003a. A generalized vernalization response function for winter wheat. *Agronomy Journal*, 95(1): 155-159.
- Streck, N.A., Weiss, A., Xue, Q., Baenziger, P.S., 2003b. Improving predictions of developmental stages in winter wheat: a modified Wang and Engel model. *Agr Forest Meteorol*, 115(3-4): 139-150.
- Svetlitchnyi, A.A., Plotnitskiy, S.V., Stepovaya, O.Y., 2003. Spatial distribution of soil moisture content within catchments and its modelling on the basis of topographic data. *Journal of Hydrology*, 277(1-2): 50-60.
- Teuling, A.J., Troch, P.A., 2005. Improved understanding of soil moisture variability dynamics. *Geophysical Research Letters*, 32(5): L05404.
- Waldhoff, G., 2010. Land use classification of 2009 for the Rur catchment. 10.1594/GFZ.TR32.1.
- Western, A.W., Blöschl, G., Grayson, R.B., 1998. Geostatistical characterisation of soil moisture patterns in the Tarrawarra a catchment. *Journal of Hydrology*, 205(1-2): 20-37.
- Western, A.W., Grayson, R.B., 1998. The Tarrawarra data set: Soil moisture patterns, soil characteristics, and hydrological flux measurements. *Water Resources Research*, 34(10): 2765-2768.
- Western, A.W., Grayson, R.B., Blöschl, G., Willgoose, G.R., McMahon, T.A., 1999a. Observed spatial organization of soil moisture and its relation to terrain indices. *Water Resources Research*, 35(3): 797-810.
- Western, A.W., Grayson, R.B., Green, T.R., 1999b. The Tarrawarra project: high resolution spatial measurement, modelling and analysis of soil moisture and hydrological response. *Hydrological Processes*, 13(5): 633-652.
- Western, A.W. et al., 2004. Spatial correlation of soil moisture in small catchments and its relationship to dominant spatial hydrological processes. *Journal of Hydrology*, 286(1-4): 113-134.

Whittle, P., 1962. Topographic Correlation, Power-Law Covariance Functions, and Diffusion. *Biometrika*, 49(3-4): 305-314.

Willmott, C., 1981. On the validation of models. *Phys. Geogr.*, 2: 184-194.

Wösten, J.H.M., Lilly, A., Nemes, A., Le Bas, C., 1999. Development and use of a database of hydraulic properties of European soils. *Geoderma*, 90(3-4): 169-185.

Yin, X., van Laar, H.H., 2005. *Crop Systems Dynamics*. Wageningen Academic Publishers, Wageningen, 155 pp.

6. Summary of results and conclusions

In this thesis spatial patterns and temporal dynamics of surface soil moisture, their controlling parameters and underlying processes were investigated on different scales. The investigation area was the catchment of the river Rur (2364 km²), which can be separated in a low mountain range in the southern part with mostly forest and grassland (~1300 km²), and an intensively agriculturally used northern part (~1100 km²), where predominantly crops are grown on a virtually flat area. Our small grassland test site with 9 test fields was established within the southern part, our arable land test site with 6 test fields was located within the northern part of the Rur catchment.

The spatial organization of the investigation can be characterized by three scales (spacing, extent and support, see also section 2.2. Spacing refers to the distance between single measurements, extent to the overall size of the investigation area and support to the resolution of the investigation. The investigation was conducted on varying spatial scales:

- I) Small scale (extent): Extensive field measurements (soil moisture campaigns, long-term soil moisture stations, plant measurements, soil measurements and meteorological stations) were conducted in the grassland test site (~0.4 km x 1.1 km) and the arable land test site (~0.9 km x 1.2 km). The soil moisture data was used to investigate spatial and temporal variability of surface soil moisture at the field scale within small catchments. This measurement data was also used to validate the other methods used in this thesis (radar remote sensing and ecohydrological modeling).
- II) Large scale (extent): Estimation of surface soil moisture patterns at the scale of the whole Rur catchment from field measurements is generally not feasible. Thus, we derived spatially distributed soil moisture maps from radar remote sensing and ecohydrological modeling, both with support of 150 meters. The spatial variability of surface soil moisture and the underlying processes were analyzed with respect to their scaling properties:

- Estimated surface soil moisture from radar remote sensing data was analyzed regarding a varying spatial extent.
- Estimated surface soil moisture from spatially distributed model runs was analyzed with regard to a varying support.

6.1. Small scale surface soil moisture patterns

The basis for the investigation of small scale surface soil moisture patterns were spatially distributed field measurements conducted within our grassland (slopes from 0 to 10°) and arable land test site (slopes from 0 to 4°). Distributed soil moisture measurements of the top soil layer (top 6 cm) were performed with a spacing of approximately 50 meters on 14 campaigns for the grassland and 17 campaigns for the arable land test site. To analyze the spatial and temporal patterns from the distributed soil moisture measurements, an Empirical Orthogonal Function (EOF) analysis was applied.

The analysis in the grassland test site resulted in one significant EOF (spatial pattern, remaining stable over time), explaining 57.5 % of the spatial soil moisture variability in whole dataset. This EOF was related to soil properties and topography. Its dominance was largest during or shortly after wet periods, because under wet conditions, the lateral redistribution of water and the varying infiltration by different soil types became more important. Another significant EOF accounting for the differences in land management (grazing, cutting, fertilizing) could not be identified for the grassland site. The highest temporal soil moisture variability was found in the lower parts of the grassland test site. These locations with a high soil organic carbon content were associated with areas where higher soil moisture content prevailed over longer time periods resulted from and indicated by the soil type.

At the arable land test site, two significant EOFs controlling the major part of the spatial variability were determined. The first EOF, accounting for 38.4 % of the variability, was strongly related to soil properties and pointed to the importance of spatial differences in soil porosity in relation to soil moisture dynamics. The impact of this pattern was more pronounced during dry periods, indicating a compensating effect of precipitation. The second EOF explained 28.3 % of the variance and could be assigned to land management patterns, influencing soil properties and increased evaporation due to tillage as well as transpiration, due to different crops and different dates of sowing and fertilization. More than 66 % of the spatial variability of surface soil moisture at the arable test site was explained by these two

EOFs. The highest temporal variability of soil moisture was found at locations with low porosity. At these locations higher thermal conductivity and lower water holding capacity, caused by higher content of the coarse fraction in the soil, led to a higher temporal variance of soil moisture. The structure of our dataset with alternating management patterns at the arable test site in two consecutive years of measurements allowed for detecting not only the stable pattern (connected with soil parameters), but also the non-stable pattern of different land management on different fields.

Both test sites were small enough to assume homogeneous precipitation conditions for all measuring locations, but while the surface soil moisture variability increases with increasing soil moisture conditions in the grassland test site, a reversed relationship was found in the arable land test site. Hence, the wet state on the grassland test site was non-locally controlled, with catchment terrain leading to pattern (e.g., by lateral redistribution of water), whereas the wet state on the arable land was locally controlled, with mainly vertical fluxes leading to the pattern (see section 2.4).

The identification of management as one main factor controlling surface soil moisture patterns had implications for the analysis on larger scales. We used a spatial support of 150 m in the large scale analysis, to account for the land use and management induced small scale variability.

6.2. Large scale surface soil moisture patterns

Spatially distributed soil moisture maps were derived from radar remote sensing and ecohydrological modeling. Data from the field measurements were used to validate the DANUBIA model and soil moisture estimates from the empirical retrieval algorithm for the Advanced Synthetic Aperture Radar (ASAR) onboard the ENVISAT satellite.

6.2.1. Validation of methods

The dynamically coupled, process based and spatially distributed ecohydrological model DANUBIA was used and validated in the northern part of the Rur catchment. The model study focused on the northern part of the Rur catchment, since 46 % of the area is arable land. Water uptake from the vegetation strongly influences soil moisture dynamics during the growing season. In turn, water demand of the vegetation strongly depends on vegetation type and development state. Thus, it is important to adequately model the vegetation dynamics. Therefore the plant growth model was validated during two growing seasons for the three

main crops in the investigation area: Winter wheat, sugar beet, and maize. The index of agreement for the total aboveground biomass yielded values of 0.96 or higher and values ranging from 0.81 to 0.98 for green LAI supporting our confidence to adequately simulate the key effects of plant growth dynamics upon the temporal course and spatial dynamics of soil moisture. The validation of surface soil moisture yielded RMSE values that range from 1.8 to 7.8 Vol.-% for both years and all crops and an average RMSE of 3.4 Vol.-%. However, a change in soil infiltration, which was clearly discernible in the field measurements, lead to significantly larger RMSE values for maize and sugar beet at the end of the growing season. Considering only the first phase of the measurements for these crops, the RMSE showed values between 1.3 and 3.0 Vol.-%. Possible processes leading to the observed changes in soil infiltration might be clogging of the pores by siltation or crust formation.

The validation of ASAR derived soil moisture values for bare soil, cereal, harvested fields, grassland and root crops yielded an overall RMSE of 5.0 Vol.-%. Very high soil moisture values, exceeding 45 Vol.-%, were measured under grassland, where the thatch layer of the grass cover and the organic topsoil layer provided a porosity exceeding the porosity of mineral soils. The empirical retrieval algorithm did not appropriately account for this effect. By excluding soil moisture values above 45 Vol.-% the overall RMSE value diminished to 4.3 Vol.-%.

6.2.2. Large scale patterns

We analyzed the statistical properties of the surface soil moisture patterns in terms of the relationship between soil moisture variability and mean soil moisture. Using the data from all eight ASAR soil moisture images from the whole Rur catchment, a linear relationship between the spatial coefficient of variation (CV) and the mean soil moisture was found. The relationship showed decreasing soil moisture variability with increasing mean soil moisture values. When investigating this relationship separately for the northern part and the southern part of the Rur catchment, the relationship in the northern part was close to that of the whole catchment, while in contrast the relationship for the southern area showed high variability even at high soil moisture means. While the soil texture in the northern part was rather uniform, the soil textures in the southern part varied considerably from mineral soils saturating at moisture values between 45 and 50 Vol.-% to organic soil or soils with an organic top soil layer with surface soil moisture values in excess of 60 Vol.-%. Thus, even at or close to saturation, the soils in the southern part showed large spatial variability. Moreover, the hilly topography of the southern part also caused larger spatial variations of precipitation

and more heterogeneity due to lateral redistribution of water on the soil surface or subsurface. A similar behavior of the relationship between variability and mean value was found using the daily surface soil moisture maps of the northern part of the Rur catchment calculated by the DANUBIA model. Here we found a negative exponential relationship, leading to slightly lower CV values at a given mean value than calculated from the ASAR data. For example, for the mean value of 30 Vol.-%, the relationship derived from the model data results in a CV of 12.3 %, and from the remote sensing data in a CV of 17.7 %. These differences could be explained by additional variability induced by the grassland in the northern part of the Rur catchment, which is included in the ASAR data, but not in the model and by differences in the soil volume for the soil moisture estimation between the two methods. Furthermore, the relationships are derived from different years with different land use classifications. Moreover, modeled spatial patterns tend to reduce the spatial variability of the natural system, because the full detail of all processes involved cannot be implemented in a model and models are simplifications by definition. Also the input data for the model (e.g., soil map, precipitation data) cannot include the full heterogeneity of the natural system.

An advantage of using the DANUBIA model for the analysis of spatial surface soil moisture patterns on large scales is the higher temporal resolution of the data (daily soil moisture maps), compared to radar remote sensing with one image every 35 days. The higher temporal resolution of the data enables the potential to analyze the main processes leading to soil moisture dynamics during the course of the year. To investigate the influence of the single factors land use, precipitation and soil on surface soil moisture patterns, we performed, besides a model run with the full complexity, several additional model runs, holding one of these factors spatially constant. The generated maps from these four model runs served as a basis for autocorrelation analyses of the spatial patterns. With these analyses, we could distinguish between three different major factors influencing the soil moisture patterns in the northern part of the Rur catchment: 1) precipitation events with large autocorrelation lengths, 2) soil properties with medium autocorrelation lengths, and 3) land use patterns with small autocorrelation lengths. At the beginning and the end of the year when the overall soil moisture is high, surface soil moisture patterns depended mainly on the soil properties (field capacity). During the main growing season in the spring and summer, the patterns resulting from soil properties were modified by the small scale land use pattern and the resulting small scale variability of evapotranspiration. Due to their high autocorrelation lengths, precipitation events increased soil moisture autocorrelation even beyond the autocorrelation lengths

resulting from the soil properties. The strength of this effect depends on the variability and amount of the precipitation and upon the preceding soil moisture conditions.

6.3. Scaling properties of surface soil moisture patterns

Scaling properties of surface soil moisture patterns were analyzed regarding the influence of the extent on the relationship between soil moisture variability and mean soil moisture. This was done on the basis of ASAR soil moisture maps and field measurements. The relationship was calculated for the whole Rur catchment, for the northern part of the Rur catchment, for 1.5 km x 1.5 km boxes (non-overlapping 10 x 10 pixels moving box) within the northern part of the Rur catchment and for the field scale (winter wheat and sugar beet). At all scales (extent) the variability of soil moisture decreased with increasing mean soil moisture, but the slope of this linear relationship decreases with decreasing extent. Hence, at a given mean soil moisture level, we observed the highest variability on the scale of the entire Rur catchment and the smallest variability on the field scale. This can be attributed to the fact that the controlling factors of surface soil moisture variability are much more variable on the large scale. Precipitation as the dominant driver for soil moisture was much more heterogeneous on the catchment scale with annual mean values between 600 mm in the northern part and over 1200 mm in the southern part of the Rur catchment, than on individual fields or small catchments, where it could be assumed to be homogeneous. But also the heterogeneities of influencing factors like soil, vegetation and topography became generally larger at larger scales (larger extent).

The scaling properties in terms of the variation of the support were investigated by aggregating the results of the DANUBIA model runs to spatial resolutions from 0.3 km x 0.3 km up to 5.55 km x 5.55 km. Surface soil moisture patterns are determined by soil patterns across the analyzed scales. Land use patterns disturb these patterns in times of high evapotranspiration, but disturbance decreased with coarser spatial resolution. Precipitation typically results in large scale patterns that are superimposed upon other patterns at all scales for a short time. The scaling behavior (regarding the support) of patterns is of importance when data must be scaled down to finer resolutions. A power law relationship could be used for downscaling purposes. Fitting the daily spatial variance of surface soil moisture to spatial resolutions from 0.3 km x 0.3 km up to 5.55 km x 5.55 km yielded daily values of the scaling factor β . High negative values of β occurred during periods of high small scale spatial variability and denoted a strong decrease of surface soil moisture variability with increasing support, while lower negative β -values indicate periods of reduced scale

dependence. High negative β -values occurred mainly during dry periods in summer, which again indicates the influence of small scale variability of evapotranspiration during the growing season. To be suitable for downscaling, the temporal course of the scaling factor β has to be derivable from independent parameters. 53 % of the variance of β could be explained by an independent LAI parameter to account for the small scale variability of plant controlled water fluxes and a precipitation parameter to account for the temporal variability of the precipitation. This indicated a potential to estimate the subscale surface soil moisture heterogeneity from coarse scale data. The derived scaling properties resulted partly from the specific field sizes and management structures in the northern part of the Rur catchment and might not apply to areas with a significantly different agricultural field structure.

6.4. General conclusions

This thesis improves the knowledge about surface soil moisture patterns in agriculturally used areas, namely the river Rur catchment. The northern part of the Rur catchment was of special interest, due to the strong influence of agricultural management (e.g., dates of planting and harvesting for different crops). The fact, that different patterns with their underlying processes are encountered at different temporal or spatial scales intrinsically connects the two terms of pattern and scale. Therefore the identification of different processes and the importance of these processes for surface soil moisture patterns had to be considered in the context of the scale. The following three paragraphs summarize the conclusions with respect to the research questions:

- Precipitation, vegetation patterns, topography and soil properties are the dominant factors for soil moisture patterns in an agriculturally used landscape. Precipitation can be assumed to be homogeneous at the small scale, having a uniformly raising effect on surface soil moisture for the time of the event, but can be very heterogeneous on the large scale at the same time. Vegetation patterns influence soil moisture patterns by controlling evapotranspiration. Especially during the growing season large differences in evapotranspiration on neighboring fields could be identified, causing high small scale variability. This small scale pattern smoothes out with coarser resolutions of the investigation. Topography is a source of small scale patterns on wet surface soil moisture states, due to the lateral redistribution of water during or shortly after precipitation events. Soils have a major influence on the variability of surface soil moisture on all scales, due to the large heterogeneity of soil properties within a given

soil type (small scale) and between different soil types (large scale). These varying soil properties led to large spatial differences in the hydraulic behavior of a soil (e.g., infiltration or water holding capacity).

- These influencing factors and their underlying processes control the variability of surface soil moisture patterns in our investigation. Based on the scale analysis of the radar remote sensing data (scale: extent) and the model data (scale: support) we come to the conclusion, that the variability of surface soil moisture increases with an increasing size of the investigation area (extent) and an increasing resolution within the investigation area (support).
- In the course of the year surface soil moisture patterns and their scaling properties depend on different varying factors. Two main periods with different general patterns and scaling behavior can be distinguished. A) In the beginning and towards the end of the year (outside the growing season) the patterns and their scaling properties are mainly determined by soil properties. B) During the growing season these patterns are superimposed by the small scale land use pattern and the resulting small scale variability of evapotranspiration. At this time of high small scale variability of evapotranspiration, the variability of surface soil moisture decreases much stronger with increasing spatial scale (support) than during times outside the growing season. During the whole year precipitation events superimpose their large scale patterns for a short period of time and diminish the small scale variability induced by evapotranspiration.

6.5. Outlook

The comprehensive analysis of surface soil moisture patterns in an agricultural landscape and the understanding of the different influencing factors on different scales at different times upon these patterns are of great importance within the SFB/TR32 project, because soil moisture is one of the key components in the soil-vegetation-atmosphere system. The improved knowledge could be used to access the subscale surface soil moisture heterogeneity from coarse scale data, derived for example from SMOS (Soil Moisture and Ocean Salinity) or SMAP (Soil Moisture Active Passive) satellite measurements. Our analysis showed the importance of small scale land use patterns and the usability of vegetation (e.g., leaf area index) and meteorological parameters for downscaling purposes. The combined analysis of

radar remote sensing and modeling provide an opportunity to improve the parameterization of surface soil properties. Outside the growing season soil moisture patterns are mainly determined by soil properties. Hence, the analysis of systematic and stable differences between estimates from remote sensing and modeling can be utilized to identify heterogeneity of soil parameters, which is not differentiated in soil maps. The assimilation of remote sensing data could potentially be used to improve the precision of surface soil moisture estimates from the model. This will depend on the accuracy of the data sets and the temporal resolution of the remote sensing data. The daily distributed data produced by the DANUBIA model (e.g., biomass) will be used for biomass correction in radar remote sensing retrieval algorithms for soil moisture and can be used as input data for models operating on larger scales and for model comparisons within the SFB/TR32 project. Plans are to implement a forest and a grassland model into the DANUBIA model, to extend the coverage within the Rur catchment.

References*

- Arnell, N.W., 1999. Climate change and global water resources. *Global Environ Chang*, 9: 31-49.
- Barth, M., Hennicker, R., Kraus, A., Ludwig, M., 2004. DANUBIA: An integrative simulation system for global change research in the Upper Danube Basin. *Cybernet Syst*, 35(7-8): 639-666.
- Barthel, R. et al., 2012. Integrated Modeling of Global Change Impacts on Agriculture and Groundwater Resources. *Water Resour Manag*, 26(7): 1929-1951.
- Blöschl, G., Sivapalan, M., 1995. Scale Issues in Hydrological Modeling - a Review. *Hydrological Processes*, 9(3-4): 251-290.
- Bogena, H.R., Huisman, J.A., Oberdorster, C., Vereecken, H., 2007. Evaluation of a low-cost soil water content sensor for wireless network applications. *Journal of Hydrology*, 344(1-2): 32-42.
- Charpentier, M.A., Groffman, P.M., 1992. Soil-Moisture Variability within Remote-Sensing Pixels. *J Geophys Res-Atmos*, 97(D17): 18987-18995.
- Choi, M., Jacobs, J.M., 2011. Spatial soil moisture scaling structure during Soil Moisture Experiment 2005. *Hydrological Processes*, 25(6): 926-932.
- Eagleson, P.S., 1978. Climate, Soil, and Vegetation .3. Simplified Model of Soil-Moisture Movement in Liquid-Phase. *Water Resources Research*, 14(5): 722-730.
- Entekhabi, D., Rodriguez-Iturbe, I., 1994. Analytical framework for the characterization of the space-time variability of soil moisture. *Advances in Water Resources*, 17(1-2): 35-45.
- Falloon, P., Jones, C.D., Ades, M., Paul, K., 2011. Direct soil moisture controls of future global soil carbon changes: An important source of uncertainty. *Global Biogeochem. Cycles*, 25(3): GB3010.
- Famiglietti, J.S. et al., 1999. Ground-based investigation of soil moisture variability within remote sensing footprints during the Southern Great Plains 1997 (SGP97) Hydrology Experiment. *Water Resources Research*, 35(6): 1839-1851.
- Famiglietti, J.S., Rudnicki, J.W., Rodell, M., 1998. Variability in surface moisture content along a hillslope transect: Rattlesnake Hill, Texas. *Journal of Hydrology*, 210(1-4): 259-281.

* for chapters 1,2, and 6

- Flügel, W.-A., 1995. Delineating hydrological response units by geographical information system analyses for regional hydrological modelling using PRMS/MMS in the drainage basin of the River Bröl, Germany. *Hydrological Processes*, 9(3-4): 423-436.
- Gaskin, G.J., Miller, J.D., 1996. Measurement of Soil Water Content Using a Simplified Impedance Measuring Technique. *Journal of Agricultural Engineering Research*, 63(2): 153-159.
- Grayson, R., Blöschl, G., 2000. *Spatial patterns in catchment hydrology : observations and modelling*. Cambridge University Press, New York, 404 pp.
- Grayson, R.B., Western, A.W., Chiew, F.H.S., Blöschl, G., 1997. Preferred states in spatial soil moisture patterns: Local and nonlocal controls. *Water Resources Research*, 33(12): 2897-2908.
- Green, T.R., Erskine, R.H., 2004. Measurement, scaling, and topographic analyses of spatial crop yield and soil water content. *Hydrological Processes*, 18(8): 1447-1465.
- Hansen, J.R., Refsgaard, J.C., Hansen, S., Ernstsens, V., 2007. Problems with heterogeneity in physically based agricultural catchment models. *Journal of Hydrology*, 342(1-2): 1-16.
- Hawley, M.E., Jackson, T.J., McCuen, R.H., 1983. Surface Soil-Moisture Variation on Small Agricultural Watersheds. *Journal of Hydrology*, 62(1-4): 179-200.
- Hillel, D., 1998. *Environmental soil physics*. Academic Press, San Diego, CA, 771 pp.
- Huisman, J.A., Sperl, C., Bouten, W., Verstraten, J.M., 2001. Soil water content measurements at different scales: accuracy of time domain reflectometry and ground-penetrating radar. *Journal of Hydrology*, 245(1-4): 48-58.
- Jackson, T.J., Schmugge, T.J., 1989. Passive Microwave Remote-Sensing System for Soil-Moisture - Some Supporting Research. *Ieee T Geosci Remote*, 27(2): 225-235.
- Jawson, S.D., Niemann, J.D., 2007. Spatial patterns from EOF analysis of soil moisture at a large scale and their dependence on soil, land-use, and topographic properties. *Advances in Water Resources*, 30(3): 366-381.
- Jones, C.A., Kiniry, J.R., 1986. *CERES-Maize: A simulation Model of Maize Growth and Development*. Texas A & M University Press, College Station, 194 pp.
- Kemna, A., Vanderborght, J., Kulesa, B., Vereecken, H., 2002. Imaging and characterisation of subsurface solute transport using electrical resistivity tomography (ERT) and equivalent transport models. *Journal of Hydrology*, 267(3-4): 125-146.
- Kim, G., Barros, A.P., 2002. Space-time characterization of soil moisture from passive microwave remotely sensed imagery and ancillary data. *Remote Sensing of Environment*, 81(2-3): 393-403.
- Kitanidis, P.K., Bras, R.L., 1980. Real-Time Forecasting with A Conceptual Hydrologic Model .1. Analysis of Uncertainty. *Water Resources Research*, 16(6): 1025-1033.

- Klar, C.W., Fiener, P., Neuhaus, P., Lenz-Wiedemann, V.I.S., Schneider, K., 2008. Modelling of soil nitrogen dynamics within the decision support system DANUBIA. *Ecol. Model.*, 217(1-2): 181-196.
- Lenz-Wiedemann, V.I.S., Klar, C.W., Schneider, K., 2010. Development and test of a crop growth model for application within a Global Change decision support system. *Ecol. Model.*, 221(2): 314-329.
- Ludwig, R. et al., 2003. Web-based modelling of energy, water and matter fluxes to support decision making in mesoscale catchments - the integrative perspective of GLOWA-Danube. *Phys. Chem. Earth*, 28(14-15): 621-634.
- Manfreda, S., McCabe, M.F., Fiorentino, M., Rodríguez-Iturbe, I., Wood, E.F., 2007. Scaling characteristics of spatial patterns of soil moisture from distributed modelling. *Advances in Water Resources*, 30(10): 2145-2150.
- Mausser, W., Bach, H., 2009. PROMET - Large scale distributed hydrological modelling to study the impact of climate change on the water flows of mountain watersheds. *Journal of Hydrology*, 376(3-4): 362-377.
- Moore, I.D., Burch, G.J., Mackenzie, D.H., 1988. Topographic Effects on the Distribution of Surface Soil-Water and the Location of Ephemeral Gullies. *Transactions of the ASABE*, 31(4): 1098-1107.
- Muerth, M., Mauser, W., 2012. Rigorous evaluation of a soil heat transfer model for mesoscale climate change impact studies. *Environ Modell Softw*, 35: 149-162.
- Navarro, V., Candej, M., Yustres, A., Merlo, O., Mena, M., 2006. Analysis of installation of FDR sensors in a hard soil. *Geotech Test J*, 29(6): 462-466.
- Oh, Y., Sarabandi, K., Ulaby, F.T., 1992. An Empirical-Model and an Inversion Technique for Radar Scattering from Bare Soil Surfaces. *Ieee T Geosci Remote*, 30(2): 370-381.
- Oki, T., Kanae, S., 2006. Global hydrological cycles and world water resources. *Science*, 313(5790): 1068-1072.
- Perry, M.A., Niemann, J.D., 2007. Analysis and estimation of soil moisture at the catchment scale using EOFs. *Journal of Hydrology*, 334(3-4): 388-404.
- Peters-Lidard, C.D., Pan, F., Wood, E.F., 2001. A re-examination of modeled and measured soil moisture spatial variability and its implications for land surface modeling. *Advances in Water Resources*, 24(9-10): 1069-1083.
- Philip, J.R., 1960. General Method of Exact Solution of the Concentration-dependent Diffusion Equation. *Aust J Phys*, 13: 1-12.
- Pitman, A.J., 2003. The evolution of, and revolution in, land surface schemes designed for climate models. *International Journal of Climatology*, 23(5): 479-510.

- Reynolds, S.G., 1970a. The gravimetric method of soil moisture determination Part I A study of equipment, and methodological problems. *Journal of Hydrology*, 11(3): 258-273.
- Reynolds, S.G., 1970b. The gravimetric method of soil moisture determination Part III An examination of factors influencing soil moisture variability. *Journal of Hydrology*, 11(3): 288-300.
- Rodriguez-Iturbe, I. et al., 1995. On the Spatial-Organization of Soil-Moisture Fields. *Geophysical Research Letters*, 22(20): 2757-2760.
- Rombach, M., Mauser, W., 1997. Multi-annual analysis of ERS surface soil moisture measurements of different land uses, Proc. 3rd ERS Scientific Symposium. Eur. Space Agency, Florence, pp. 703-708.
- Roth, C.H., Malicki, M.A., Plagge, R., 1992. Empirical evaluation of the relationship between soil dielectric constant and volumetric water content as the basis for calibrating soil moisture measurements by TDR. *Journal of Soil Science*, 43(1): 1-13.
- Sayde, C. et al., 2010. Feasibility of soil moisture monitoring with heated fiber optics. *Water Resources Research*, 46: W06201.
- Schneider, K., 2003. Assimilating remote sensing data into a land-surface process model. *International Journal of Remote Sensing*, 24(14): 2959-2980.
- Sellers, P.J. et al., 1997. Modeling the exchanges of energy, water, and carbon between continents and the atmosphere. *Science*, 275(5299): 502-509.
- Seneviratne, S.I. et al., 2010. Investigating soil moisture-climate interactions in a changing climate: A review. *Earth-Sci Rev*, 99(3-4): 125-161.
- Sheets, K.R., Hendrickx, J.M.H., 1995. Noninvasive Soil Water Content Measurement Using Electromagnetic Induction. *Water Resour. Res.*, 31(10): 2401-2409.
- Šimůnek, J., van Genuchten, M.T., Šejna, M., 2008. Development and Applications of the HYDRUS and STANMOD Software Packages and Related Codes. *Vadose Zone J.*, 7(2): 587-600.
- Steele-Dunne, S.C. et al., 2010. Feasibility of soil moisture estimation using passive distributed temperature sensing. *Water Resources Research*, 46: W03534.
- Teuling, A.J., Troch, P.A., 2005. Improved understanding of soil moisture variability dynamics. *Geophysical Research Letters*, 32(5): L05404.
- Topp, G.C., Davis, J.L., Annan, A.P., 1980. Electromagnetic Determination of Soil-Water Content - Measurements in Coaxial Transmission-Lines. *Water Resources Research*, 16(3): 574-582.
- Verhoest, N.E.C. et al., 2008. On the soil roughness parameterization problem in soil moisture retrieval of bare surfaces from synthetic aperture radar. *Sensors-Basel*, 8(7): 4213-4248.
- Vogel, H.J., Ippisch, O., 2008. Estimation of a critical spatial discretization limit for solving Richards' equation at large scales. *Vadose Zone Journal*, 7(1): 112-114.

- Von Hippel, A.R., Labounsky, A.S., 1995. Dielectrics and Waves. Microwave Library. Artech House, 304 pp.
- Wagner, W. et al., 2007. Operational readiness of microwave remote sensing of soil moisture for hydrologic applications. *Nord Hydrol*, 38(1): 1-20.
- Western, A.W., Blöschl, G., Grayson, R.B., 1998. Geostatistical characterisation of soil moisture patterns in the Tarrawarra a catchment. *Journal of Hydrology*, 205(1-2): 20-37.
- Western, A.W., Grayson, R.B., 1998. The Tarrawarra data set: Soil moisture patterns, soil characteristics, and hydrological flux measurements. *Water Resources Research*, 34(10): 2765-2768.
- Western, A.W., Grayson, R.B., Green, T.R., 1999. The Tarrawarra project: high resolution spatial measurement, modelling and analysis of soil moisture and hydrological response. *Hydrological Processes*, 13(5): 633-652.
- Western, A.W. et al., 2004. Spatial correlation of soil moisture in small catchments and its relationship to dominant spatial hydrological processes. *Journal of Hydrology*, 286(1-4): 113-134.
- Yin, X., van Laar, H.H., 2005. *Crop Systems Dynamics*. Wageningen Academic Publishers, Wageningen, 155 pp.
- Yoo, C., Kim, S., 2004. EOF analysis of surface soil moisture field variability. *Advances in Water Resources*, 27(8): 831-842.
- Zreda, M., Desilets, D., Ferre, T.P.A., Scott, R.L., 2008. Measuring soil moisture content non-invasively at intermediate spatial scale using cosmic-ray neutrons. *Geophysical Research Letters*, 35(21): L21402.

Eigene Beteiligung an den Veröffentlichungen

An allen drei Artikeln habe ich maßgeblich von Feldmessungen und Modellierung bis hin zur Analyse der Ergebnisse sowie Konzeption und Ausarbeitung der Artikel mitgewirkt, was auch meine Erstautorenschaft in zwei der drei Artikel belegt. Die von Herrn Dr. Koyama in Erstautorenschaft eingereichte Publikation besteht aus zwei Aspekten: der Prozessierung der Fernerkundungsdaten und einer Musteranalyse dieser Daten und der durchgeführten Feldmessungen. Die Prozessierung und Validierung der Radar-Fernerkundungsdaten erfolgte durch Herrn Dr. Koyama und begründet seine Erstautorenschaft. Die Auswertung der Bodenfeuchtedaten beruhen überwiegend auf meiner wissenschaftlichen Arbeit.

Erklärung

Ich versichere, dass ich die von mir vorgelegte Dissertation selbständig angefertigt, die benutzten Quellen und Hilfsmittel vollständig angegeben und die Stellen der Arbeit – einschließlich Tabellen, Karten und Abbildungen –, die anderen Werken im Wortlaut oder dem Sinn nach entnommen sind, in jedem Einzelfall als Entlehnung kenntlich gemacht habe; dass diese Dissertation noch keiner anderen Fakultät oder Universität zur Prüfung vorgelegen hat; dass sie – abgesehen von unten angegebenen Teilpublikationen – noch nicht veröffentlicht worden ist sowie, dass ich eine solche Veröffentlichung vor Abschluss des Promotionsverfahrens nicht vornehmen werde. Die Bestimmungen der Promotionsordnung sind mir bekannt. Die von mir vorgelegte Dissertation ist von Prof. Dr. Karl Schneider betreut worden.

Köln, den

Folgende Teilpublikationen liegen vor:

Korres, W., Koyama, C.N., Fiener, P., Schneider, K., 2010. Analysis of surface soil moisture patterns in agricultural landscapes using Empirical Orthogonal Functions. *Hydrology and Earth System Science*, 14(5): 751-764.

Koyama, C.N., Korres, W., Fiener, P., Schneider, K., 2010. Variability of Surface Soil Moisture Observed from Multitemporal C-Band Synthetic Aperture Radar and Field Data. *Vadose Zone Journal*, 9(4): 1014-1024.

Korres, W., Reichenau T.G., Schneider, K., 2012. Patterns and scaling properties of surface soil moisture in an agricultural landscape: An ecohydrological modeling study. *Journal of Hydrology*, eingereicht am 23.10.2012, in review seit 05.11.2012.